

# Molecular Epitaxy on Two-Dimensional Materials: the Interplay between Interactions

Tian Tian and Chih-Jen Shih\*

*Institute for Chemical and Bioengineering, ETH Zürich, Vladimir Prelog Weg 1, CH-8093  
Zürich, Switzerland*

E-mail: chih-jen.shih@chem.ethz.ch

## Abstract

Molecular epitaxy – the process of growing a crystalline overlayer onto a substrate – at the two-dimensional (2D) material interfaces, opens new avenues towards the integration of 2D materials with a large variety of functional molecules. ~~Together with recent advances in synthesis and transfer techniques of 2D hybrid materials, The emerging field of~~ controlling molecular epitaxy on 2D materials interfaces ~~represents a fundamental technique towards 2D materials-based heterostructures and opens new opportunities in~~ towards functional heterostructures and novel optoelectronic devices. ~~Owing to the unique physical and chemical nature of 2D materials surfaces, the understanding of interplays clearly requires the understanding of the interplay~~ between molecular interactions at the interfaces~~is an emerging field and clearly plays a crucial role in engineering the interface properties and subsequent applications.~~ In this article, we review the mechanisms governing ~~the~~ molecular epitaxy on 2D materials, with an emphasize on the diverse interactions involved, including: (i) the intermolecular interactions between the deposited molecules, (ii) the molecule-2D material interactions and (iii) the molecule-substrate interactions through the 2D material. ~~Depending on the system considered, the~~ The interplay between these interactions determines the

dimension, interfacial orientation, crystal packing, morphology, and electronic properties of the epitaxial layer. We further review the state-of-art applications, which might be benefited from tailoring molecular interactions at 2D materials interfaces.

## 1 Introduction

Two-dimensional (2D) materials, the one- or few-atom thick crystalline films, have continuously inspired the design and applications of functional materials since their emergence.<sup>1–5</sup> While the theoretical and synthetic effort for novel 2D materials has steadily increased the number of members in the 2D materials family,<sup>5,6</sup> a considerable steeper rising number of applications has also been developed for the hybridization of 2D materials and their combinations in various dimensions, including the 2D-material-organic interfaces,<sup>7,8</sup> 2D material heterostructures,<sup>3,6,9</sup> and mixed-dimensional complex structures.<sup>10</sup> Because it remains unrealistic to find a 2D material which can satisfy all the requirements concerning high-performance applications (e.g., electronic properties, mechanical strength, chemical stability and synthetic difficulty), the flexibility of combining 2D materials with existing functional materials through playing with the interactions at their heterointerfaces may offer opportunities to fully exploit the potential of 2D materials.

Molecular epitaxy refers to the process of growing crystalline materials over a substrate.<sup>11</sup> Within the scope of this review, we refer molecular epitaxy to the general concept of growing ordered and/or crystalline structures in various dimensions, adhering to the underlying 2D material. This concept is broader than the technique in semiconductor industry known as “molecular beam epitaxy” (MBE)<sup>11</sup>, which grows crystalline semiconducting epitaxial layer under high vacuum, since we cover various fabrication methods in this review. The molecular epitaxy on 2D material interfaces provides a mighty approach for fabricating 2D material-based heterostructures in various dimensions. Compared with the micro-mechanical assembly techniques mainly used to fabricate 2D stacked heterostructures, molecular epitaxy not only reduces the interfacial contamination, but also provides flexibility over the

choice of epitaxial molecules. By controlling the interfacial interactions, the epitaxy can vary from sub-monolayer assembly of organic molecules,<sup>12,13</sup> templated growth of 2D vertical heterostructures,<sup>4</sup> and 3D epitaxial crystals.<sup>10</sup> The versatility of molecular epitaxy on 2D material interfaces has led to research in both fundamental understanding and applications. Clearly, due to the ultrathickness of 2D materials, their interfacial molecular interactions may differ from that at the interfaces of their 3D counterparts.<sup>14</sup> In addition, the interfacial molecular interactions have already been demonstrated to be tunable by modulating the electronic states of 2D materials,<sup>15,16</sup> offering another dimension to modify the properties of the epitaxial structures. On the other hand, the epitaxial structure may in turn change the properties of 2D materials and therefore allows the integration of mixed-dimensional functional devices. In this sense, understanding the mechanism governing the molecular epitaxy on 2D materials is undoubtedly crucial for the design of novel 2D hybrid functional structures.

Since the first discovery of graphene more than a decade ago,<sup>17</sup> the family of inorganic 2D materials has largely extended, offering a wide spectrum of electronic properties, including insulating (e.g. hexagonal boron nitride (hBN)), semiconductors (e.g. transitional transition metal (Mo, W) dichalcogenides (TMDCs) and phosphorene), semimetals (e.g. graphene, silicene, germanene and borophene) and metallic or superconducting materials (e.g. dichalcogenides of Nb and Ta). Although recent advances of non-covalent and covalent organic 2D materials such as 2D polymers, 2D covalent- or metal-organic frameworks (2D COFs or MOFs) have shown promising approaches for synthesizing large library of 2D materials,<sup>18</sup> the molecular epitaxy-epitaxial behaviors on these materials are less understood. The focus of this article will be mainly on the molecular epitaxy at interfaces of graphene, hBN, TMDCs and phosphorene (see Figure 1), due to the fact that the synthesis methods for their large area crystalline films are better developed, such that these 2D materials can be supported by a large variety of substrates. As will be discussed in this review, the molecular epitaxy on 2D materials interfaces can be distinct from that on a metal surface, and even

the 3D counterparts. Important features of a 2D material interface include the reduced density of states and screening compared to that on a metal surface<sup>19</sup>. Due to the low 2D density of states, significant charge redistribution may be observed at the molecule-2D material interface. As a result of the reduced screening in 2D materials, the contribution of the substrate to the molecular epitaxy cannot be ignored. Moreover, the orientation and preferential binding sites of adsorbed molecules on a 2D material interface can be different from the that on a metal surface, due to the diverse geometry and atomic environment of 2D materials. The substrate effect may also cause different molecular epitaxy behavior on a 2D material interface, compared to that on its 3D counterpart. Moreover, the distinctions of lattice parameter, charge density, polarity and polarizability between different 2D materials also come into play. In this review, we will cover both the unicity of molecular epitaxy on 2D materials interfaces, as well as the diverse inter-species behaviors.

Molecular epitaxy on 2D material interfaces essentially involves a combination of interactions. As schematically illustrated in Figure 2, the interactions can be divided mainly into three categories: (i) the intermolecular interactions between the epitaxial molecules, (ii) the interactions between the epitaxial molecules and the 2D materials, and (iii) the interactions between the epitaxial molecules and the supporting substrate. Note that different from the molecular epitaxy on the bulk material surfaces, the substrate effect should be taken into account, due to the fact that the dispersion and long-range interactions from the substrate cannot be completely screened by the ultrathin 2D barrier.<sup>20-22</sup> The interplay between the interactions determines the packing and morphology of the molecular **epitaxy-epitaxial** structures. A general principle is that, when the interfacial interactions are weak, the **epitaxy-epitaxial** structures are consistent with their crystalline packing as the bulk form; on the other hand, with strong interactions at the 2D interfaces, the interfacial molecule packing and orientation can be greatly distinct from the bulk form, resulting in new epitaxial structures at such interfaces.<sup>23</sup> In that sense, the substrate which supports the 2D material acts as a control variable for engineering the interfacial molecular epitaxy, because: (i) the in-

teractions from the substrate can partially penetrate through the 2D material, and (ii) the underlying substrate can alter the electronic and geometric properties of the 2D material, such as doping and formation of moiré patterns and electronic corrugation, which further influences the molecule-2D material interactions.

Based on the fundamental knowledge of 2D materials and the interfacial molecular interactions, we believe that molecular epitaxy on 2D materials is a promising approach towards scalable 2D materials-based devices. In this article To obtain a comprehensive understanding of the mechanism and modulation of molecular epitaxy, we need to focus on the interfacial interactions. In Section 2, we first overview different types of provide an overview of different interactions involved in molecular epitaxy on 2D materials interfaces. We next In Section 3, we discuss the interplay of between molecular interactions by studying several multi-dimensional model systems. Finally, we review the applications based on the epitaxial heterostructures –in Section 4, as well as giving a summary concerning the challenges and opportunities of the researches in this field in Section 5. This review article is aimed to provide a general view of the 2D-interfacial molecular epitaxy and its design rules, complementary to several recent reviews that only briefly cover this topic.<sup>8,10,12,24</sup> As the review mainly focuses on the phenomenological theory, the discussion of fundamental physical and chemical properties of 2D materials, fabrication methods, applications and device performance are not extensively discussed here. We encourage the interested readers to refer to several other reviews covering these topics<sup>1,3,4,7,10,25</sup>.

## 2 Interactions Involving Molecular Epitaxy on 2D Materials

The concepts of interactions in the process of molecular epitaxy on 2D materials interfaces, can be learned from the field of epitaxy and self-assembly on bulk interfaces<sup>11,19,23,26</sup>. A molecule in the bulk form and on a densely-covered surface feels the interactions from the

other epitaxial molecules, known as the intermolecular interactions. On the other hand, a molecule undergoes various processes on a 2D surface, including adsorption, diffusion, rotation, and vibration, which is governed by the molecule-2D material interactions. Note that we will only discuss about the interactions at equilibrium. As discussed in the introduction, a unique property of the 2D material interface is the effect of the underlying substrate, where the molecule-substrate interactions come into play. In this section, we will introduce the diverse interactions of each type, and their role in the molecular epitaxy on 2D materials.

## 2.1 Intermolecular Interactions between Epitaxial Molecules

The

In this section, we discuss the intermolecular interactions ~~in this context refer to the intermolecular interactions~~ between the deposited molecules on 2D materials. The intermolecular interactions govern the epitaxial packing behavior several atoms away from the 2D material surface: the strength and the direction of intermolecular interactions determine the packing density as well as the orientation of the molecular epitaxy. Here we categorize the intermolecular interactions into van der Waals (vdW) interactions, hydrogen bonds, and covalent bonds.

### 2.1.1 van der Waals (vdW) Interactions

The van der Waals (vdW) interactions are dispersion forces between charge-neutral molecules. The interactions of many organic molecules belong to this category, such as fullerene C<sub>60</sub>,<sup>27–33</sup> metal-phthalocyanine (MPc),<sup>34–53</sup> pentacene,<sup>41,54–60,60–66</sup> perfluoropentacene,<sup>67,68</sup> rubrene,<sup>69</sup> perylene-3,4,9,10-tetracarboxylic dianhydride (PTCDA),<sup>70–76</sup> 7,7,8,8,-Tetracyanoquinodimethane (TCNQ) and its fluorinated derivative 2,3,5,6-Tetrafluoro-7,7,8,8-tetracyanoquinodimethane (F<sub>4</sub>-TCNQ),<sup>77–82,82–84</sup> and even crystalline polymers.<sup>85</sup> The molecule structures of C<sub>60</sub>, MPc, pentacene, perfluoropentacene, PTCDA, TCNQ and F<sub>4</sub>-TCNQ are shown in Figure 3, since they will be frequently discussed in this review.

Due to its non-directional and weak force nature, if the vdW interaction governs the molecular epitaxy (on weak interacting 2D interfaces), the molecules tends to form close-packed structures in 2D or 3D assemblies. The dimension of molecular epitaxy by vdW interactions is usually dependent on the surface coverage, as the molecule growth mechanism is similar to that of adsorption isotherm. Although the vdW interactions usually have an energy less than  $4 \text{ kJ}\cdot\text{mol}^{-1}$ , the collective interactions between molecules with large electron cloud can be stronger. For the  $\pi$ -conjugated aromatic molecules listed above, an effect known as the  $\pi$ - $\pi$  interaction, a combined effect of vdW interactions and charge transfer<sup>86</sup>, can lead to preferential stacking and orientation of the molecules, due to maximal overlapping of  $\pi$ -electron clouds.

### 2.1.2 Hydrogen Bonds (H-Bonds)

The hydrogen bond (H-bond) ~~provides directional forces between covalently bonded H atom and refers to the directional electrostatic forces between an H atom covalently-bonded to an atom of high electronegativity in adjacent molecules, (such as O, N and F) and another highly electronegative atom in adjacent molecules.~~ Different from the vdW interactions, hydrogen bonds usually have higher energy and preferred direction, which favors certain assembly structure on 2D materials. ~~Examples of molecular epitaxy by H-bond include The H-bonds are usually stronger than vdW interactions between molecules rich of N, O, F, such as modified PTCDA compounds,<sup>64,76</sup> perylene tetracarboxylic diimide (PTCDI),<sup>87,88</sup> carboxylic-substituted aromatic compounds,<sup>89,90</sup> polycyclic aromatic compounds<sup>91–93</sup> and phosphonic acid.<sup>94</sup> The existence of H-bond is shown to stabilize the assembled structures in low dimensions, such as linear supramolecular assemblies<sup>87</sup> or two-dimensional sheets.<sup>94</sup> It is also found that the specific adsorption sites on 2D materials (such as the moiré patterns) also play an important role in the assembly of H-bond-governed molecular epitaxy.~~

### 2.1.3 Covalent Bonds

Covalent bonds, including the metal coordination bonds, have also been demonstrated in the molecular epitaxy on 2D materials interfaces. In general, the interactions between the epitaxial molecules and 2D material (vdW and Coulombic interactions) are much weaker than the covalent bond, resulting in a large variety of epitaxial structures.<sup>95</sup> One example is the van der Waals epitaxy (vdWE) which allows 2D or 3D crystalline growth on 2D materials, regardless of the lattice mismatch between the two materials at the interface, as will be discussed in latter in Section 3.2.2. A number of 2D vertical heterostructures have been demonstrated by the vdWE approach, including (the former being the epitaxial layer): TMDC/graphene,<sup>96–105</sup> TMDC/hBN,<sup>106–109</sup> graphene/hBN,<sup>110–114</sup> and TMDC/TMDC<sup>115–120</sup> heterostructures. Moreover, the 2D epitaxial layer can also serve as template for ~~sequent~~ subsequent vdWE process, allowing the growth of multilayer 2D heterostructures on a large scale.<sup>101</sup> The vdWE has also been used to grow 3D heterostructures on mono- or multilayer 2D materials interfaces, by utilizing non-planar electron pairs, such as tetrahedral and octahedral orbitals. A variety of 3D inorganic materials have been shown the possibility to be grown on 2D materials, including dielectric Al<sub>2</sub>O<sub>3</sub>,<sup>121,122</sup> and HfO<sub>2</sub><sup>123</sup> by atomic layer deposition, semiconducting TiO<sub>2</sub> with various morphology (mesoporous, nanowire and nanowall),<sup>124–126</sup> ZnO on graphene,<sup>125,127</sup> ZnO on hBN,<sup>128</sup> GaN on graphene,<sup>129–133</sup> GaAs on graphene,<sup>133,134</sup> GaN on hBN<sup>135</sup> as well as CdS and CdTe on layered MoTe<sub>2</sub> or WTe<sub>2</sub>.<sup>136,137</sup>

Apart from the vdWE approach, covalently bonded structures can also be formed by on-surface chemical reactions and metal coordination bonds. Two-dimensional covalent organic frameworks (2D COFs), which are formed by linking monomers by boron ester or imine groups, have shown to be grown on graphene layer with highly ordered orientation,<sup>138–140</sup> by fine tuning the aromatic building blocks and bond formation process. Metal coordination bonding also shows the feasibility of making long-range ordered 2D<sup>141</sup> and 3D<sup>142</sup> structures on weakly interacting or functionalized 2D materials. The choice of the linker is crucial for

the formation of COF and MOF on 2D materials: planar sp<sub>2</sub>-type bonds such as boron ester, imine and square planar metal coordination are generally required for the formation of stable 2D epitaxial structure.

## 2.2 Interactions between Epitaxial Molecules and 2D Material

The interactions between the epitaxial molecules and 2D material determine the molecular packing behavior of the first few overayers. In addition, the interactions also have great impact on the molecular adsorption process, thereby influencing the heterogeneous nucleation characteristics. As discussed above, the interplay between the intermolecular and molecule-2D material interactions is the key factor in controlling the molecular epitaxial structure. Here we categorize the molecule-2D material interactions into weak (dispersion and electrostatic), charge-transfer interactions, site-specific adsorption, and covalent bond formation.

### 2.2.1 Weak Interactions

The weak molecule-2D material interactions involve the short-range dispersion (vdW) and long-range electrostatic (Coulombic) interactions. In the case of graphene, the delocalized  $\pi$ -electrons are the basis for the non-covalent interactions. A large variety of planar aromatic molecules, including PTCDA, PTCDI, C<sub>60</sub>, MPc are shown to assemble on graphene with their aromatic rings parallel to the graphene surface, in order to lower the adsorption energy by maximizing the  $\pi$ -electron overlapping. Such phenomenon is often termed as the  $\pi$ - $\pi$  interaction.<sup>143,144</sup> The  $\pi$ - $\pi$  interactions between graphene and aromatic  $\pi$ -conjugated molecules play a significant role in the orientation of planar organic molecules on graphene, which is also widely known as the graphene template effect.<sup>145</sup> MPc molecules (e.g. M=Cu, Fe, Co and AlCl) and substituted MPc (e.g. F<sub>16</sub>CuPc) are well known to form a “face-on” orientation on graphene interface, relative to the “edge-on” orientation that are usually found on the deposition of these molecules on amorphous substrates such as SiO<sub>2</sub> or glass.<sup>35,36,38,41,42,44,146,147</sup>

Similarly, the graphene-templated orientation of organic molecules have also been discovered for pentacene,<sup>54,58,62</sup> C<sub>60</sub>,<sup>31,148</sup> p-sexiphenyl (6P),<sup>149</sup> and dibenzotetrathienocoronene (DBTC)<sup>150</sup> molecules, revealing a general mechanism behind their assembly behavior.

Apart from graphene, the weak interactions on hBN and MoS<sub>2</sub> surfaces are also studied. The packing configuration of pentacene and perfluoropentacene on MoS<sub>2</sub> are studied through X-ray diffraction, near edge X-ray absorption fine structure (NEXAFS)<sup>59,68</sup> and atomic force microscopy (AFM).<sup>55</sup> A comparison between the packing configurations of the molecules on pristine MoS<sub>2</sub>, SiO<sub>2</sub>, and defective MoS<sub>2</sub> surfaces indicates that the growth of pentacene and perfluoropentacene on MoS<sub>2</sub> is also an epitaxial process. Theoretical calculations show that the molecule-MoS<sub>2</sub> interactions are also dependent on the MoS<sub>2</sub> phase: adsorbed pentacene molecules on the 2H-MoS<sub>2</sub> (hexagonal symmetry, semiconducting) is dominated by the weak interactions, while the charge-transfer interactions (see next section) between pentacene and 1T-MoS<sub>2</sub> (trigonal symmetry, metallic) turns out to be the major effect.<sup>56</sup> More detailed definition and characteristics of the 2H- and 1T- phases of MoS<sub>2</sub> can be found in Ref. 151. The results show that although the dipole intensity of MoS<sub>2</sub> is larger than graphene, its 2D interface is still of weakly interactive nature, which can be also revealed from recent theoretical studies on the wettability of monolayer MoS<sub>2</sub>.<sup>152</sup> 6P molecules on hBN also exhibits a “face on” configuration,<sup>153</sup> similar to that observed in its molecular epitaxy on graphene. Moreover, in the case of rubrene on hBN, due to the non-planar structure of rubrene,<sup>69</sup> the “edge-on” configuration is more predominant than the “face-on” configuration, reflecting the fact that the molecule-hBN interaction is weakly dispersive. The vdW interaction is also found to lower the binding energy in the rubrene-hBN system.

Another important feature of 2D materials is their low quantum capacitance nature due to low density of states (DOS) near the intrinsic Fermi level,<sup>5,154</sup> which enables practical doping by either substrate-2D material interaction<sup>155–157</sup> or by an electric displacement field.<sup>158,159</sup> Recent atomistic simulation and scanning tunneling microscopy studies<sup>15,16</sup> indicate that the vdW interaction between the 2D material and epitaxial molecule can be tuned by the doping

density of graphene (Figure 4(a) and 4(b)). In principle, the doping of 2D materials may also influence the electrostatic interactions with the molecules above, as supported by the studies of doping-induced wettability change of 2D materials.<sup>160–163</sup>

### 2.2.2 Charge-Transfer Interactions

The charge-transfer (CT) interactions, or the donor-acceptor (DA) interactions, refer to the process that electrons undergo redistribution between the epitaxial molecules and the underlying 2D material. Due to the locally enhanced carrier density in the formed CT complex, the CT interactions tend to be stronger than the dispersion and electrostatic interactions. The formation of a CT heterostructure requires alignment of the energy levels between the 2D material and the overlayer molecules.<sup>164</sup> The CT interactions may change the electronic structure of the 2D material through non-covalent interactions, which have benefited the electronic modification of 2D materials.<sup>144,165,166</sup> 7,7,8,8,-Tetracyanoquinodimethane (TCNQ) and its fluorinated derivative 2,3,5,6-Tetrafluoro-7,7,8,8-tetracyanoquinodimethane ( $F_4$ -TCNQ) tend to form CT complexes with graphene,<sup>77,78</sup> with a degree of charge transfer of  $\sim 0.3\text{ e}$  for TCNQ and  $\sim 0.4\text{ e}$  for  $F_4$ -TCNQ.<sup>79</sup> Molecular assembly of  $F_4$ -TCNQ on epitaxial graphene is shown to be determined by the moiré pattern, while the assembled TCNQ molecules exhibit close-packed geometry,<sup>79</sup> indicating that the molecular-2D material interaction becomes predominant, when the degree of charge transfer increases. More interestingly,  $F_4$ -TCNQ exhibits an “edge-on” orientation on graphene, with the electron-withdrawing C  $\equiv$  N groups adjacent to graphene,<sup>167</sup> which supports the existence of strong interacting CT complex, overwhelming the  $\pi$ - $\pi$  interactions. Since the charge transfer may occur when the HOMO and LUMO energy levels of the epitaxial molecule and 2D material match, it is also expected to play a role in the molecular epitaxy on 2D semiconductors, such as TMDCs. Density functional theory (DFT) studies reveal that pentacene adsorbed on 1T-type monolayer MoS<sub>2</sub> has a large degree of charge transfer ranging from 0.44-0.87 e, and in turn changes the Fermi energy level of MoS<sub>2</sub> by up to 1 eV.<sup>56</sup> Similarly, the interface

between C<sub>60</sub> and MoS<sub>2</sub> is found to be a pn-junction, with charge depleted at the bottom of the C<sub>60</sub> and accumulated at the interface.<sup>32</sup> On the other hand, the tendency of forming CT-induced orientation is attenuated on bulk MoS<sub>2</sub> crystal,<sup>168</sup> due to an increase of the quantum capacitance compared with its monolayer counterpart. Theoretical studies also disclose strong CT between phosphorene and electron-donating tetrathiafulvalene (TTF), as well as electron-accepting TCNQ molecules.<sup>169</sup>

### 2.2.3 Site-Specific Adsorption

The electronic and geometric properties of a 2D material are known to be influenced by its ~~underneath~~underlying substrate. When there is a lattice mismatch between the 2D material and the substrate, a long-range periodic superposition known as moiré pattern forms, as has been found in the case of graphene/metal<sup>170</sup> (Figure 5(a)) and hBN/metal<sup>171</sup> (Figure 5(b)). The moiré pattern does not only cause a geometric interference, but indeed changes the local electronic ~~state and~~ structure of the 2D material. Although structural corrugation up to 1 Å exists in the moiré patterns formed on strongly interacting surfaces, we still regard the system as a 2D material due to the confined thickness. In the case of graphene sitting on a metal surface, a longer carbon-metal distance than average was found to be formed when a metal atom rests under the center of the carbon ring (the “hill” or top region). The regions with a lower carbon-metal distance (“valley” regions) can be further categorized to the face-centered cubic (fcc) and hexagonal close-packed (hcp) sites. In the hBN/metal system, due to the ~~weak~~weakly interaction nature of hBN, there are pore sites where the average metal-2D material distance is reduced, when the strongly interacting N atoms sit on top of metal atoms. The edges that connect the pore regions in hBN/metal are referred to the “wire” regions. The height difference within the graphene or hBN layer can be used to quantify the degree of metal-2D material interaction strength. The weakly interacting surfaces include graphene/Ir(111),<sup>170,172,173</sup> graphene/Pt(111),<sup>174</sup> hBN/Ir(111),<sup>171</sup> hBN/Pt(111),<sup>175</sup> hBN/Cu(111),<sup>176</sup> in which the average 2D material-metal distance is com-

parable with that in the bulk material (3.3~3.4 Å) and the corrugation in the 2D layer is typically small (<0.5 Å). The strongly interacting surfaces including graphene/Ru(0001),<sup>177</sup> graphene/Rh(111),<sup>178</sup> hBN/Ru(0001),<sup>178</sup> and hBN/Rh(111),<sup>179</sup> in which the height corrugation in the 2D layer can be as large as 1 Å, and the electronic fluctuation can be up to 0.5 eV. In the strongly interacting systems, the moiré pattern creates a local difference in the adsorption potential, which in turn results in site-specific adsorption of small molecules on these surfaces. The site-specific adsorption behavior has been observed in a variety of organic semiconductor molecules deposited on the graphene/Ru(0001) surface, including MPc (M=Fe, Ni, Zn, Mn),<sup>41,43,180</sup> pentacene,<sup>41,58</sup> C<sub>60</sub>,<sup>28,29</sup> PTCDA,<sup>92,181</sup> TCNQ.<sup>81,82</sup> Similar behavior has also been found on the surface of hBN/Ru(0001) for MPc (M=H<sub>2</sub>, Cu, Co),<sup>179,182,183</sup> TCNQ,<sup>184</sup> and C<sub>60</sub>.<sup>27</sup> The molecules on the strongly interacting surfaces prefer to first adsorb on the sites with a lower adsorption energy, such as the hcp and fcc sites on the graphene/Ru(0001) surface, and the pore regions in the hBN/Ru(0001) surface. Adsorption onto ~~The~~the sites with a higher energy, e.g., the top regions of the graphene/Ru(0001) surface, may occur after the lower-energy sites are fully occupied. Therefore under a low coverage, the molecules adsorbed on the strongly interacting moiré pattern typically show ordered sub-2D assembly, composed of the molecules trapped at the specific sites.

Recently, more experimental and theoretical studies have also demonstrated the moiré pattern formation on TMDC/metal,<sup>157,185,186</sup> TMDC/TMDC,<sup>115,116,120,187,188</sup> and TMDC/hBN<sup>188</sup> surfaces. Following the discussion of the strongly interacting surface of graphene/Ru(0001), it is believed that the moiré pattern formed between the strongly coupled layers, e.g. TMDC/Ru(0001)<sup>157</sup> and TMDC/TMDC<sup>188</sup> heterostructures may also lead to the site-specific adsorption phenomenon,<sup>116</sup> in contrast to the close-packing structure formed on the weakly interacting surfaces, as discussed in the previous section.

#### 2.2.4 Covalent Bonds

Covalent bonds formed perpendicular to the 2D material plane open an opportunity for functionalizing 2D materials and provide anchor sites for post-modification. Compared with the vdWE approach, chemical modification of 2D material is less used for growing epitaxy structures, due to a relatively limited choice of chemical reactions available and the potential structural destruction during modification. It is also noteworthy that heteroepitaxy based on covalent bonds on 2D material is almost impossible, because the 2D basal structure is destroyed by the geometric change of the molecular orbital (e.g. planar  $sp^2$  to tetrahedral  $sp^3$  in graphene). ~~Indeed, covalent modifications with sparse sites distribution on~~ ~~Although the covalent molecule-2D bonding is less relevant to the content of this review since we mainly focus on the non-covalent epitaxy, there are several examples which binds the epitaxial layer to the~~ 2D materials have been shown to change their electronic properties. The attachment of  $\pi$ -conjugated structures can also be employed in the covalent modification of graphene, due to the large electron cloud material covalently, and showing the potential of tuning the electronic properties of the 2D materials<sup>189–194</sup>. The chemical grafting of graphene mainly involves free-radical reaction, using 2,2,6,6-tetramethyl-1-piperridinyloxy (TEMPO),<sup>190</sup> 4-amino-2,2,6,6-tetramethyl-1-piperridinyloxy (amino-TEMPO),<sup>195</sup> and 4-nitrophenyldiazonium salt (NPD) derivatives.<sup>142,191,196–198</sup> ~~The work function of graphene is found to be changed by the density of aryl substitution sites, which enables stable modification of its electronic properties.~~ More interestingly, a “Janus” functionalized graphene can be realized by the covalent modification on both sides of a free-standing graphene sheet,<sup>191</sup> demonstrating the potential of asymmetric fabrication of complex 2D functional materials. ~~From the classical chemical reaction model, the reaction rate between NPD and graphene can be modeled by the overlap of DOS between the LUMO of NPD and the Fermi level graphene.~~ A ~~The~~ low DOS in a 2D materials further makes it possible to fine-tune the interfacial chemical reaction rate by the doping density of 2D materials, for instance through the substrate doping of graphene.<sup>198</sup> Several approaches have also show the pos-

sibility of functionalizing other 2D materials, including nucleophilic substitution between anionized TMDCs and organohalides<sup>193</sup> and aryl diazonium salts.<sup>199</sup> The functional groups on 2D materials may further serve as anchoring sites for chain-reaction,<sup>197</sup> MOF growth,<sup>142</sup> and functionalization of bioactive molecules.<sup>198</sup> ~~It is expected that further Future~~ advance of covalently modified 2D materials with site-specific and programmable chemical functionalization ~~will~~may combine the 2D with the 3D materials in a controllable manner.

### 2.3 Interactions between Epitaxial Molecules and Substrate

One of the major differences of the molecular epitaxy on 2D materials compared with that on the bulk materials is that the interactions from the underlying substrate is not fully screened by the atomically thin 2D barrier. Note that this phenomenon is distinguished from the effect of strongly interacting surface or substrate doping, with the latter two referring to the change of 2D material's electronic and geometric properties, which then influence the molecule-2D material interactions. The penetration of the molecule-substrate interactions through monolayer 2D material is first observed in the experiments of wettability of substrate-supported graphene: the water contact angle of water on graphene is found to be influenced by the vdW force between the water molecules and the substrate, known as the wetting "transparency" or "translucency" of graphene.<sup>20-22</sup> The transparency can be even pronounced for electrostatic interactions, which has longer length scale than the vdW force.<sup>148,200</sup>

Recent studies have extended the concept of the molecule-substrate interactions to the topic covered in this review. The influence of the molecule-substrate interactions on molecular epitaxy can be examined indirectly via changing the layer number of 2D materials, due to the fact that the interactions decay drastically by increasing the interaction distance. Kratzer et al. reported that the morphology of the 6P molecules deposited on SiO<sub>2</sub>-supported graphene shows layer-dependent morphology.<sup>201</sup> The needle-like crystalline structures of 6P deposited on graphene/SiO<sub>2</sub> underwent morphological change by increasing graphene layer

number increasing from 1 to 4. No further change of morphology was observed after more than 5 layers (Figure 6(a)). The author attributed the layer-dependent morphology change to the dewetting caused by increasing the number of graphene layers, which corresponds well with the decay of the vdW interaction between the 6P molecule and the SiO<sub>2</sub> surface as a function of graphene layers. Similarly, Chhikara et al also reported the layer-dependent morphology change of pentacene layer deposited on graphene/SiO<sub>2</sub>,<sup>65</sup> with the domain size of pentacene on single layer graphene (SLG) larger than that on bilayer graphene (BLG), and a lower activation energy on SLG. Direct evidence of the molecule-substrate interaction is also revealed by the comparison between different substrates. Nguyen et al. showed that the chemical composition and wettability of the substrate surface has an impact on the morphology of pentacene molecules deposited on the supported graphene film.<sup>63</sup> On graphene supported by the hydrophobic SiO<sub>2</sub> substrate with an alkyl self-assembled monolayer (SAM), the domain size of the pentacene film increases compares to that on graphene supported by pristine SiO<sub>2</sub>, and the pentacene molecules are mainly packed with the “face-on” orientation. On the contrary, on graphene supported by ozone-plasma-treated SiO<sub>2</sub>, the domain size of pentacene decreases and the percentage of standing orientation of pentacene increases (see Figure 6(b)). Recently the vdW transparency of graphene has also been employed in the remote vdWE of GaAs on graphene/GaAs substrate.<sup>133</sup> Kim et al. showed that the strong interactions between the Ga-As and As-As atoms can penetrate through a gap of up to 9 Å, which is essentially larger than the thickness of graphene (Figure 6(c)). As a result the vdW interaction of the GaAs substrate is not fully screened by the graphene layer on the top, and highly crystalline GaAs film can be grown following the underlying GaAs orientation (Figure 6(d)). In addition to the vdW and Coulombic interactions, graphene layer is also found to be transparent to the charge transfer process.<sup>202</sup> The reduction rate of AuCl<sub>4</sub><sup>-</sup> on graphene surface are found to be faster when graphene is coated on a reductive surface, such as Al, Ge and Cu surfaces. Due to the fact that the intrinsic Fermi level of graphene (-4.6 eV) is higher than that of Cu (-4.8 eV) while the reduction rate is even lower, such phenomenon

cannot be solely ascribed to the substrate doping of graphene. DFT calculations reveal the depletion of charges in the Al supporting layer and accumulation near the  $\text{AuCl}_4^-$  ion across the graphene membrane, while the charge density in graphene is negligible compared with graphene supported by  $\text{SiO}_2$ , implying that the charge transfer interaction can also penetrate through the graphene layer. Recently, the modulation of molecule-substrate interactions has also been used for controlled add-layer growth<sup>203–205</sup> and modulation of optical properties on vdW interfaces<sup>206</sup>.

Note that although the molecule-substrate interaction has an impact on the molecular epitaxy on 2D materials, the following conditions have to be satisfied for observing the phenomenon experimentally. First, the interaction strength between the epitaxial molecules and the substrate is comparable with the molecule-2D material and intermolecular interactions. In addition, the molecule-substrate distance should be sufficiently small to allow the penetration of short-range vdW and charge-transfer interactions, requiring high degree of surface cleanliness in fabrication and precise control over surface wrinkle and overlayers. We believe the molecule-substrate interaction is universal but may be negligible in some systems, in which the molecule-substrate interactions may be screened by 2D materials.<sup>30,207–210</sup> By replacing graphene with TMDC, the molecule-substrate distance increases, which causes greatly-attenuated molecule-substrate interaction at both nano- to micro- length scale<sup>208,209</sup> and macroscopic scale.<sup>210</sup> In order to precisely determine the contribution of molecule-substrate interactions experimentally, one needs to decouple it from the substrate-induced doping effect of 2D materials, which may also change the molecule-2D material interaction, as addressed earlier.<sup>15,16,162,163</sup>

## 2.4 Summary

To obtain a clear view of the interactions involved in the molecular epitaxy on 2D materials interfaces, we have summarized the major forms of interactions and their energy range in Table 1. As can be seen, both strong interactions ( $> 100 \text{ kJ}\cdot\text{mol}^{-1}$  for covalent bonds,

metal-coordination and some hydrogen bonds), and weak interactions ( $< 50 \text{ kJ}\cdot\text{mol}^{-1}$  vdW and  $\pi-\pi$  interactions) exist between the epitaxial molecules and at the molecule-2D material interface. On the other hand, the molecule-substrate interactions mainly have a weak nature, and relatively weaker than the intermolecular and molecule-2D weak interactions due to the increasing of molecule-substrate distance.

Table 1: Types of interfacial interactions involved in the molecular epitaxy on 2D materials interfaces, showing the typical forms of interaction and energy range.

Type of Interfacial Interaction	Form of Interaction	Typical Energy Range ( $\text{kJ}\cdot\text{mol}^{-1}$ )
Intermolecular	van der Waals	$\leq 5$
	$\pi - \pi$	$\leq 50$
	H-bonds	4 - 120 <sup>211</sup>
	Covalent Bonds	100 - 400
Molecule-2D	Weak Interactions	10 - 60 <sup>212</sup>
	Charge-Transfer	50 - 200
	Site-Specific Adsorption	30 - 100
	Covalent Bonds	100 - 400
Molecule-Substrate	Weak Interactions	$\leq 20$

We would like to point out that the interactions discussed here are at the molecular level and represent the nanoscale properties of the epitaxial system. The macroscopic properties, such as the morphology, density and domain size of the epitaxial structures, do not solely depend on single type of interaction. Some macroscopic properties, such as the surface energy, as a combined effect of the interactions discussed here, are used more frequently to describe the macroscopic behavior. We will cover this topic in Section 3 when discussing the 3D epitaxy.

### 3 Molecular Epitaxy of Different Dimensions

As shown in the previous section, the molecular epitaxy on 2D materials is controlled by a variety of interactions, which essentially dominate the epitaxial structure of the first few monolayers. Various growth methods are considered in this section, including thermal evaporation deposition of small molecules, gas phase chemical vapor deposition of 2D heterostructures, and liquid phase nucleation. Upon thin film growth, the morphology of the grown structure can range from 0D to 3D, depending on the interfacial interactions. Various characterization techniques are involved. For 0D-1D assemblies, the ordering is mainly characterized by scanning tunneling microscopy (STM). On the other hand, for 2D and 3D assemblies, the morphology and thickness are mainly revealed by scanning electron microscopy (SEM), transmission electron microscopy (TEM) and atomic force microscopy (AFM). The packing and orientation information of the epitaxial structure are generally measured by X-ray diffraction techniques, in particular grazing X-ray incidence diffraction (GIXD). Understanding the role of different interactions and their interplay in multi-dimensional molecular epitaxial structure is important for tailoring 2D material-based heterostructures. In this section, we review several model systems of different dimensions, with the focus on how the interactions determine the morphological dimension. Note that here we discuss the dimension of the epitaxial structure, rather than the dimension of epitaxial molecules in some other studies.<sup>10</sup>

#### 3.1 **Sub-2D Sub-monolayer Assembly**

We refer the **sub-2D sub-monolayer** assembly on 2D material to the formation of discrete 0D clusters, 1D nanowires or incomplete 2D assembly such as porous and network structures. Note that several prerequisites exist for the formation of sub-2D assembly on a 2D material surface. First, the surface coverage should be less than 1 monolayer (ML), as determined by the surface adsorption mechanism. Subsequently, in the assembled structures, one or more

preferred interactions must dominate the sub-2D structure. Molecular dynamics (MD) simulations have shown that the weak intermolecular and molecule-2D interactions alone, do not result in the formation of ~~sub-2D~~sub-monolayer assembly, such as the case of pentacene and PTCDA on graphene or hBN,<sup>213</sup> and organic semiconductor molecules dominated by vdW force on phosphorene.<sup>214</sup> Even when the starting configuration of the adsorbed molecules on 2D material is less than 1 ML, due to a low energy barrier of on-plane diffusion and non-directional nature of the vdW and Coulombic interactions, the epitaxial molecules always thermodynamically favor to form ordered 2D assemblies. In order to form sub-2D assembly, either a higher diffusion barrier has to be created, or the intermolecular interactions are sufficiently strong to stabilize the low dimensional structure.

### 3.1.1 0D Assembly

To form 0D clusters distributed on 2D materials during molecular epitaxy, specific adsorption sites have to trap the molecules coming to the 2D interface. The moiré pattern formed in the graphene/metal and hBN/metal surfaces are shown to be able to trap metal clusters<sup>215–221</sup> and individual organic semiconductor molecules.<sup>29,92,179,184,222</sup> N'Diaye et al. studied the deposition of Ir on epitaxial graphene/Ir(111) surface.<sup>223</sup> The preferred nucleation sites for Ir atoms were found to be the hcp sites of the moiré pattern. Isolated Ir clusters in a hexagonal arrangement were found on the graphene surface with a coverage less than 0.8 ML (see Figure 7(a)). Sicot et al. reported similar findings for Ni clusters on graphene/Ru(0001) surface,<sup>219</sup> while the Ni clusters preferred to nucleate in the fcc regions of the moiré pattern. Accordingly, Ni clusters of up to 3.1 nm in diameter were created with a surface coverage of 0.25 ML. Goriachko et al. studied the deposition of Au on strongly interacting hBN/Ru(0001) surface, and found that at a low surface coverage of Au (< 0.3 ML), the nucleation of Au almost exclusively occurs in the pore sites, where there are stronger hBN-Ru interactions and a shorter hBN-Ru distance,<sup>215,216</sup> resulting in isolated Au nanoclusters after annealing (Figure 7(b)). Further increase of Au coverage resulted in 2D islands, followed by multilayer

formation, indicating the Au-Au interaction overwhelms the effect of local trapping. The mechanism of the selective nucleation of metal clusters on graphene/metal and hBN/metal surfaces were also investigated by first principles calculations.<sup>220,221</sup> Wang et al. compared the adsorption energy between different sites on these surfaces.<sup>220</sup> The adsorption energy of Au on the hill and valley regions of graphene/Ru(0001) surface reaches 1.1 eV, with the adsorption on the hcp regions more preferred over the FCC region by 0.2 eV. On the contrary, the valley in graphene/Rh(111) surface provides a considerably high adsorption energy drop up to 1.0 eV while the fcc region is more favorable for nucleation with an energy preference of 0.3 eV compared to the hcp region. Similarly the valley regions in the hBN/Ru(0001) surface provides an energy decrease of 1.2 eV for Au nucleation. Zhang et al. further demonstrated that the strong sp<sup>3</sup> hybridization of the graphene/metal surface and the partially occupied HOMO orbital of the adsorbate are responsible for the formation of dispersion of metal clusters on the 2D interface.

The moiré pattern of 2D/metal surface can also be used for trapping of organic semiconductor molecules to form isolated 0D clusters. The preference of adsorption in the valley regions of the moiré pattern leads to isolation of individual molecules at the 2D plane, thereby screening the intermolecular interactions. Dil et al. first observed the trapping of CuPc molecules on the hBN/Ru(111) surface.<sup>179</sup> The CuPc molecules at a very low surface coverage were found to adsorb specifically near the rim of the 2-nm-diameter BN nanomesh, as confirmed by the emission spectra of the Xe atoms on the hBN/Rh(111). Similar results have also been demonstrated in the off-center adsorption on the hBN nanomesh, including CoPc on hBN/Ir(111),<sup>183</sup> H<sub>2</sub>Pc and CuPc on hBN/Rh(111) surface<sup>52</sup> (see Figure 7(c)). A maximum potential gradient of ~10<sup>9</sup> V/m on the hBN nanomesh has been found near the edge of the pore, revealing the mechanism for site-specific trapping of individual molecules on hBN/metal surfaces. The concept of using the moiré pattern on graphene/metal surface has been used for trapping other small molecules. Lu et al. revealed that the adsorption energy of C<sub>60</sub> on the HCP region of the graphene/Ru(0001) surface is lower than that

on the TOP region by  $\sim$ 160 meV.<sup>29</sup> The energy difference allows to trap C<sub>60</sub> molecules in the valley regions of the graphene moiré pattern at room temperature (Figure 7(d)). The highly-ordered trapped C<sub>60</sub> molecules serve as nucleation sites for later C<sub>60</sub> epitaxy, leading to dendritic growth of the C<sub>60</sub> islands with inherited corrugation morphology from the underlying graphene moiré pattern. The isolation of single molecules using graphene moiré pattern has also been demonstrated for FePc,<sup>41</sup> and TCNQ<sup>82</sup> molecules. It is also found that the site-specific isolation of small molecules is not limited to strongly interacting surfaces such as graphene and hBN supported by Ru or Rh, but also weakly interacting surfaces like hBN/Cu(111) with a small degree of corrugation but strong electronic patterning,<sup>176,184</sup> Joshi et al. showed that the work function difference between the hill and valley regions of the hBN/Cu surface reaches up to 0.3 V.<sup>176</sup> The local work function difference of the moiré pattern, or surface potential was found to locally trap the free-base porphine (2H-P) on the hill regions, distinct from those trapped in the valley regions on the strongly-interacting hBN/metal surfaces.<sup>52,179,183</sup> The trapped 2H-P molecules form isolated clusters as large as 18 molecules, which significantly differed from the observations on hBN/Ru surface. The reduced molecule-substrate electronic coupling refers to the hill-preferred adsorption which results in the formation of small molecule clusters. TCNQ molecules are also found to form individual clusters on the hBN/Cu surfaces,<sup>184</sup> suggesting the electronic nature behind such phenomenon.

### 3.1.2 1D and Fractal Assembly

With increasing surface coverage or introducing directional intermolecular interactions, 1D and fractal (with fractal dimension between 1 and 2) assemblies may be formed on 2D material interfaces, in the form of nanowires, nanoporous and network structures. Note that we categorize the formation of incomplete 2D assembly as sub-2D assembly, due to the fact that the interactions behind these assembly forms are essentially different from the close packing 2D assembly.

As we discussed earlier, the strongly interacting surfaces, including graphene/Ru(0001), graphene/Rh(111) and hBN/Ru(0001) result in the moiré pattern that serves as specific binding sites for trapping small molecules at low surface coverage. By increasing the surface coverage, the specifically adsorbed molecules further act as nucleation sites for subsequent epitaxial growth. Due to the existence of local energy barrier, adsorption on the sites with a high energy would not be covered until the low-energy sites are fully-occupied. The intermolecular interactions, in combination with the geometry of moiré pattern, result in a specific arrangement of the molecules on the surface, varying from nanowire, nanorope to Kagome lattice [—\(a form of trihexagonal tilting, see Ref. 224\)](#). In the case of Ref. 41, when the coverage of FePc on Gr/Ru(0001) increases, the assembled structure changed from 0D isolated molecules to hexagonal ring-like structure, and finally to a Kagome lattice, at the coverage of 0.75 ML.<sup>180</sup> The top sites remain unoccupied at this stage, in good agreement with the calculated site-specific adsorption energy profile. Similarly, ~~epitaxy~~[epitaxial](#) growth of TCNQ molecules on graphene/Ru(0001) also shows a transition from isolated clusters at 0.3 ML to Kagome lattice at 0.6 ML<sup>82</sup> (see Figure 8(a)). Note that the clusters still form at a relatively higher coverage compared to other molecules on graphene, such as MPc, possibly due to a strong charge-transfer interaction between TCNQ and graphene. On the other hand, increasing molecular coverage on the strongly interacting hBN/metal surfaces didn't show apparent formation of Kagome lattice,<sup>52,171,183,184</sup> due to the different surface potential distribution compared with the moiré pattern of graphene. Bazarnik et al. further showed that sub-ML epitaxy of MPc molecules on graphene/Ir(111) surface is tunable by Fe- or Co- intercalation sites below the graphene layer.<sup>51,225</sup> For example, the close-packed assembly of MPc molecules on weakly interacting graphene/Ir surface completely changes to one-dimensional chain growth, honeycomb, or Kagome lattice for CuPc and CoPc molecules, when Fe or Co atoms were intercalated between graphene and Ir substrate. The increased corrugation caused by intercalation atoms was found to be the mechanism responsible for the change of epitaxial structure. The influence of the intercalated metal atoms can be regarded

as the molecule-substrate interaction, which indirectly affect the surface potential of the 2D material.

In addition to the epitaxial behavior induced by the specific adsorption site on 2D materials, a rich set of sub-2D assembled structures can be obtained by tailoring the intermolecular and molecule-substrate interactions. The concept of 2D supramolecular self-assembly<sup>26,226</sup> which was previously extensively studied on bulk surfaces, such as metal and highly oriented pyrolytic graphite (HOPG), has been shown to be also extendable under the scope of 2D materials, yielding a broad possibility for fabricating hybrid function 2D heterostructures. Intermolecular hydrogen bonding is widely used to guide the orientation of surface-assisted self-assemblies,<sup>227</sup> due to its relatively high strength. In addition, in a hydrogen-bond-bounded self-assembled structure, the interactions perpendicular to the surface is usually weak, thereby reducing the molecular epitaxy in the vertical direction. Pollard et al. first studied the assembly of PTCDI derivatives on graphene/Rh(111) surface.<sup>87</sup> It is found that the PTCDI molecules packed into discrete linear assemblies, distinct from those grown on highly oriented pyrolytic graphite (HOPG) surface, in which HOPG surface, where the PTCDI molecules form the close-packed structures. The graphene-substrate superlattice was found to be responsible for this phenomenon, by offering local binding sites for the PTCDI molecules, followed by directional growth mediated by the intermolecular hydrogen bonds. PTCDI derivatives with alkyl side chains exhibit stronger network and Kagome-like structures, as a result of increases side-to-side intermolecular interaction.<sup>87</sup> Other complex supramolecular assemblies were also found on strongly interacting graphene/metal surface, by tailoring the molecular orientation and number of hydrogen bonds. On graphene/Ru(0001) surface, supramolecular assembly of two specific molecules, 2,4'-bis(terpyridine) (2,4'-BTP) and 3,3'-bis(terpyridine) (3,3'-BTP) which possess nearly identical backbone and geometry but different pyridine substitution sites, is a good example demonstrating the impact of the hydrogen bond orientation on molecular assembly<sup>92,93,222</sup> (see Figure 8(b)). The C-H ... N hydrogen bonds formed between 3,3'-BTP molecules were

found to allow the molecules to pack with a larger rotation angle than 2,4'-BTP. Clearly, the ~~he~~-minor change in the functional group exhibited great influence on the assembled morphology. The 3,3'-BTP molecules assembled in a curved fashion, forming nanoropes with triangle or hexagonal shape around the top regions of the graphene moiré pattern.<sup>92</sup> On the other hand, molecular packing of 2,4'-BTP forms linear assemblies connecting the valley regions.<sup>222</sup> It appears that in this case, the strong intermolecular hydrogen bonds dominate the molecular assembly, even on the surface with site-specific molecule-2D material interactions. 2D growth of deposited molecules can also be facilitated with heteromolecular hydrogen bonds. Pioneer work of Theobald et al. showed that triple hydrogen bonds between PTCDI and melamine could form highly ordered 2D epitaxy with Kagome lattice structure on metal surface<sup>228</sup>. The same idea can also be applied to the the molecular epitaxy on 2D materials. Karmel et al. demonstrated the formation of a periodic nanoporous network by the triple hydrogen bonds formed between PTCDI and melamine molecules on epitaxial graphene/SiC.<sup>64</sup> On the weakly interacting graphene/SiC surface, the triple hydrogen bonds formed between PTCDI and melamine molecules show good lattice match, resulting in a hexagonal nanoporous network with a lateral lattice parameter of 3.45 nm, and each node comprised of one melamine molecule connected three PTCDI separated by 120<sup>deg</sup>. Due to a lack of intermolecular hydrogen bonds between PTCDI molecules, the epitaxial structure for the molecules alone show close-packed behavior.<sup>88</sup> Interestingly, although the molecule-2D material interactions are weaker than the multivalent hydrogen bonds, the hexagonal network was found to maintain the same orientation uniformly, indicating the weak interactions are sufficient to keep the epitaxial layer in registry with the 2D material lattice.

In addition to hydrogen bond, several other interactions were also found to facilitate the stabilization of sub-2D assemblies on 2D materials. The interactions between long alkyl chains are known to favor the formation of highly crystalline epitaxial structures.<sup>226</sup> Molecules with long alkyl chain, including 10,12-pentacosadiynoic acid (PCDA),<sup>229</sup> phosphonic acid,<sup>94</sup> dehydrobenzo[12]annulene (DBA) and lauroyl peroxide<sup>230</sup> were found to form

ordered nanowire to porous network structures on graphene and MoS<sub>2</sub> surfaces. The assembly of DBA molecules on graphene/SiC is shown in Figure 8(c). In these examples the close-packed long alkyl chains were found to stabilize the structure. By proper chain length design, herringbone<sup>229</sup> and nanoporous network with tunable diameter<sup>231</sup> were reported. Covalent and metal coordination bonds were also shown for constructing sub-2D assembly on 2D materials. Successful examples include COF on graphene connected by boronate ester<sup>138,139</sup> and imine coupling,<sup>140</sup> as well as MOF on hBN by on-surface chelation between free porphyrin and Co.<sup>141</sup> A variety of examples have also shown the importance of molecule-2D material interaction. The orientation of the nanoporous network formed in Ref. 64,138 was found to be in line with the lattice of graphene. On the other hand, the assemblies on MoS<sub>2</sub><sup>230</sup> and other polar substrates (e.g. mica, SiO<sub>2</sub>)<sup>64,229,230</sup> lose the orientation or even fail to form ordered structure. The above examples clearly show that the  $\pi$ - $\pi$  interactions and collective dispersion are critical for stabilizing the aromatic molecules on the 2D interface, while increasing dipole and Coulombic interactions decrease the stability of such assembly.

## 3.2 2D Assembly

In principle, under sub-ML coverage, when the diffusion of molecules on 2D material is not limited by interfacial traps, close-packed 2D assembly can be formed in molecular epitaxy. The molecular epitaxy with 2D assembled structures can be categorized into two classes, namely the self-assembled small organic molecules on 2D material, and the 2D heterostructures grown by vdWE.

### 3.2.1 Monolayer Self-Assembly of Small Molecules

The assembly of small molecules on 2D materials with low geometric and electronic corrugation have usually been found to form close-packed structures. Molecular dynamics (MD) simulations is a good tool to rationalize the role of intermolecular, molecule-2D material and molecule-substrate interactions. Zhao et al. studied the self-assembly of non-polar pentacene

and polar PTCDA molecules on planar graphene and hBN.<sup>213</sup> Starting from a disordered state with sub-ML adsorption, both pentacene and PTCDA molecules ended up in forming an ordered 2D assembled structure, within the timescale of 100 ns. Subsequent adsorption of molecules was found to fill the gaps in the assembled structures within 1 ns, regardless of the initial orientation. For non-polar pentacene, the intermolecular vdW interactions which decreased dominate structure, while the Coulombic interactions, on the other hand, have much less effect on the packing. However both the Coulombic and vdW interactions were found to play important roles in stabilizing the epitaxy structure of PTCDA. The molecule-2D material interactions determine the orientation of the interfacial molecules. Decreasing the pentacene-graphene potential to half of its optimized force field value changed the packing of pentacene molecules from the face-on to edge-on configuration (see Figure 9). Using a similar approach, Mukhopadhyay et al. studied the interactions involved in the self-assembly of various small organic molecules (including benzene derivatives, TCNQ, pentacene, C<sub>60</sub>) on top of phosphorene.<sup>214</sup> For non-polar molecules such as pentacene and mesitylene, the vdW potential decreases upon assembly while the Coulombic potential slightly increases. For polar molecules (1,3,5-trifluorobenzene, 1,3,5-trihydroxybenzene and TCNQ), the long-range intermolecular Coulombic interactions are more dominant. The calculated molecule-phosphorene interaction free energies for TCNQ (-45.4 kJ/mol) and pentacene (-28.6 kJ/mol) were comparable to those on graphene and hBN, which explain the similar packing behavior observed on phosphorene as compared to graphene and hBN systems. The results indicate that the non-aromatic nature of phosphorene does not affect the stability of epitaxial molecules in assemblies, and therefore the experimentally observed packing structures on phosphorene may be analog to those on graphene and hBN. To our knowledge, the effect of underlying substrate on 2D epitaxial assembly has not been investigated under the scope of MD simulations. However with the recently-developed knowledge of substrate-influenced effects in wettability of 2D materials by MD simulations,<sup>20,232</sup> it would be straightforward to consider the substrate effect in further work.

Although the above findings that are based on the MD-calculated interaction energies have not taken into account the kinetic phenomena involved in epitaxy experiments, the formation of ordered 2D crystalline organic films on 2D materials generally correlates well to the theoretical framework. A general feature in the 2D epitaxy of small molecules is that the sub-2D packing formed on the strongly interacting 2D surfaces, as discussed in the previous sections, changes to close-packed arrangements on a weakly interacting 2D material surface for molecules including MPc,<sup>35,36,39,40,42,233</sup> TCNQ,<sup>79</sup> C<sub>60</sub>.<sup>31–33</sup> The comparisons between the epitaxial behavior on the strongly and weakly interacting 2D material substrate have been addressed, such as FePc on graphene/Ru(0001) and graphene/Pt(111),<sup>43</sup> TCNQ on graphene/Ru(0001)<sup>82</sup> and graphene/Ir(111),<sup>79</sup> CoPc on graphene/Ru(0001)<sup>234</sup> and graphene/Ir(111),<sup>42</sup> F<sub>4</sub>-TCNQ on graphene/Ru(0001)<sup>83</sup> and graphene/hBN,<sup>84</sup> as shown in Figure 10.

Due to a low surface corrugation for 2D materials on the weakly interacting surfaces, more freedom for surface adsorption and diffusion of the small molecule is observed, resulting in the close-packed structures. Note that a strongly interacting 2D material does not always lead to sub-2D packing, as the molecular geometry and intermolecular interactions also come into play. Such phenomena has been observed in the systems of PTCDA molecules epitaxially grown on graphene<sup>70,71,75,235</sup>, and supported by *ab initio* simulations<sup>76</sup>. Due to the existence of intermolecular C-H ... O hydrogen bonds, the moiré pattern of graphene/Ru(0001) surface is not sufficiently strong to trap individual PTCDA molecules,<sup>70</sup> and therefore a close-packed 2D assembly forms, similar to that found on weakly interacting graphene/SiC surface.<sup>75,235</sup> The hydrogen bond energy per unit PTCDA herringbone lattice (400 ~ 600 meV)<sup>71</sup> was found to be comparable with the adsorption energy on the top sites of the moiré pattern (~700 meV),<sup>92</sup> revealing a competition between the intermolecular and molecule-2D interactions. Therefore, there is a small degree of morphological change by changing the weak interacting substrate to the strongly-interacting substrate, as vacancies are be found in the 2D PTCDA deposited on graphene/Ru(0001) located on the top sites. The close-packed assemblies on the

strongly interacting 2D surface are also be found in other molecules including pentacene<sup>236</sup> and C<sub>60</sub>,<sup>28,29</sup> in which the potential barrier on the surface was overcome by kinetic energy. On the other hand, the influence of molecule-substrate interaction has been demonstrated in the systems of CoPc deposited on graphene/SiO<sub>2</sub> and graphene/hBN.<sup>233</sup> Specifically, although CoPc forms cubic close-packed structures on both surfaces, the domain size on graphene/SiO<sub>2</sub> was found to be significantly smaller than that on graphene/hBN. The LUMO energy level fluctuation of CoPc on graphene/hBN was found to be less than that on graphene/SiO<sub>2</sub>, revealing the influence of the underlying substrate.

Following the discussions of 2D assembly, molecular packing of small organic molecules on 2D materials other than graphene is essentially determined by the molecule-2D material interactions, as well as the geometry and electronic structure of the 2D material. Shen et al. predicted the phase-dependent charge transfer between pentacene and MoS<sub>2</sub> monolayer,<sup>56</sup> as briefly mentioned in Section 2.2. A considerable degree of charge transfer between pentacene and 1T MoS<sub>2</sub> (i.e. enhanced molecule-2D material interactions) may lead to unprecedented 2D self-assembly. The dipole MoS<sub>2</sub> surface has shown to orient the butyl-substituted PTCDI derivative (PTCDI-C<sub>4</sub>) differently from the graphene surface.<sup>24</sup> X-ray photoelectron spectroscopy (XPS), NEXAFS and resonant photoemission spectroscopy (RPES) where used to reveal the edge-on orientation of PTCDI-C<sub>4</sub>, compared with the normally found face-on configuration of PTCDI compounds on graphene.<sup>88</sup> The molecule-MoS<sub>2</sub> interactions have been found to be weaker than that between the alkyl chains, leading to a tilted packing configuration. Another example is the dioctylbenzothienobenzothiophene (C8-BTBT) epitaxy on MoS<sub>2</sub>,<sup>237</sup> compared with that on graphene.<sup>238</sup> The ML thickness of C8-BTBT on MoS<sub>2</sub> was found to be ~1.2 nm, significantly larger than that on graphene (~0.7 nm), because the interfacial C8-BTBT molecules are with the “edge-on” orientation on MoS<sub>2</sub>. Clearly, the reduced vdW molecular-2D material interaction is responsible for the substrate-dependent packing configuration. Due to the fact that monolayer molecular assembly on 2D materials other than graphene and hBN has not been well studied by STM, more detailed studies will

be required to uncover the molecule-2D interaction on these 2D materials.

### 3.2.2 2D van der Waals Heterostructures

We refer the 2D vdW heterostructures to the epitaxial ~~assembled-assembly~~ of covalently bonded 2D materials. Chemical vapor deposition (CVD) and van der Waals epitaxy (vdWE) are the two major methods to grow the 2D vdW heterostructures.<sup>4</sup> In the view point of molecular interactions at the interface, these two methods are essentially similar. Therefore here we do not specify the preparation method for the 2D vdW heterostructure in this review. Note that the definition of 2D vdWE refers to the growth of single- or few-layer 2D materials on top of another 2D material. The use of vdWE for both small molecule<sup>168,239</sup> and layered materials<sup>240–243</sup> on layered TMDCs has been demonstrated long before the first discovery of graphene. The benefit of vdWE over conventional heteroepitaxy is less constraint in lattice mismatch. In conventional heteroepitaxy, dangling bonds exist on the substrate surface, thereby limiting the growth of lattice-mismatch overlayer. On the other hand for 2D materials, the interactions perpendicular to the 2D plane are mainly vdW or Coulombic interaction, so that the overlaying 2D material can be grown with less constraint in lattice mismatch. Figure 11(a) schematically shows the principle of van der Waals epitaxy process. As introduced in the section of intermolecular covalent bond, a large variety of 2D vdW heterostructures have been synthesized by vdWE approach. In this section we discuss the interplay between the covalent bond and inter-layer interactions in the vdWE growth of 2D vdW heterostructures.

Graphene, hBN and TMDC (in particular MoS<sub>2</sub>) are the most-studied 2D materials for vdWE growth of 2D heterostructures, due to their large area accessibility. Epitaxial graphene,<sup>110</sup> MoS<sub>2</sub><sup>106,107</sup> and WS<sub>2</sub><sup>108</sup> have been grown by vdWE on multilayer hBN. The epitaxial graphene on hBN was grown by plasma-enhanced CVD at ~500 °C, which is much lower than that required for metal-catalyzed CVD growth of graphene (~1000 °C).<sup>110</sup> The orientation of epitaxial graphene was found to be uniform on hBN, as revealed by

the moiré pattern formation in STM (see Figure 11(b)). Similar to the previous discussion about the 2D assembly of organic molecules, the interlayer interaction is also shown to govern the stacking of 2D heterostructure. On epitaxial or CVD-grown graphene, the vdWE technique has been used to grow hBN,<sup>100</sup> MoS<sub>2</sub>,<sup>96–98,100,103,104</sup> WS<sub>2</sub>,<sup>103</sup> WSe<sub>2</sub>,<sup>101,102</sup> and non-layered Pb<sub>1-x</sub>Sn<sub>x</sub>Se.<sup>244</sup> Monolayer epitaxial MoS<sub>2</sub> was successfully grown following on graphene, whereas the growth on bulk SiC surface remains negligible, following the principle of vdWE.<sup>100</sup> Monolayer TMDCs were also used for vdWE of TMDC/TMDC hybrid heterostructure, including MoTe<sub>2</sub>/MoS<sub>2</sub>,<sup>116</sup> WS<sub>2</sub>/MoS<sub>2</sub>,<sup>117</sup> GaSe/MoSe<sub>2</sub><sup>120</sup> (see Figure 11(c)), MoS<sub>2</sub>/SnS<sub>2</sub>.<sup>115</sup> More complex vdW heterostructures can also be synthesized using the vdWE approach. Lin et al. used repeated vdWE on epitaxial graphene at different temperatures for the synthesis of MoS<sub>2</sub>/WSe<sub>2</sub>/graphene and WS<sub>2</sub>/MoSe<sub>2</sub>/graphene heterostructures.<sup>101</sup> Alemayehu et al. synthesized ordered stacks of GeSe<sub>2</sub>/VSe<sub>2</sub> heterostructures<sup>118</sup> with controlled GeSe<sub>2</sub> layer number modulation by tuning the nucleation process.

One challenge in the vdWE growth of 2D vdW heterostructures is the controlled growth of monolayer 2D overlayer. We note that in many 2D heterostructures systems (mainly TMDC/graphene or TMDC/hBN) grown by vdWE, the growth of mono- and multi- overlayers have both been reported, including MoS<sub>2</sub>/graphene,<sup>96–100,103</sup> WSe<sub>2</sub>/graphene<sup>100,103</sup> and MoS<sub>2</sub>/hBN.<sup>106</sup> The stacking sequence seems also relevant to the layer number of the epitaxial layers. For example almost all hBN/graphene heterostructures reported showed multilayer hBN growth,<sup>100,245</sup> while graphene grown on hBN tend to be monolayer.<sup>110,245</sup> These results reveal the importance of chemical kinetics in the vdWE heterostructure growth, since the interplay between the interactions alone cannot explain the discrepancy. The proposed mechanisms include preferred nucleation sites,<sup>106</sup> non-epitaxial growth<sup>103</sup> and synthesis method.<sup>103</sup> Further studies are required to elucidate the mechanism underlying the layer-controlled growth.

### 3.3 3D Assembly

3D assembly on 2D material can be made by layer-by-layer deposition of small molecules or epitaxy of covalently bonded structure. When the thickness of 3D assembly increases, the intermolecular (or interatomic) interactions become dominant over the molecule-2D material and molecule-substrate interactions. However, this does not mean the interfacial interactions are negligible. In fact, as will be discussed later, the interfacial layer plays an important role in determining the molecular orientation and morphology in the 3D assembled structures. 3D epitaxy on 2D material interfaces may result in various forms of nanostructures other than simple stacked layers. The morphology of the 3D assembly greatly influence several key properties in organic semiconductors, including carrier transport, interfacial barrier, which motivates understanding of the underlying mechanism. The diversity of 3D **epitaxy** epitaxial morphology addresses the question of how the macroscopic structure is influenced by the interplay between the interactions. In this section, we review the interactions involved in a variety of 3D epitaxial structures, with more focus on the theoretical work in this field.

#### 3.3.1 Layer-by-Layer Assembly of Small Molecules

Layer-by-layer (LbL) self-assembly of small molecules can be viewed as the vertical epitaxy of 2D assembled structure. The molecular orientation and packing of the interfacial layers, i.e., the first few layers of the molecules, are strongly influenced by the molecule-2D material and molecule-substrate interactions, compared to the molecules far from the interface. The maximum molecule layer number influenced by the 2D material and substrate highly depends on the choice of molecule. The transition of orientation is a consequence of the **competence** competition between the interfacial and the bulk packing orientations. In the case of C<sub>60</sub> on corrugated graphene/Ru(0001) surface,<sup>29</sup> the first layer of C<sub>60</sub> forms isolated single molecules trapped in the HCP valley of the moiré pattern, which also serves as the nucleation sites for the second layer. The second layer C<sub>60</sub> molecules pack in a hexagonal pattern around the trapped C<sub>60</sub> molecules, namely the corrugation-guided packing. From the third layer on,

subsequent packing of C<sub>60</sub> molecules experience from dendritic to compact growth; in other words, the influence of graphene corrugation does not go beyond the third layer (Figure 12(a)). Similarly, TCNQ assembly on graphene/Ru(0001) also show transition from sub-2D Kagome packing to bulk phase close-packed order when coverage is slight higher than 1ML.<sup>82</sup> On the other hand, the second layer CoPc molecules adsorbed on hBN/Ir(111) still prefer to occupy the pore regions of hBN moiré pattern which have already been covered by the first layer CoPc molecules.<sup>183</sup> Multilayer assembly of pentacene molecules on graphene is another interesting example of layer-dependent molecule-2D material interactions. On epitaxial graphene/SiC surface, the first layer of pentacene shows the face-on orientation, with long-range ordering.<sup>61</sup> The second pentacene layer shows a tiled angle with respect to the graphene plane, corresponding to partial turn-over of the pentacene molecules.<sup>246</sup> After the fifth layer, the pentacene molecules pack in an edge-on manner, consistent with that in the bulk pentacene film<sup>247</sup> (Figure 12(b)). By increasing pentacene-graphene interactions, a strained polymorph of pentacene was observed,<sup>60</sup> stabilizing the epitaxial structure with consistent face-on orientation throughout the entire film. C8-TBTB is another example that exhibits a structural transition during epitaxial assembly. The first layer of C8-TBTB molecules packs with the polycyclic TBTB group in contact with graphene, forming long-range ordered linear structure,<sup>238</sup> as a result of the  $\pi$ - $\pi$  interactions between TBTB core and graphene, together with the alignment of the alkyl chains. In the bulk phase, the C8-TBTB molecules assemble with the edge-on orientation and form cubic lattice. The transition of orientation is found exclusively at the second layer, as revealed by the average layer thickness change (Figure 12(c)). The observation slightly changes for C8-TBTB deposited on single layer MoS<sub>2</sub><sup>237</sup> (Figure 12(d)). Due to a weaker molecule-2D material interaction, the first layer of C8-TBTB already shows an intermediate degree of tilted orientation between the face-on and edge-on configurations. From second layer on, the C8-TBTB molecules completely become the bulk phase packing. A general trend of the mono- to multi-layer transition can be observed: the molecule-2D material interactions have more influence on

the first ML and decays rapidly with the increase of layer numbers. When the direction of molecule-2D material interaction differs from that of intermolecular interaction in the bulk phase, a transition of the molecular orientation can be observed from monolayer to multi-layer. The effective depth of the molecule-2D material interactions is usually less than 2~3 ML, and dependent on the type of epitaxial molecules.

For molecules with a large planar structure such as CuPc and F<sub>16</sub>CuPc, the strong intermolecular interactions tend to pack the molecules along their c-axis.<sup>34,47,48</sup> Due to the fact that MPc molecules also take face-on orientation on graphene surface,<sup>36,53,146</sup> the face-on orientation can be maintained after the second layer and continue in its 3D epitaxy structure. On the other hand, the MPc molecules prefer to form the edge-on orientation on amorphous polar surface such as SiO<sub>2</sub> and glass.<sup>35,36,46</sup> As a result, molecular orientation of epitaxial CuPc and F<sub>16</sub>CuPc is templated by the graphene layer, screening the interactions from the SiO<sub>2</sub> or glass substrates. The idea of graphene-templated growth is also applied to the epitaxy of pentacene,<sup>54</sup> perfluoropentacene,<sup>67</sup> C<sub>60</sub><sup>31</sup> and DBTTC.<sup>150</sup> On the contrary, the epitaxy structure of thin-layer CuPc on MoS<sub>2</sub><sup>50</sup> shows less stability which undergo a face-on to edge-on transition upon air exposure and forming 1D-ordered structures. The face-on orientation, however, can be maintained at higher deposition temperature to create a compact structure and high turn-over barrier.

The morphology of the grown 3D epitaxial film is a consequence of both thermodynamic and kinetic effects.<sup>11</sup> Classical theory of thin film organic molecular epitaxy identifies three typical growth mechanisms, depending on their morphology, as follows: (i) Volmer-Weber (VW) type, where the assemblies are majorly island-like, (ii) ~~Fran-van-Frank-van~~ der Merwe (FM) type, where flat epitaxial layers are formed, and (iii) Stranski-Krastanov (SK) type, where island formation follows flat interfacial layer. The macroscopic phenomenon of morphology can be explained by the interplay of surface energies of different interfaces, including the 2D material surface  $\gamma_{2D}$ , surface of epitaxial molecules  $\gamma_M$ , and molecule-2D interface  $\gamma_{M-2D}$ , under the scope of 2D-interfacial epitaxy. In VW type growth, it's usually observed

that  $\gamma_M + \gamma_{M-2D} > \gamma_{2D}$ , indicating a non-wetting of molecules at the interface, while in the FM type growth,  $\gamma_M + \gamma_{M-2D} < \gamma_{2D}$ , corresponding to wetting of the molecules. The different models of thin film growth is shown in Figure 13(a). Since the surface energy is a macroscopic property related to the intermolecular and interfacial interactions, the growth models can also be rationalized by the interplay between the interactions. In VW-type growth, the intermolecular interaction is usually stronger than the molecule-2D and molecule-substrate interactions, as the molecules tend to grow on nuclei and form islands, while in FM- and SK-type growth, the strong interfacial interactions lead to the formation of interfacial wetting layer. After the first few layers, the kinetic parameters, in particular the surface diffusivity of epitaxial molecules, play a crucial role.<sup>248</sup>

The morphological control of 3D molecular epitaxy is also studied by fine-tuning the chemical structure of epitaxial molecules, such as the cases of CuPc/F<sub>16</sub>CuPc, and pentacene/perfluoropentacene. Several reports have indicated that the fluorination has great impact on the assembly morphology. On graphene surface, both CuPc<sup>35,36</sup> and F<sub>16</sub>CuPc<sup>146</sup> molecules form the face-on orientation, as indicated by X-ray diffraction (XRD) and grazing incidence X-ray diffraction (GIXD) spectroscopy. For the following layers of both molecules, a uniform diffraction peak corresponds to the face-on orientation is observed. However the macroscopic morphology shows different features: CuPc tends to form a dense film on graphene, with the grain size larger than that on SiO<sub>2</sub>,<sup>35,36</sup> F<sub>16</sub>CuPc forms vertical nanowires on PTCDA-template surface (similar to graphene with rich  $\pi$ -electrons)<sup>249</sup> (Figure 13(b)). Pentacene and perfluoropentacene on MoS<sub>2</sub> are also shown to have different morphologies.<sup>68</sup> Individual close-packed islands were formed in 30 nm-thick the pentacene/MoS<sub>2</sub> film, while the deposited film of perfluoropentacene on MoS<sub>2</sub> showed much a smoother surface, with the island size larger than 10  $\mu$ m, as has been observed in the case of pentacene and perfluoropentacene deposited on graphene or graphite<sup>67,250</sup> (Figure 13(c)). However the interfacial layer for both molecules were found to be the face-on orientation. Indeed, the morphology change caused by fluorination demonstrate how minor chemical composition change of the

epitaxial molecule may affect the macroscopic behavior in 3D molecular epitaxy. While the detailed mechanism is still not fully understood, the change of film surface energy  $\gamma_M$  caused by the fluorine atoms may be a possible explanation, as indicated by the different epitaxial growth models.

Another variable to control the macroscopic morphology is the interfacial energy  $\gamma_{M-2D}$ , following the previous discussion of molecular-substrate interactions. The wetting transparency of graphene layer enables the modulation of interfacial energy between pentacene and graphene by changing the wettability of the underlying substrate.<sup>63</sup> Although the growth mechanism remains to be VW-type, epitaxy on a graphene-coated hydrophobic surface shows a larger domain size, by reducing the heterogeneous nucleation rate, since  $\gamma_{M-2D}$  is small. A smaller domain size, on the other hand, has been observed on the graphene-coated hydrophobic surface.

### 3.3.2 Van der Waals Epitaxy of 3D Crystals

3D vdWE on 2D material interface shares the same mechanism with the 2D vdWE. Here we limit the discussion of 3D vdWE to the growth of crystalline material with non-planar (such as sp<sup>3</sup>) bonding. The absence of dangling bonds at the interface enables the growth of 3D bulk crystal with lattice mismatch. Similar to the vdWE of 2D heterostructures, the growth of 3D vdWE structure on layered 2D material is not a new idea. Layered TMDCs (MoTe<sub>2</sub>, WSe<sub>2</sub>) have been used for the growth of 3D crystalline semiconductors like CdS and CdTe.<sup>136,137</sup> In the case of epitaxial CdTe/MoTe<sub>2</sub> and CdTe/WSe<sub>2</sub>, the lattice mismatch is as high as 30% and 40%, respectively,<sup>137</sup> showing the power of vdWE in fabricating 3D crystalline structures. Recent examples have shown using 2D material as template for 3D vdWE of crystalline semiconductors, include GaAs/graphene,<sup>133,134</sup> GaN/graphene,<sup>127,129,129–132</sup> GaN/hBN,<sup>135,251</sup> InGaN/hBN,<sup>251</sup> ZnO/graphene<sup>127</sup> and ZnO/hBN.<sup>128</sup> In these systems, the 2D material not only serves as the buffer layer for vdWE, but also acts as a transferable layer which enables separation of the 3D crystal from the substrate to allow fabrication of semiconductor

devices.<sup>132,133,135,251</sup> However a general problem encountered in the 3D vdWE process is the low density of nucleation sites and formation of smaller clusters instead of continuous film.<sup>129,135–137</sup> In 2D vdWE process, the covalent bonds are confined in-plane which enable the growth of large area 2D layer. On the contrary, in 3D vdWE process, the 3D covalent bonds lead to comparable growth rate in all directions, so that the crystal size highly depends on the interfacial nucleation density. On the other hand, the growth of metal oxides (e.g. Al<sub>2</sub>O<sub>3</sub>, ZnO, TiO<sub>2</sub>) on graphene or hBN lead to more uniform films,<sup>121,122,124–128,252</sup> due to an increased interfacial adsorption of precursors. 2D materials with a ZnO or AlN buffer layers have thus been used for vdWE of large area crystalline semiconductors.<sup>127,130,131,135</sup> Kim et al. showed the nucleation density of GaN on graphene can be enhanced by the periodic step edges of epitaxial graphene/SiC surface.<sup>132</sup> Large-area single crystalline film of epitaxial GaN with high lattice ordering has been achieved, despite the 23% lattice mismatch between graphene and GaN. For epitaxy of metal-oxide films, the monolayer assembled organic molecules can also be used for seeded growth of high-quality metal oxide films on 2D materials. For instance, Alaboson et al. used single layer close-packed PTCDA molecules adsorbed on the epitaxial graphene/SiC for the seeding growth of Al<sub>2</sub>O<sub>3</sub> and HfO<sub>2</sub>.<sup>123</sup> The ALD-grown high-k metal oxide films showed smoother morphology and less current leakage compared to those grown in identical ALD conditions without the PTCDA seeding layer. Besides the molecule-2D material interactions, recently Kim et al. also showed that the 3D vdWE growth can be guided by the interaction between the epitaxial overlayer and the underlying substrate, in the case of the homoepitaxy of III-V semiconductors (GaAs, InP and GaP).<sup>133</sup> In other words, graphene serves as a buffer layer for 3D vdWE. Since the thickness of graphene (~3 Å) is smaller than the vdW interaction distance of the bulk material (~9 Å for GaAs), the lattice of the underneath substrate can guide remote homoepitaxy of the overlayer. In principle, a series of single layer 2D materials can serve as the vdW buffer layer for such homoepitaxy, and benefit the design and fabrication of tandem 2D-3D heterostructures.

### **3.4 Summary**

Table 2 summarizes the representative examples of multidimensional molecular epitaxy on 2D materials interfaces, and outlines the governing interactions and the comparison between the interactions that discussed in this section. A clear relation between the interaction and the dimension of assembly can be observed: molecular epitaxy of higher dimension is favored with increasing intermolecular interactions. In the case of 2D and 3D vdWE, the intermolecular interactions (covalent bond) can be much greater than the molecule-2D interactions (vdW). It can also be found that the molecule-substrate interactions are constantly weaker than the other two types of interactions, as a result of increased interaction distance and partial screening effect of the 2D material layer. However as seen in the examples in this section, the absolute order of interaction strength is not the only factor that determines the packing and orientation of the molecular epitaxy. Understanding the role of weak interactions in determining the molecular epitaxy poses a challenge towards comprehensive theory framework, and is crucial for the designing of epitaxial systems on 2D materials interfaces.

Table 2: Summary of representative examples of multidimensional molecular epitaxy on 2D materials interfaces, the governing interactions involved and the comparison between the interactions discussed in this section.

Dimension	Governing interaction(s)	Comparison between interactions
Examples		
0D	Site-specific	Molecule-2D $\gg$ intermolecular
Strongly interacting surface		
1D	H-bond, site-specific	Molecule-2D $\approx$ intermolecular
Strongly interacting surface		
Fractal	H-bond, site-specific	Molecule-2D $\approx$ intermolecular
Strongly interacting surface		
	Multivalent H-bond	
Weakly interacting surface		Intermolecular $\gtrsim$ molecule-2D
2D	(H-bond), CT, $\pi-\pi$	Molecule-2D $\gtrsim$ intermolecular
ML on graphene		
	(H-bond), CT, vdW	Intermolecular $\gtrsim$ molecule-2D
ML on TMDC		
	Covalent bond, vdW	Intermolecular $\gg$ molecule-2D
2D vdWE		
3D	(H-bond), CT, $\pi-\pi$ , vdW	Depending on the 2D material
LbL assembly		
	Covalent bond, vdW	Intermolecular $\gg$ molecule-2D
3D vdWE		

## 4 Engineering 2D-Interfacial Molecular Epitaxy for Applications

Molecular epitaxy on 2D materials as an emerging route for synthesizing functional structures with mixed dimensions have generated research interest in their applications. Extensive reviews have been made on the applications of 2D material hybrid structures, including 2D vdW heterostructures,<sup>1,4,253</sup> 2D-organic interfaces,<sup>7,8,12,165,189</sup> and mixed dimension assemblies.<sup>10</sup> With the advance of thin-film technology, it is expected that the existing and even theoretically-proposed 2D hybrid structures can be eventually fabricated by molecular epitaxy. The tunability of molecular epitaxy also provides flexible control over the dimension, orientation, packing and morphology of the resulting films, which may be difficult to achieve with other methods. Here we do not review in details the applications of 2D-interfacial molecular epitaxy, but rather put our focus on how 2D material-based applications can benefit from engineering of 2D-interfacial molecular epitaxy, in particular about the modulation of interactions at different length scales.

### 4.1 Engineering the Properties of 2D Materials

The electronic properties, including Fermi level, bandgap, photoluminescence, and carrier mobility of 2D materials are widely tunable by a variety of physical and chemical approaches. Molecular epitaxy offers two potential routes to modulate 2D material properties, including non-covalent adsorption and interlayer coupling in 2D heterostructures<sup>178,253</sup>. Non-covalent adsorption with molecular epitaxy enables doping<sup>156,157,165,166,254</sup>, bandgap engineering<sup>167,255</sup>, vibration mode modulation<sup>256,257</sup> and magnetism control<sup>81–83,258</sup> of 2D materials. Interlayer coupling of 2D heterostructure, on the other hand, has shown to tune the bandgap<sup>253</sup>, spin state, [photoluminescence](#), [interlayer stress](#),<sup>259,260</sup> [photoluminescence](#)<sup>188,261</sup>, and interfacial carrier transport<sup>262,263</sup> due to the coupling of vdW interactions. Mechanism and examples of molecular doping of 2D materials can be found in Refs. 144,165,166 and the coupling-induced

tuning of 2D heterostructures can be found in Refs. 4,253.

## 4.2 Interfacial Engineering for Electronic Applications

The orientation of interfacial layer has been well-known to influence the interfacial electronic properties, such as the carrier injection barrier,<sup>57,146</sup> binding energy<sup>36,53,66</sup> and anisotropic charge transfer.<sup>264</sup> As discussed earlier, the template effect of 2D materials offers a feasible approach to create functional heterojunctions. ~~As an example, One important property which greatly affects the performance of 2D material-based applications is the carrier mobility. Tailoring the interfacial interactions on 2D materials interfaces provides the opportunity for modulating the carrier mobility via packing and orientation of the epitaxial molecules.~~ Lee et al. employed the orientation difference between pentacene molecules on graphene and polymer to create high-resistance lateral junctions.<sup>54</sup> By using the pentacene/graphene as source and drain electrode, and pentacene/polymer in the channel region, lateral field effect transistor with high on-off current ratio of up to  $10^8$  was demonstrated. ~~The highly ordered packing behavior of hBN can also serve as template for epitaxial growth of highly-crystalline rubrene, which greatly enhance the carrier mobility compared with the single crystal counterpart~~<sup>69</sup>. Lee et al. demonstrated that by using graphene as electrical contacts, the rubrene layer on hBN can reach carrier mobility as high as  $11.5 \text{ cm}^2 \cdot \text{V}^{-1} \cdot \text{s}^{-1}$ . The hBN layer not only provides a template for highly ordered single layer epitaxial layer of rubrene, but also creates an atomically sharp interface with reduced trap density. hBN is also shown to provide high mobility in  $\text{C}_{60}$  epitaxial layers due to templated packing. Lee et al reported a maximal carrier mobility of  $2.9 \text{ cm}^2 \cdot \text{V}^{-1} \cdot \text{s}^{-1}$  in  $\text{C}_{60}/\text{hBN}$  transistor, superior to the performance of  $\text{C}_{60}$  grown on conventional dielectric layers such as  $\text{SiO}_2$ <sup>204</sup>. The benefit of highly ordered packing molecules on 2D material templates have also been employed for other lateral<sup>55,59</sup> and vertical<sup>31,148</sup> field effect transistors, photosensors<sup>265</sup> and light emitting diodes (LED)<sup>132,133,135,251</sup>, proving that 2D material-induced interfacial engineering is a promising approach for improving device performance.

### 4.3 Nanostructure-Based Applications

Finally, the morphological change induced by the 2D material in molecular epitaxial may enable new approaches to tailor the physical properties of the 2D complexes, especially when hierarchical or high aspect-ratio nanostructures are formed. For example, Wang et al. used graphene as template to grow highly-ordered vertical arrays of oligoaniline.<sup>266</sup> The  $\pi$ - $\pi$  molecule-graphene interaction leads to selective ~~modification of graphene adsorption on graphene compared with the bulk SiO<sub>2</sub> substrate~~, which further enables patterned growth of vertical oligoaniline arrays. The ordered packing of oligoaniline resulted in high conductivity of 12.3 S/cm. Zheng et al. used graphene as a template for the solution-based growth of dense array of vertical 9,10-bis(phenylethynyl) anthracene (BPEA) semiconducting nanowires.<sup>267</sup> The high aspect ratio and narrowly dispersed diameter of the nanowires enable high-performance array of cavities with strong optical dispersion. Another example of the nanostructures grown by molecular epitaxy using molecular epitaxy on 2D materials is the growth of nanowall-nanowire hybrid structures of ZnO on graphene by controlling the interfacial nucleation density.<sup>125</sup> Combining the piezoelectric effect of ZnO, the high aspect ratio of nanowires, the specific electron dynamics of the nanowall-nanowire interface, and the high conductance of graphene, the hybrid structure was used as an effective nanoscale power generator.

## 5 Opportunities and Challenges

In the previous sections we have shown the diverse nature of molecular epitaxy on 2D materials interfaces, especially the role of the interactions involved in the process. The flexibility of tuning molecular epitaxy enables various high-performance devices and other applications. However as we have pointed out in previous sections, our understanding of the mechanism of the interactions on the 2D interface is far from complete. On the other hand, controllable and scalable fabrication technique still needs to be improved. These challenges

would also mean future opportunities in the emerging research field of 2D materials. In this section we will summarize several important issues concerning the molecular epitaxy on 2D materials.

## 5.1 Choice of 2D Materials

The past decade witnessed the booming of the 2D materials family, in particular the rich applications of graphene, hBN, and TMDCs due to their wide availability. We noticed a constant relationship between the numbers of publications dealing with molecular epitaxy on 2D materials and the maturity of the fabrication technique of the 2D material studied. Early-stage studies were mainly focusing on the molecular assembly on metal-supported graphene and hBN, with Ref. 70 and 179 as typical examples. Following the scalable synthesis of large area single layer graphene<sup>268</sup>, studies of molecular interactions on graphene are guaranteed with rich selection of substrates<sup>198</sup> and even isolating the substrate effect<sup>269,270</sup>. Similar trend can also be found in the studies of TMDCs, where studies regarding epitaxy on single layer TMDCs experience a fast increase from 2013, after the development of its large are synthesis method<sup>271</sup>. Therefore it is foreseeable the studies of molecular epitaxy and interfacial interactions on other types of 2D materials will be greatly increased after future advanced in their fabrication techniques. Our understanding of the interfacial interactions may be refreshed by 2D materials with unique properties, such as (i) different symmetry, such as phosphorene, (ii) different configuration, such as planar and buckling forms of silicene, and (iii) unique electro- and magneto-properties, such as superconducting Lanthanide-based 2D materials.

## 5.2 Linking the 2D Electronic Properties with Interfacial Interactions

It has been widely revealed that a 2D material owns unique electronic properties, such as low DOS, indirect-direct transition of band gap and attenuated screening compared with its 3D counterpart. Although a large number of applications have taken advantage of

such promising features, it is less understood how the internal electronic properties of an 2D material would affect the interfacial interactions. One example is the doping-induced modulation of vdW interactions on 2D interface, as discussed in Section 2.2.1. We note that most of such interactions are of a weak and dispersive nature, making them sensitive to the spatial charge distribution of 2D materials. As a result the classical adsorption theory on bulk surface is inapplicable. In addition, the interaction energies of dispersion and charge-transfer systems are known to be challenging for state-of-art *ab initio* simulations, such as density functional theory (DFT)<sup>272,273</sup> due to the fact that such interaction energies are usually much less than the total energy of the system. Another issue we have addressed previously is to isolate the contribution of the molecule-substrate interactions from the molecule-2D interactions, when the electronic properties of the 2D material is also sensitive to its support.

### 5.3 Enriching the Theoretical Framework

Theoretical and computational chemistry has constantly gained its importance in the study of 2D material science, including the study of molecular interactions on 2D materials interfaces. State-of-art quantum chemistry, molecular dynamics and empirical macroscopic models have provided the opportunities of multiscale study of the interfacial phenomena. However they are still far from perfect in elucidating what happens at the 2D interface. Due to limitation of computing force, the *ab initio* simulations of adsorption on 2D materials usually only deal with few epitaxial molecules, and sub-2D coverage. The intermolecular interactions are usually omitted or underestimated under such circumstance. Moreover, the molecules widely used for epitaxy have large number of atoms per molecule (e.g. 36 atoms for pentacene, 57 atoms for MPc, and 72 atoms for C8-BTBT), requiring large computation resources. On the other hand, N-body simulations such as molecular dynamics (MD) provide more insights into the intermolecular interactions and statistical configurations. However the accuracy of MD simulations rely heavily on the estimation of the force field at the 2D interface,

which can be very problematic when transition metals are in the system (e.g. MPc, TMDC)  
<sup>274</sup>. The van der Waals interactions are also crucial for a large variety of 2D materials, as  
discussed in the previous section, and should also be carefully treated in both atomistic-  
and molecular-scale simulations. Lastly, accurate empirical models are necessary to bridge  
the gap between interaction potential calculated by quantum chemistry and MD approaches,  
and the macroscopic packing/morphology of the epitaxial structures, which may be hopefully  
achieved by the fast experimental development of 2D materials.

## 6 Summary

Molecular epitaxy on 2D materials has been proven to be a powerful approach to create multidimensional hybrid structures. Understanding the mechanism, in particular the interplay between the interactions behind the complex epitaxial structures is important towards engineering the heterostructures. In this article, we review the interactions involved in the molecular epitaxy on 2D materials, including the intermolecular, molecule-2D material and molecule-substrate interactions. By looking into various examples of the epitaxial assemblies, we discuss the influence of each interaction on the dimension, interfacial orientation, lattice packing and morphology of the resulting heterostructures. By increasing the molecule-2D material and molecule-substrate interactions, the epitaxial structure tends to be more surface-specific, and different from that in bulk phase. It is often observed that even weak molecule-2D material interactions can be crucial in stabilizing the interfacial structure and its orientation. The unique surface-induced assembled structures enable a variety of applications, including tailoring the electronic properties of 2D materials, high performance field effect devices and multifunctional nanostructure surfaces. Here we highlight that there are several key issues regarding molecular epitaxy on 2D materials that remain poorly understood, including (i) the relationship between the electronic structure of the 2D material and the interfacial interactions, (ii) the effective interaction range of the underlying substrate in

different 2D material systems, (iii) a general model describing the molecule-2D material and molecule-substrate interactions, and (iv) the governing factors for the morphology of the resulting structure. Further theoretical and experimental investigations are required to address the above questions. We believe that reproducible, high throughput, and controllable fabrication of the 2D hybrid heterostructures will ~~be benefited benefit~~ from the fundamental principles covered in this review.

## Acknowledgement

The authors are grateful for the financial support from the ETH startup funding.

## References

- (1) Novoselov, K. S.; Geim, A. K.; Morozov, S. V.; Jiang, D.; Zhang, Y.; Dubonos, S. V.; Grigorieva, I. V.; Firsov, A. A. A roadmap for graphene. *Nature* **2012**, *490*, 192–200.
- (2) Lin, Z.; McCreary, A.; Briggs, N.; Subramanian, S.; Zhang, K.; Sun, Y.; Li, X.; Borys, N. J.; Yuan, H.; Fullerton-Shirey, S. K.; et al., 2D materials advances: from large scale synthesis and controlled heterostructures to improved characterization techniques, defects and applications. *2D Mater.* **2016**, *3*, 042001.
- (3) Geim, A. K.; Grigorieva, I. V. Van der Waals heterostructures. *Nature* **2013**, *499*, 419–425.
- (4) Novoselov, K. S.; Mishchenko, A.; Carvalho, A.; Castro Neto, A. H. 2D materials and van der Waals heterostructures. *Science* **2016**, *353*, aac9439.
- (5) Bhimanapati, G. R.; Lin, Z.; Meunier, V.; Jung, Y.; Cha, J.; Das, S.; Xiao, D.; Son, Y.; Strano, M. S.; Cooper, V. R.; et al., Recent Advances in Two-Dimensional Materials beyond Graphene. *ACS Nano* **2015**, *9*, 11509–11539.

- (6) Das, S.; Robinson, J. A.; Dubey, M.; Terrones, H.; Terrones, M. Beyond Graphene: Progress in Novel Two-Dimensional Materials and van der Waals Solids. *Annu. Rev. Mater. Res.* **2015**, *45*, 1–27.
- (7) Kim, C.-H.; Kymmissis, I. Graphene–organic hybrid electronics. *J. Mater. Chem. C* **2017**, *5*, 4598–4613.
- (8) Hong, G.; Wu, Q.-H.; Ren, J.; Wang, C.; Zhang, W.; Lee, S.-T. Recent progress in organic molecule/graphene interfaces. *Nano Today* **2013**, *8*, 388–402.
- (9) Lee, G.-H.; Lee, C.-H.; van der Zande, A. M.; Han, M.; Cui, X.; Arefe, G.; Nuckolls, C.; Heinz, T. F.; Hone, J.; Kim, P. Heterostructures based on inorganic and organic van der Waals systems. *APL Mater.* **2014**, *2*, 092511.
- (10) Jariwala, D.; Marks, T. J.; Hersam, M. C. Mixed-dimensional van der Waals heterostructures. *Nat. Mater.* **2016**, *16*, 170–181.
- (11) Kowarik, S.; Gerlach, A.; Schreiber, F. Organic molecular beam deposition: fundamentals, growth dynamics, and in situ studies. *J. Phys. Cond. Matter* **2008**, *20*, 184005.
- (12) MacLeod, J. M.; Rosei, F. Molecular Self-Assembly on Graphene. *Small* **2013**, *10*, 1038–1049.
- (13) Kumar, A.; Banerjee, K.; Liljeroth, P. Molecular assembly on two-dimensional materials. *Nanotechnology* **2017**, *28*, 082001.
- (14) Israelachvili, J. N. *Intermolecular and surface forces*; Academic press, 2011.
- (15) Huttmann, F.; Martínez-Galera, A. J.; Caciuc, V.; Atodiresei, N.; Schumacher, S.; Standop, S.; Hamada, I.; Wehling, T. O.; Blügel, S.; Michely, T. Tuning the van der Waals Interaction of Graphene with Molecules via Doping. *Phys. Rev. Lett.* **2015**, *115*, 236101.

- (16) Muruganathan, M.; Sun, J.; Imamura, T.; Mizuta, H. Electrically Tunable van der Waals Interaction in Graphene–Molecule Complex. *Nano Lett.* **2015**, *15*, 8176–8180.
- (17) Novoselov, K. S.; Geim, A. K.; Morozov, S. V.; Jiang, D.; Zhang, Y.; Dubonos, S. V.; Grigorieva, I. V.; Firsov, A. A. Electric Field Effect in Atomically Thin Carbon Films. *Science* **2004**, *306*, 666–669.
- (18) Boott, C. E.; Nazemi, A.; Manners, I. Synthetic Covalent and Non-Covalent 2D Materials. *Angew. Chem. Int. Ed.* **2015**, *54*, 13876–13894.
- (19) Barth, J. V. Molecular Architectonic on Metal Surfaces. *Annu. Rev. Phys. Chem.* **2007**, *58*, 375–407.
- (20) Shih, C.-J.; Wang, Q. H.; Lin, S.; Park, K.-C.; Jin, Z.; Strano, M. S.; Blankschtein, D. Breakdown in the Wetting Transparency of Graphene. *Phys. Rev. Lett.* **2012**, *109*, 176101.
- (21) Shih, C.-J.; Strano, M. S.; Blankschtein, D. Wetting translucency of graphene. *Nat. Mater.* **2013**, *12*, 866–869.
- (22) Rafiee, J.; Mi, X.; Gullapalli, H.; Thomas, A. V.; Yavari, F.; Shi, Y.; Ajayan, P. M.; Koratkar, N. A. Wetting transparency of graphene. *Nat. Mater.* **2012**, *11*, 217–222.
- (23) Whitesides, G. M. Self-Assembly at All Scales. *Science* **2002**, *295*, 2418–2421.
- (24) Arramel,; Yin, X.; Wang, Q.; Zheng, Y. J.; Song, Z.; bin Hassan, M. H.; Qi, D.; Wu, J.; Rusydi, A.; Wee, A. T. S. Molecular Alignment and Electronic Structure of N,N -Dibutyl-3,4,9,10-perylene-tetracarboxylic-diimide Molecules on MoS<sub>2</sub> Surfaces. *ACS Appl. Mater. Interfaces* **2017**, *9*, 5566–5573.
- (25) Lin, Z.; McCreary, A.; Briggs, N.; Subramanian, S.; Zhang, K.; Sun, Y.; Li, X.; Borys, N. J.; Yuan, H.; Fullerton-Shirey, S. K.; et al., 2D materials advances: from

large scale synthesis and controlled heterostructures to improved characterization techniques, defects and applications. *2D Mater.* **2016**, *3*, 042001.

- (26) Phillips, A. G.; Beton, P. H.; Champness, N. R. *Supramolecular Chemistry*; John Wiley & Sons, Ltd, 2012.
- (27) Corso, M. Boron Nitride Nanomesh. *Science* **2004**, *303*, 217–220.
- (28) Li, G.; Zhou, H. T.; Pan, L. D.; Zhang, Y.; Mao, J. H.; Zou, Q.; Guo, H. M.; Wang, Y. L.; Du, S. X.; Gao, H.-J. Self-assembly of C<sub>60</sub> monolayer on epitaxially grown, nanostructured graphene on Ru(0001) surface. *Appl. Phys. Lett.* **2012**, *100*, 013304.
- (29) Lu, J.; Yeo, P. S. E.; Zheng, Y.; Yang, Z.; Bao, Q.; Gan, C. K.; Loh, K. P. Using the Graphene Moiré Pattern for the Trapping of C<sub>60</sub> and Homoepitaxy of Graphene. *ACS Nano* **2012**, *6*, 944–950.
- (30) Cho, J.; Smerdon, J.; Gao, L.; Süzer, Ö.; Guest, J. R.; Guisinger, N. P. Structural and Electronic Decoupling of C<sub>60</sub> from Epitaxial Graphene on SiC. *Nano Lett.* **2012**, *12*, 3018–3024.
- (31) Kim, K.; Lee, T. H.; Santos, E. J. G.; Jo, P. S.; Salleo, A.; Nishi, Y.; Bao, Z. Structural and Electrical Investigation of C<sub>60</sub>–Graphene Vertical Heterostructures. *ACS Nano* **2015**, *9*, 5922–5928.
- (32) Chen, R.; Lin, C.; Yu, H.; Tang, Y.; Song, C.; Yuwen, L.; Li, H.; Xie, X.; Wang, L.; Huang, W. Templating C<sub>60</sub> on MoS<sub>2</sub> Nanosheets for 2D Hybrid van der Waals p–n Nanoheterojunctions. *Chem. Mater.* **2016**, *28*, 4300–4306.
- (33) Jung, M.; Shin, D.; Sohn, S.-D.; Kwon, S.-Y.; Park, N.; Shin, H.-J. Atomically resolved orientational ordering of C<sub>60</sub> molecules on epitaxial graphene on Cu(111). *Nanoscale* **2014**, *6*, 11835–11840.

- (34) Ren, J.; Meng, S.; Wang, Y.-L.; Ma, X.-C.; Xue, Q.-K.; Kaxiras, E. Properties of copper (fluoro-)phthalocyanine layers deposited on epitaxial graphene. *J. Chem. Phys.* **2011**, *134*, 194706.
- (35) Singha Roy, S.; Bindl, D. J.; Arnold, M. S. Templating Highly Crystalline Organic Semiconductors Using Atomic Membranes of Graphene at the Anode/Organic Interface. *J. Phys. Chem. Lett.* **2012**, *3*, 873–878.
- (36) Xiao, K.; Deng, W.; Keum, J. K.; Yoon, M.; Vlassiouk, I. V.; Clark, K. W.; Li, A.-P.; Kravchenko, I. I.; Gu, G.; Payzant, E. A.; et al., Surface-Induced Orientation Control of CuPc Molecules for the Epitaxial Growth of Highly Ordered Organic Crystals on Graphene. *J. Am. Chem. Soc.* **2013**, *135*, 3680–3687.
- (37) Pandey, P. A.; Rochford, L. A.; Keeble, D. S.; Rourke, J. P.; Jones, T. S.; Beanland, R.; Wilson, N. R. Resolving the Nanoscale Morphology and Crystallographic Structure of Molecular Thin Films: F16CuPc on Graphene Oxide. *Chem. Mater.* **2012**, *24*, 1365–1370.
- (38) Dou, W.-D.; Lee, C.-S. Controllable growth of copper-phthalocyanine thin film on rough graphene substrate. *Appl. Phys. Lett.* **2014**, *105*, 223110.
- (39) Wang, Y.-L.; Ren, J.; Song, C.-L.; Jiang, Y.-P.; Wang, L.-L.; He, K.; Chen, X.; Jia, J.-F.; Meng, S.; Kaxiras, E.; et al., Selective adsorption and electronic interaction of F16CuPc on epitaxial graphene. *Phys. Rev. B* **2010**, *82*, 245420.
- (40) Wu, Q.-H.; Hong, G.; Lee, S. Modification of CuPc/graphene interfacial electronic structure with F16CuPc. *Org. Electron.* **2013**, *14*, 542–547.
- (41) Zhang, H. G.; Sun, J. T.; Low, T.; Zhang, L. Z.; Pan, Y.; Liu, Q.; Mao, J. H.; Zhou, H. T.; Guo, H. M.; Du, S. X.; et al., Assembly of iron phthalocyanine and pentacene molecules on a graphene monolayer grown on Ru(0001). *Phys. Rev. B* **2011**, *84*, 245436.

- (42) Hämäläinen, S. K.; Stepanova, M.; Drost, R.; Liljeroth, P.; Lahtinen, J.; Sainio, J. Self-Assembly of Cobalt-Phthalocyanine Molecules on Epitaxial Graphene on Ir(111). *J. Phys. Chem. C* **2012**, *116*, 20433–20437.
- (43) Yang, K.; Xiao, W. D.; Jiang, Y. H.; Zhang, H. G.; Liu, L. W.; Mao, J. H.; Zhou, H. T.; Du, S. X.; Gao, H.-J. Molecule–Substrate Coupling between Metal Phthalocyanines and Epitaxial Graphene Grown on Ru(0001) and Pt(111). *J. Phys. Chem. C* **2012**, *116*, 14052–14056.
- (44) Ying Mao, H.; Wang, R.; Wang, Y.; Chao Niu, T.; Qiang Zhong, J.; Yang Huang, M.; Chen Qi, D.; Ping Loh, K.; Thye Shen Wee, A.; Chen, W. Chemical vapor deposition graphene as structural template to control interfacial molecular orientation of chloroaluminium phthalocyanine. *Appl. Phys. Lett.* **2011**, *99*, 093301.
- (45) Ogawa, Y.; Niu, T.; Wong, S. L.; Tsuji, M.; Wee, A. T. S.; Chen, W.; Ago, H. Self-Assembly of Polar Phthalocyanine Molecules on Graphene Grown by Chemical Vapor Deposition. *J. Phys. Chem. C* **2013**, *117*, 21849–21855.
- (46) de Oteyza, D. G.; Barrena, E.; Sellner, S.; Ossó, J. O.; Dosch, H. Structural Rearrangements During the Initial Growth Stages of Organic Thin Films of F16CuPc on SiO<sub>2</sub>. *J. Phys. Chem. B* **2006**, *110*, 16618–16623.
- (47) Yoon, S. M.; Song, H. J.; Hwang, I.-C.; Kim, K. S.; Choi, H. C. Single crystal structure of copper hexadecafluorophthalocyanine (F16CuPc) ribbon. *Chem. Commun.* **2010**, *46*, 231–233.
- (48) Jiang, H.; Ye, J.; Hu, P.; Wei, F.; Du, K.; Wang, N.; Ba, T.; Feng, S.; Kloc, C. Fluorination of Metal Phthalocyanines: Single-Crystal Growth, Efficient N-Channel Organic Field-Effect Transistors, and Structure-Property Relationships. *Sci. Rep.* **2014**, *4*, 7573.

- (49) Pak, J.; Jang, J.; Cho, K.; Kim, T.-Y.; Kim, J.-K.; Song, Y.; Hong, W.-K.; Min, M.; Lee, H.; Lee, T. Enhancement of photodetection characteristics of MoS<sub>2</sub> field effect transistors using surface treatment with copper phthalocyanine. *Nanoscale* **2015**, *7*, 18780–18788.
- (50) Zhang, L.; Yang, Y.; Huang, H.; Lyu, L.; Zhang, H.; Cao, N.; Xie, H.; Gao, X.; Niu, D.; Gao, Y. Thickness-Dependent Air-Exposure-Induced Phase Transition of CuPc Ultra-thin Films to Well-Ordered One-Dimensional Nanocrystals on Layered Substrates. *J. Phys. Chem. C* **2015**, *119*, 4217–4223.
- (51) Avvisati, G.; Lisi, S.; Gargiani, P.; Della Pia, A.; De Luca, O.; Pacilé, D.; Cardoso, C.; Varsano, D.; Prezzi, D.; Ferretti, A.; et al., FePc Adsorption on the Moiré Superstructure of Graphene Intercalated with a Cobalt Layer. *J. Phys. Chem. C* **2017**, *121*, 1639–1647.
- (52) Iannuzzi, M.; Tran, F.; Widmer, R.; Dienel, T.; Radican, K.; Ding, Y.; Hutter, J.; Gröning, O. Site-selective adsorption of phthalocyanine on h-BN/Rh(111) nanomesh. *Phys. Chem. Chem. Phys.* **2014**, *16*, 12374.
- (53) Mativetsky, J. M.; Wang, H.; Lee, S. S.; Whittaker-Brooks, L.; Loo, Y.-L. Face-on stacking and enhanced out-of-plane hole mobility in graphene-templated copper phthalocyanine. *Chem. Commun.* **2014**, *50*, 5319–5321.
- (54) Lee, W. H.; Park, J.; Sim, S. H.; Lim, S.; Kim, K. S.; Hong, B. H.; Cho, K. Surface-Directed Molecular Assembly of Pentacene on Monolayer Graphene for High-Performance Organic Transistors. *J. Am. Chem. Soc.* **2011**, *133*, 4447–4454.
- (55) Jariwala, D.; Howell, S. L.; Chen, K.-S.; Kang, J.; Sangwan, V. K.; Filippone, S. A.; Turrisi, R.; Marks, T. J.; Lauhon, L. J.; Hersam, M. C. Hybrid, Gate-Tunable, van der Waals p–n Heterojunctions from Pentacene and MoS<sub>2</sub>. *Nano Lett.* **2016**, *16*, 497–503.

- (56) Shen, N.; Tao, G. Charge Transfer and Interface Engineering of the Pentacene and MoS<sub>2</sub> Monolayer Complex. *Adv. Mater. Interfaces* **2017**, *4*, 1601083.
- (57) Oh, G.; Kim, J.-S.; Jeon, J. H.; Won, E.; Son, J. W.; Lee, D. H.; Kim, C. K.; Jang, J.; Lee, T.; Park, B. H. Graphene/Pentacene Barristor with Ion-Gel Gate Dielectric: Flexible Ambipolar Transistor with High Mobility and On/Off Ratio. *ACS Nano* **2015**, *9*, 7515–7522.
- (58) Zhou, H.; Zhang, L.; Mao, J.; Li, G.; Zhang, Y.; Wang, Y.; Du, S.; Hofer, W. A.; Gao, H.-J. Template-directed assembly of pentacene molecules on epitaxial graphene on Ru(0001). *Nano Res.* **2013**, *6*, 131–137.
- (59) Kim, J.-K.; Cho, K.; Kim, T.-Y.; Pak, J.; Jang, J.; Song, Y.; Kim, Y.; Choi, B. Y.; Chung, S.; Hong, W.-K.; et al., Trap-mediated electronic transport properties of gate-tunable pentacene/MoS<sub>2</sub> p-n heterojunction diodes. *Sci. Rep.* **2016**, *6*, 36775.
- (60) Kim, K.; Santos, E. J. G.; Lee, T. H.; Nishi, Y.; Bao, Z. Epitaxially Grown Strained Pentacene Thin Film on Graphene Membrane. *Small* **2015**, *11*, 2037–2043.
- (61) Jung, W.; Oh, D.-H.; Song, I.; Shin, H.-C.; Ahn, S. J.; Moon, Y.; Park, C.-Y.; Ahn, J. R. Influence of graphene-substrate interactions on configurations of organic molecules on graphene: Pentacene/epitaxial graphene/SiC. *Appl. Phys. Lett.* **2014**, *105*, 071606.
- (62) Zhang, L.; Roy, S. S.; Hamers, R. J.; Arnold, M. S.; Andrew, T. L. Molecular Orientation-Dependent Interfacial Energetics and Built-in Voltage Tuned by a Template Graphene Monolayer. *J. Phys. Chem. C* **2015**, *119*, 45–54.
- (63) Nguyen, N. N.; Jo, S. B.; Lee, S. K.; Sin, D. H.; Kang, B.; Kim, H. H.; Lee, H.; Cho, K. Atomically Thin Epitaxial Template for Organic Crystal Growth Using Graphene with Controlled Surface Wettability. *Nano Lett.* **2015**, *15*, 2474–2484.

- (64) Karmel, H. J.; Chien, T.; Demers-Carpentier, V.; Garramone, J. J.; Hersam, M. C. Self-Assembled Two-Dimensional Heteromolecular Nanoporous Molecular Arrays on Epitaxial Graphene. *J. Phys. Chem. Lett.* **2014**, *5*, 270–274.
- (65) Chhikara, M.; Pavlica, E.; Matković, A.; Beltaos, A.; Gajić, R.; Bratina, G. Pentacene on graphene: Differences between single layer and bilayer. *Carbon* **2014**, *69*, 162–168.
- (66) Betti, M. G.; Kanjilal, A.; Mariani, C. Electronic States of a Single Layer of Pentacene: Standing-Up and Flat-Lying Configurations†. *J. Phys. Chem. A* **2007**, *111*, 12454–12457.
- (67) Salzmann, I.; Moser, A.; Oehzelt, M.; Breuer, T.; Feng, X.; Juang, Z.-Y.; Nabok, D.; Della Valle, R. G.; Duham, S.; Heimel, G.; et al., Epitaxial Growth of  $\pi$ -Stacked Perfluoropentacene on Graphene-Coated Quartz. *ACS Nano* **2012**, *6*, 10874–10883.
- (68) Breuer, T.; Maßmeyer, T.; Mänz, A.; Zoerb, S.; Harbrecht, B.; Witte, G. Structure of van der Waals bound hybrids of organic semiconductors and transition metal dichalcogenides: the case of acene films on MoS<sub>2</sub>. *Phys. Status Solidi RRL* **2016**, *10*, 905–910.
- (69) Lee, C.-H.; Schiros, T.; Santos, E. J. G.; Kim, B.; Yager, K. G.; Kang, S. J.; Lee, S.; Yu, J.; Watanabe, K.; Taniguchi, T.; et al., Epitaxial Growth of Molecular Crystals on van der Waals Substrates for High-Performance Organic Electronics. *Adv. Mater.* **2014**, *26*, 2812–2817.
- (70) Wang, Q. H.; Hersam, M. C. Room-temperature molecular-resolution characterization of self-assembled organic monolayers on epitaxial graphene. *Nat. Chem.* **2009**, *1*, 206–211.
- (71) Tian, X. Q.; Xu, J. B.; Wang, X. M. Self-Assembly of PTCDA Ultrathin Films on Graphene: Structural Phase Transition and Charge Transfer Saturation. *J. Phys. Chem. C* **2010**, *114*, 20917–20924.

- (72) Huang, H.; Chen, S.; Gao, X.; Chen, W.; Wee, A. T. S. Structural and Electronic Properties of PTCDA Thin Films on Epitaxial Graphene. *ACS Nano* **2009**, *3*, 3431–3436.
- (73) Meissner, M.; Gruenewald, M.; Sojka, F.; Udhardt, C.; Forker, R.; Fritz, T. Highly ordered growth of PTCDA on epitaxial bilayer graphene. *Surf. Sci.* **2012**, *606*, 1709–1715.
- (74) Liu, X.; Gu, J.; Ding, K.; Fan, D.; Hu, X.; Tseng, Y.-W.; Lee, Y.-H.; Menon, V.; Forrest, S. R. Photoresponse of an Organic Semiconductor/Two-Dimensional Transition Metal Dichalcogenide Heterojunction. *Nano Lett.* **2017**, *17*, 3176–3181.
- (75) Lauffer, P.; Emtsev, K. V.; Graupner, R.; Seyller, T.; Ley, L. Molecular and electronic structure of PTCDA on bilayer graphene on SiC(0001) studied with scanning tunneling microscopy. *Phys. Status Solidi B* **2008**, *245*, 2064–2067.
- (76) Mura, M.; Sun, X.; Silly, F.; Jonkman, H. T.; Briggs, G. A. D.; Castell, M. R.; Kantorovich, L. N. Experimental and theoretical analysis of H-bonded supramolecular assemblies of PTCDA molecules. *Phys. Rev. B* **2010**, *81*, 195412.
- (77) Voggu, R.; Das, B.; Rout, C. S.; Rao, C. N. R. Effects of charge transfer interaction of graphene with electron donor and acceptor molecules examined using Raman spectroscopy and cognate techniques. *J. Phys.: Condens. Matter* **2008**, *20*, 472204.
- (78) Chen, W.; Chen, S.; Qi, D. C.; Gao, X. Y.; Wee, A. T. S. Surface Transfer p-Type Doping of Epitaxial Graphene. *J. Am. Chem. Soc.* **2007**, *129*, 10418–10422.
- (79) Barja, S.; Garnica, M.; Hinarejos, J. J.; Vázquez de Parga, A. L.; Martín, N.; Miranda, R. Self-organization of electron acceptor molecules on graphene. *Chem. Commun.* **2010**, *46*, 8198–8200.

- (80) Hong, G.; Wu, Q.-H.; Wang, C.; Ren, J.; Xu, T.; Zhang, W.; Lee, S.-T. Surface doping of nitrogen atoms on graphene via molecular precursor. *Appl. Phys. Lett.* **2013**, *102*, 051610.
- (81) Garnica, M.; Stradi, D.; Barja, S.; Calleja, F.; Díaz, C.; Alcamí, M.; Martín, N.; Vázquez de Parga, A. L.; Martín, F.; Miranda, R. Long-range magnetic order in a purely organic 2D layer adsorbed on epitaxial graphene. *Nat. Phys.* **2013**, *9*, 368–374.
- (82) Maccariello, D.; Garnica, M.; Niño, M. A.; Navío, C.; Perna, P.; Barja, S.; Vázquez de Parga, A. L.; Miranda, R. Spatially Resolved, Site-Dependent Charge Transfer and Induced Magnetic Moment in TCNQ Adsorbed on Graphene. *Chem. Mater.* **2014**, *26*, 2883–2890.
- (83) Stradi, D.; Garnica, M.; Díaz, C.; Calleja, F.; Barja, S.; Martín, N.; Alcamí, M.; Vazquez de Parga, A. L.; Miranda, R.; Martín, F. Controlling the spatial arrangement of organic magnetic anions adsorbed on epitaxial graphene on Ru(0001). *Nanoscale* **2014**, *6*, 15271–15279.
- (84) Tsai, H.-Z.; Omrani, A. A.; Coh, S.; Oh, H.; Wickenburg, S.; Son, Y.-W.; Wong, D.; Riss, A.; Jung, H. S.; Nguyen, G. D.; et al., Molecular Self-Assembly in a Poorly Screened Environment: F4TCNQ on Graphene/BN. *ACS Nano* **2015**, *9*, 12168–12173.
- (85) Kim, K. L.; Lee, W.; Hwang, S. K.; Joo, S. H.; Cho, S. M.; Song, G.; Cho, S. H.; Jeong, B.; Hwang, I.; Ahn, J.-H.; et al., Epitaxial Growth of Thin Ferroelectric Polymer Films on Graphene Layer for Fully Transparent and Flexible Nonvolatile Memory. *Nano Lett.* **2016**, *16*, 334–340.
- (86) Hunter, C. A.; Sanders, J. K. M. The nature of  $\pi - \pi$  interactions. *J. Am. Chem. Soc.* **1990**, *112*, 5525–5534.
- (87) Pollard, A.; Perkins, E.; Smith, N.; Saywell, A.; Goretzki, G.; Phillips, A.; Argent, S.;

- Sachdev, H.; Müller, F.; Hüfner, S.; et al., Supramolecular Assemblies Formed on an Epitaxial Graphene Superstructure. *Angew. Chem. Int. Ed.* **2010**, *49*, 1794–1799.
- (88) Karmel, H. J.; Garramone, J. J.; Emery, J. D.; Kewalramani, S.; Bedzyk, M. J.; Hersam, M. C. Self-assembled organic monolayers on epitaxial graphene with enhanced structural and thermal stability. *Chem. Commun.* **2014**, *50*, 8852–8855.
- (89) Rochefort, A.; Wuest, J. D. Interaction of Substituted Aromatic Compounds with Graphene. *Langmuir* **2009**, *25*, 210–215.
- (90) Addou, R.; Batzill, M. Defects and Domain Boundaries in Self-Assembled Terephthalic Acid (TPA) Monolayers on CVD-Grown Graphene on Pt(111). *Langmuir* **2013**, *29*, 6354–6360.
- (91) Kozlov, S. M.; Viñes, F.; Görling, A. On the interaction of polycyclic aromatic compounds with graphene. *Carbon* **2012**, *50*, 2482–2492.
- (92) Roos, M.; Uhl, B.; Künzel, D.; Hoster, H. E.; Groß, A.; Behm, R. J. Intermolecular vs molecule–substrate interactions: A combined STM and theoretical study of supramolecular phases on graphene/Ru(0001). *Beilstein J. Nanotechnol.* **2011**, *2*, 365–373.
- (93) Meier, C.; Roos, M.; Künzel, D.; Breitrock, A.; Hoster, H. E.; Landfester, K.; Gross, A.; Behm, R. J.; Ziener, U. Concentration and Coverage Dependent Adlayer Structures: From Two-Dimensional Networks to Rotation in a Bearing. *J. Phys. Chem. C* **2010**, *114*, 1268–1277.
- (94) Prado, M. C.; Nascimento, R.; Moura, L. G.; Matos, M. J. S.; Mazzoni, M. S. C.; Cancado, L. G.; Chacham, H.; Neves, B. R. A. Two-Dimensional Molecular Crystals of Phosphonic Acids on Graphene. *ACS Nano* **2011**, *5*, 394–398.

- (95) Bakti Utama, M. I.; Zhang, Q.; Zhang, J.; Yuan, Y.; Belarre, F. J.; Arbiol, J.; Xiong, Q. Recent developments and future directions in the growth of nanostructures by van der Waals epitaxy. *Nanoscale* **2013**, *5*, 3570–3588.
- (96) Shi, Y.; Zhou, W.; Lu, A.-Y.; Fang, W.; Lee, Y.-H.; Hsu, A. L.; Kim, S. M.; Kim, K. K.; Yang, H. Y.; Li, L.-J.; et al., van der Waals Epitaxy of MoS<sub>2</sub> Layers Using Graphene As Growth Templates. *Nano Lett.* **2012**, *12*, 2784–2791.
- (97) McCreary, K. M.; Hanbicki, A. T.; Robinson, J. T.; Cobas, E.; Culbertson, J. C.; Friedman, A. L.; Jernigan, G. G.; Jonker, B. T. Large-Area Synthesis of Continuous and Uniform MoS<sub>2</sub> Monolayer Films on Graphene. *Adv. Funct. Mater.* **2014**, *24*, 6449–6454.
- (98) Miwa, J. A.; Dendzik, M.; Grønborg, S. S.; Bianchi, M.; Lauritsen, J. V.; Hofmann, P.; Ulstrup, S. Van der Waals Epitaxy of Two-Dimensional MoS<sub>2</sub>–Graphene Heterostructures in Ultrahigh Vacuum. *ACS Nano* **2015**, *9*, 6502–6510.
- (99) Liu, X.; Balla, I.; Bergeron, H.; Campbell, G. P.; Bedzyk, M. J.; Hersam, M. C. Rotationally Commensurate Growth of MoS<sub>2</sub> on Epitaxial Graphene. *ACS Nano* **2016**, *10*, 1067–1075.
- (100) Lin, Y.-C.; Lu, N.; Perea-Lopez, N.; Li, J.; Lin, Z.; Peng, X.; Lee, C. H.; Sun, C.; Calderin, L.; Browning, P. N.; et al., Direct Synthesis of van der Waals Solids. *ACS Nano* **2014**, *8*, 3715–3723.
- (101) Lin, Y.-C.; Ghosh, R. K.; Addou, R.; Lu, N.; Eichfeld, S. M.; Zhu, H.; Li, M.-Y.; Peng, X.; Kim, M. J.; Li, L.-J.; et al., Atomically thin resonant tunnel diodes built from synthetic van der Waals heterostructures. *Nat. Commun.* **2015**, *6*, 7311.
- (102) Lin, Y.-C.; Chang, C.-Y. S.; Ghosh, R. K.; Li, J.; Zhu, H.; Addou, R.; Diaconescu, B.; Ohta, T.; Peng, X.; Lu, N.; et al., Atomically Thin Heterostructures Based on Single-Layer Tungsten Diselenide and Graphene. *Nano Letters* **2014**, *14*, 6936–6941.

- (103) Azizi, A.; Eichfeld, S.; Geschwind, G.; Zhang, K.; Jiang, B.; Mukherjee, D.; Hosain, L.; Piasecki, A. F.; Kabius, B.; Robinson, J. A.; et al., Freestanding van der Waals Heterostructures of Graphene and Transition Metal Dichalcogenides. *ACS Nano* **2015**, *9*, 4882–4890.
- (104) Ago, H.; Endo, H.; Solís-Fernández, P.; Takizawa, R.; Ohta, Y.; Fujita, Y.; Yamamoto, K.; Tsuji, M. Controlled van der Waals Epitaxy of Monolayer MoS<sub>2</sub> Triangular Domains on Graphene. *ACS Appl. Mater. Interfaces* **2015**, *7*, 5265–5273.
- (105) Kim, E. S.; Hwang, J.-Y.; Lee, K. H.; Ohta, H.; Lee, Y. H.; Kim, S. W. Graphene Substrate for van der Waals Epitaxy of Layer-Structured Bismuth Antimony Telluride Thermoelectric Film. *Adv. Mater.* **2016**, *29*, 1604899.
- (106) Yan, A.; Velasco, J.; Kahn, S.; Watanabe, K.; Taniguchi, T.; Wang, F.; Crommie, M. F.; Zettl, A. Direct Growth of Single- and Few-Layer MoS<sub>2</sub> on h-BN with Preferred Relative Rotation Angles. *Nano Lett.* **2015**, *15*, 6324–6331.
- (107) Wang, S.; Wang, X.; Warner, J. H. All Chemical Vapor Deposition Growth of MoS<sub>2</sub> :h-BN Vertical van der Waals Heterostructures. *ACS Nano* **2015**, *9*, 5246–5254.
- (108) Cattelan, M.; Markman, B.; Lucchini, G.; Das, P. K.; Vobornik, I.; Robinson, J. A.; Agnoli, S.; Granozzi, G. New Strategy for the Growth of Complex Heterostructures Based on Different 2D Materials. *Chem. Mater.* **2015**, *27*, 4105–4113.
- (109) Gehring, P.; Gao, B. F.; Burghard, M.; Kern, K. Growth of High-Mobility Bi<sub>2</sub>Te<sub>2</sub>Se Nanoplatelets on hBN Sheets by van der Waals Epitaxy. *Nano Lett.* **2012**, *12*, 5137–5142.
- (110) Yang, W.; Chen, G.; Shi, Z.; Liu, C.-C.; Zhang, L.; Xie, G.; Cheng, M.; Wang, D.; Yang, R.; Shi, D.; et al., Epitaxial growth of single-domain graphene on hexagonal boron nitride. *Nat. Mater.* **2013**, *12*, 792–797.

- (111) Liu, Z.; Song, L.; Zhao, S.; Huang, J.; Ma, L.; Zhang, J.; Lou, J.; Ajayan, P. M. Direct Growth of Graphene/Hexagonal Boron Nitride Stacked Layers. *Nano Lett.* **2011**, *11*, 2032–2037.
- (112) Zhang, C.; Zhao, S.; Jin, C.; Koh, A. L.; Zhou, Y.; Xu, W.; Li, Q.; Xiong, Q.; Peng, H.; Liu, Z. Direct growth of large-area graphene and boron nitride heterostructures by a co-segregation method. *Nat. Commun.* **2015**, *6*, 6519.
- (113) Xu, Z.; Zheng, R.; Khanaki, A.; Zuo, Z.; Liu, J. Direct growth of graphene on in situ epitaxial hexagonal boron nitride flakes by plasma-assisted molecular beam epitaxy. *Appl. Phys. Lett.* **2015**, *107*, 213103.
- (114) Driver, M. S.; Beatty, J. D.; Olanipekun, O.; Reid, K.; Rath, A.; Voyles, P. M.; Kelber, J. A. Atomic Layer Epitaxy of h-BN(0001) Multilayers on Co(0001) and Molecular Beam Epitaxy Growth of Graphene on h-BN(0001)/Co(0001). *Langmuir* **2016**, *32*, 2601–2607.
- (115) Zhang, X.; Meng, F.; Christianson, J. R.; Arroyo-Torres, C.; Lukowski, M. A.; Liang, D.; Schmidt, J. R.; Jin, S. Vertical Heterostructures of Layered Metal Chalcogenides by van der Waals Epitaxy. *Nano Lett.* **2014**, *14*, 3047–3054.
- (116) Diaz, H. C.; Chaghi, R.; Ma, Y.; Batzill, M. Molecular beam epitaxy of the van der Waals heterostructure MoTe<sub>2</sub> on MoS<sub>2</sub>: phase, thermal, and chemical stability. *2D Mater.* **2015**, *2*, 044010.
- (117) Gong, Y.; Lin, J.; Wang, X.; Shi, G.; Lei, S.; Lin, Z.; Zou, X.; Ye, G.; Vajtai, R.; Yakobson, B. I.; et al., Vertical and in-plane heterostructures from WS<sub>2</sub>/MoS<sub>2</sub> monolayers. *Nat. Mater.* **2014**, *13*, 1135–1142.
- (118) Alemayehu, M. B.; Falmbigl, M.; Ta, K.; Ditto, J.; Medlin, D. L.; Johnson, D. C. Designed Synthesis of van der Waals Heterostructures: The Power of Kinetic Control. *Angew. Chem. Int. Ed.* **2015**, *54*, 15468–15472.

- (119) Xenogiannopoulou, E.; Tsipas, P.; Aretouli, K. E.; Tsoutsou, D.; Giamini, S. A.; Bazioti, C.; Dimitrakopoulos, G. P.; Komninou, P.; Brems, S.; Huyghebaert, C.; et al., High-quality, large-area MoSe<sub>2</sub>and MoSe<sub>2</sub>/Bi<sub>2</sub>Se<sub>3</sub>heterostructures on AlN(0001)/Si(111) substrates by molecular beam epitaxy. *Nanoscale* **2015**, *7*, 7896–7905.
- (120) Li, X.; Lin, M.-W.; Lin, J.; Huang, B.; Puretzky, A. A.; Ma, C.; Wang, K.; Zhou, W.; Pantelides, S. T.; Chi, M.; et al., Two-dimensional GaSe/MoSe<sub>2</sub> misfit bilayer heterojunctions by van der Waals epitaxy. *Sci. Adv.* **2016**, *2*, e1501882.
- (121) Zhang, Y.; Qiu, Z.; Cheng, X.; Xie, H.; Wang, H.; Xie, X.; Yu, Y.; Liu, R. Direct growth of high-quality Al<sub>2</sub>O<sub>3</sub> dielectric on graphene layers by low-temperature H<sub>2</sub>O-based ALD. *J. Phys. D: Appl. Phys.* **2014**, *47*, 055106.
- (122) Vaziri, S.; Lupina, G.; Henkel, C.; Smith, A. D.; Östling, M.; Dabrowski, J.; Lippert, G.; Mehr, W.; Lemme, M. C. A Graphene-Based Hot Electron Transistor. *Nano Lett.* **2013**, *13*, 1435–1439.
- (123) Alaboson, J. M. P.; Wang, Q. H.; Emery, J. D.; Lipson, A. L.; Bedzyk, M. J.; Elam, J. W.; Pellin, M. J.; Hersam, M. C. Seeding Atomic Layer Deposition of High-kDielectrics on Epitaxial Graphene with Organic Self-Assembled Monolayers. *ACS Nano* **2011**, *5*, 5223–5232.
- (124) Li, W.; Wang, F.; Liu, Y.; Wang, J.; Yang, J.; Zhang, L.; Elzatahry, A. A.; Al-Dahyan, D.; Xia, Y.; Zhao, D. General Strategy to Synthesize Uniform Mesoporous TiO<sub>2</sub>/Graphene/Mesoporous TiO<sub>2</sub> Sandwich-Like Nanosheets for Highly Reversible Lithium Storage. *Nano Lett.* **2015**, *15*, 2186–2193.
- (125) Kumar, B.; Lee, K. Y.; Park, H.-K.; Chae, S. J.; Lee, Y. H.; Kim, S.-W. Controlled Growth of Semiconducting Nanowire, Nanowall, and Hybrid Nanostructures on Graphene for Piezoelectric Nanogenerators. *ACS Nano* **2011**, *5*, 4197–4204.

- (126) Zhang, Y.; Tang, Z.-R.; Fu, X.; Xu, Y.-J. Engineering the Unique 2D Mat of Graphene to Achieve Graphene-TiO<sub>2</sub> Nanocomposite for Photocatalytic Selective Transformation: What Advantage does Graphene Have over Its Forebear Carbon Nanotube? *ACS Nano* **2011**, *5*, 7426–7435.
- (127) Chung, K.; Lee, C.-H.; Yi, G.-C. Transferable GaN Layers Grown on ZnO-Coated Graphene Layers for Optoelectronic Devices. *Science* **2010**, *330*, 655–657.
- (128) Oh, H.; Hong, Y. J.; Kim, K.-S.; Yoon, S.; Baek, H.; Kang, S.-H.; Kwon, Y.-K.; Kim, M.; Yi, G.-C. Architecture van der Waals epitaxy of ZnO nanostructures on hexagonal BN. *NPG Asia Mater.* **2014**, *6*, e145.
- (129) Chung, K.; In Park, S.; Baek, H.; Chung, J.-S.; Yi, G.-C. High-quality GaN films grown on chemical vapor-deposited graphene films. *NPG Asia Mater.* **2012**, *4*, e24.
- (130) Nepal, N.; Wheeler, V. D.; Anderson, T. J.; Kub, F. J.; Mastro, M. A.; Myers-Ward, R. L.; Qadri, S. B.; Freitas, J. A.; Hernandez, S. C.; Nyakiti, L. O.; et al., Epitaxial Growth of III–Nitride/Graphene Heterostructures for Electronic Devices. *Appl. Phys. Express* **2013**, *6*, 061003.
- (131) Yoo, H.; Chung, K.; In Park, S.; Kim, M.; Yi, G.-C. Microstructural defects in GaN thin films grown on chemically vapor-deposited graphene layers. *Appl. Phys. Lett.* **2013**, *102*, 051908.
- (132) Kim, J.; Bayram, C.; Park, H.; Cheng, C.-W.; Dimitrakopoulos, C.; Ott, J. A.; Reuter, K. B.; Bedell, S. W.; Sadana, D. K. Principle of direct van der Waals epitaxy of single-crystalline films on epitaxial graphene. *Nat. Commun.* **2014**, *5*, 4836.
- (133) Kim, Y.; Cruz, S. S.; Lee, K.; Alawode, B. O.; Choi, C.; Song, Y.; Johnson, J. M.; Heidelberger, C.; Kong, W.; Choi, S.; et al., Remote epitaxy through graphene enables two-dimensional material-based layer transfer. *Nature* **2017**, *544*, 340–343.

- (134) Alaskar, Y.; Arafin, S.; Lin, Q.; Wickramaratne, D.; McKay, J.; Norman, A. G.; Zhang, Z.; Yao, L.; Ding, F.; Zou, J.; et al., Theoretical and experimental study of highly textured GaAs on silicon using a graphene buffer layer. *J. Cryst. Growth* **2015**, *425*, 268–273.
- (135) Kobayashi, Y.; Kumakura, K.; Akasaka, T.; Makimoto, T. Layered boron nitride as a release layer for mechanical transfer of GaN-based devices. *Nature* **2012**, *484*, 223–227.
- (136) Löher, T.; Tomm, Y.; Pettenkofer, C.; Jaegermann, W. Van der Waals epitaxy of three-dimensional CdS on the two-dimensional layered substrate MoTe<sub>2</sub>(0001). *Appl. Phys. Lett.* **1994**, *65*, 555–557.
- (137) Löher, T.; Tomm, Y.; Klein, A.; Su, D.; Pettenkofer, C.; Jaegermann, W. Highly oriented layers of the three-dimensional semiconductor CdTe on the two-dimensional layered semiconductors MoTe<sub>2</sub> and WSe<sub>2</sub>. *J. Appl. Phys.* **1996**, *80*, 5718–5722.
- (138) Colson, J. W.; Mann, J. A.; DeBlase, C. R.; Dichtel, W. R. Patterned growth of oriented 2D covalent organic framework thin films on single-layer graphene. *J. Polym. Sci. A: Polym. Chem.* **2014**, *53*, 378–384.
- (139) Colson, J. W.; Woll, A. R.; Mukherjee, A.; Levendorf, M. P.; Spitler, E. L.; Shields, V. B.; Spencer, M. G.; Park, J.; Dichtel, W. R. Oriented 2D Covalent Organic Framework Thin Films on Single-Layer Graphene. *Science* **2011**, *332*, 228–231.
- (140) Sun, B.; Zhu, C.-H.; Liu, Y.; Wang, C.; Wan, L.-J.; Wang, D. Oriented Covalent Organic Framework Film on Graphene for Robust Ambipolar Vertical Organic Field-Effect Transistor. *Chem. Mater.* **2017**, *29*, 4367–4374.
- (141) Urgel, J. I.; Schwarz, M.; Garnica, M.; Stassen, D.; Bonifazi, D.; Ecija, D.; Barth, J. V.; Auwärter, W. Controlling Coordination Reactions and Assembly on a Cu(111) Supported Boron Nitride Monolayer. *J. Am. Chem. Soc.* **2015**, *137*, 2420–2423.

- (142) Kumar, R.; Jayaramulu, K.; Maji, T. K.; Rao, C. N. R. Growth of 2D sheets of a MOF on graphene surfaces to yield composites with novel gas adsorption characteristics. *Dalton Trans.* **2014**, *43*, 7383–7386.
- (143) Grimme, S. Do Special Noncovalent  $\pi$ – $\pi$  Stacking Interactions Really Exist? *Angew. Chem. Int. Ed.* **2008**, *47*, 3430–3434.
- (144) Zhang, Z.; Huang, H.; Yang, X.; Zang, L. Tailoring Electronic Properties of Graphene by  $\pi$ – $\pi$  Stacking with Aromatic Molecules. *J. Phys. Chem. Lett.* **2011**, *2*, 2897–2905.
- (145) Yang, J.; Yan, D.; Jones, T. S. Molecular Template Growth and Its Applications in Organic Electronics and Optoelectronics. *Chem. Rev.* **2015**, *115*, 5570–5603.
- (146) Zhong, S.; Zhong, J. Q.; Mao, H. Y.; Wang, R.; Wang, Y.; Qi, D. C.; Loh, K. P.; Wee, A. T. S.; Chen, Z. K.; Chen, W. CVD Graphene as Interfacial Layer to Engineer the Organic Donor–Acceptor Heterojunction Interface Properties. *ACS Appl. Mater. Interfaces* **2012**, *4*, 3134–3140.
- (147) Mativetsky, J. M.; Wang, H.; Lee, S. S.; Whittaker-Brooks, L.; Loo, Y.-L. Face-on stacking and enhanced out-of-plane hole mobility in graphene-templated copper phthalocyanine. *Chem. Commun.* **2014**, *50*, 5319–5321.
- (148) Shih, C.-J.; Pfattner, R.; Chiu, Y.-C.; Liu, N.; Lei, T.; Kong, D.; Kim, Y.; Chou, H.-H.; Bae, W.-G.; Bao, Z. Partially-Screened Field Effect and Selective Carrier Injection at Organic Semiconductor/Graphene Heterointerface. *Nano Lett.* **2015**, *15*, 7587–7595.
- (149) Hlawacek, G.; Khokhar, F. S.; van Gastel, R.; Poelsema, B.; Teichert, C. Smooth Growth of Organic Semiconductor Films on Graphene for High-Efficiency Electronics. *Nano Lett.* **2011**, *11*, 333–337.
- (150) Kim, B.; Chiu, C.-Y.; Kang, S. J.; Kim, K. S.; Lee, G.-H.; Chen, Z.; Ahn, S.; Yager, K. G.; Ciston, J.; Nuckolls, C.; et al., Vertically grown nanowire crystals of

dibenzotetrathienocoronene (DBTTC) on large-area graphene. *RSC Adv.* **2016**, *6*, 59582–59589.

- (151) Lin, Y.-C.; Dumcenco, D. O.; Huang, Y.-S.; Suenaga, K. Atomic mechanism of the semiconducting-to-metallic phase transition in single-layered MoS<sub>2</sub>. *Nat. Nanotechnol.* **2014**, *9*, 391–396.
- (152) Govind Rajan, A.; Sresht, V.; Pádua, A. A. H.; Strano, M. S.; Blankschtein, D. Dominance of Dispersion Interactions and Entropy over Electrostatics in Determining the Wettability and Friction of Two-Dimensional MoS<sub>2</sub> Surfaces. *ACS Nano* **2016**, *10*, 9145–9155.
- (153) Matković, A.; Genser, J.; Lüftner, D.; Kratzer, M.; Gajić, R.; Puschnig, P.; Teichert, C. Epitaxy of highly ordered organic semiconductor crystallite networks supported by hexagonal boron nitride. *Sci. Rep.* **2016**, *6*, 38519.
- (154) Das Sarma, S.; Adam, S.; Hwang, E. H.; Rossi, E. Electronic transport in two-dimensional graphene. *Rev. Mod. Phys.* **2011**, *83*, 407–470.
- (155) Varchon, F.; Feng, R.; Hass, J.; Li, X.; Nguyen, B. N.; Naud, C.; Mallet, P.; Veuillen, J.-Y.; Berger, C.; Conrad, E. H.; et al., Electronic Structure of Epitaxial Graphene Layers on SiC: Effect of the Substrate. *Phys. Rev. Lett.* **2007**, *99*, 126805.
- (156) Giovannetti, G.; Khomyakov, P. A.; Brocks, G.; Karpan, V. M.; van den Brink, J.; Kelly, P. J. Doping Graphene with Metal Contacts. *Phys. Rev. Lett.* **2008**, *101*, 026803.
- (157) Chen, W.; Santos, E. J. G.; Zhu, W.; Kaxiras, E.; Zhang, Z. Tuning the Electronic and Chemical Properties of Monolayer MoS<sub>2</sub> Adsorbed on Transition Metal Substrates. *Nano Lett.* **2013**, *13*, 509–514.
- (158) Das, A.; Pisana, S.; Chakraborty, B.; Piscanec, S.; Saha, S. K.; Waghmare, U. V.; Novoselov, K. S.; Krishnamurthy, H. R.; Geim, A. K.; Ferrari, A. C.; et al., Monitoring

dopants by Raman scattering in an electrochemically top-gated graphene transistor. *Nat. Nanotechnol.* **2008**, *3*, 210–215.

- (159) Perera, M. M.; Lin, M.-W.; Chuang, H.-J.; Chamlagain, B. P.; Wang, C.; Tan, X.; Cheng, M. M.-C.; Tománek, D.; Zhou, Z. Improved Carrier Mobility in Few-Layer MoS<sub>2</sub> Field-Effect Transistors with Ionic-Liquid Gating. *ACS Nano* **2013**, *7*, 4449–4458.
- (160) Ren, H.; Zhang, L.; Li, X.; Li, Y.; Wu, W.; Li, H. Interfacial structure and wetting properties of water droplets on graphene under a static electric field. *Phys. Chem. Chem. Phys.* **2015**, *17*, 23460–23467.
- (161) Ostrowski, J. H. J.; Eaves, J. D. The Tunable Hydrophobic Effect on Electrically Doped Graphene. *J. Phys. Chem. B* **2014**, *118*, 530–536.
- (162) Ashraf, A.; Wu, Y.; Wang, M. C.; Yong, K.; Sun, T.; Jing, Y.; Haasch, R. T.; Aluru, N. R.; Nam, S. Doping-Induced Tunable Wettability and Adhesion of Graphene. *Nano Lett.* **2016**, 4708–4712.
- (163) Hong, G.; Han, Y.; Schutzius, T. M.; Wang, Y.; Pan, Y.; Hu, M.; Jie, J.; Sharma, C. S.; Müller, U.; Poulikakos, D. On the Mechanism of Hydrophilicity of Graphene. *Nano Lett.* **2016**, 4447–4453.
- (164) Akiyoshi, H.; Goto, H.; Uesugi, E.; Eguchi, R.; Yoshida, Y.; Saito, G.; Kubozono, Y. Carrier Accumulation in Graphene with Electron Donor/Acceptor Molecules. *Adv. Electron. Mater.* **2015**, *1*, 1500073.
- (165) Cai, B.; Zhang, S.; Yan, Z.; Zeng, H. Noncovalent Molecular Doping of Two-Dimensional Materials. *ChemNanoMat* **2015**, *1*, 542–557.
- (166) Wehling, T. O.; Novoselov, K. S.; Morozov, S. V.; Vdovin, E. E.; Katsnelson, M. I.;

Geim, A. K.; Lichtenstein, A. I. Molecular Doping of Graphene. *Nano Lett.* **2008**, *8*, 173–177.

- (167) Coletti, C.; Riedl, C.; Lee, D. S.; Krauss, B.; Patthey, L.; von Klitzing, K.; Smet, J. H.; Starke, U. Charge neutrality and band-gap tuning of epitaxial graphene on SiC by molecular doping. *Phys. Rev. B* **2010**, *81*, 235401.
- (168) Sakurai, M.; Tada, H.; Saiki, K.; Koma, A. Van der Waals Epitaxial Growth of C60 Film on a Cleaved Face of MoS<sub>2</sub>. *Jpn. J. Appl. Phys.* **1991**, *30*, L1892–L1894.
- (169) Zhang, R.; Li, B.; Yang, J. A First-Principles Study on Electron Donor and Acceptor Molecules Adsorbed on Phosphorene. *J. Phys. Chem. C* **2015**, *119*, 2871–2878.
- (170) Hämäläinen, S. K.; Boneschanscher, M. P.; Jacobse, P. H.; Swart, I.; Pussi, K.; Moritz, W.; Lahtinen, J.; Liljeroth, P.; Sainio, J. Structure and local variations of the graphene moiré on Ir(111). *Phys. Rev. B* **2013**, *88*, 201406(R).
- (171) Schulz, F.; Drost, R.; Hämäläinen, S. K.; Demonchaux, T.; Seitsonen, A. P.; Liljeroth, P. Epitaxial hexagonal boron nitride on Ir(111): A work function template. *Phys. Rev. B* **2014**, *89*, 235429.
- (172) Pletikosić, I.; Kralj, M.; Pervan, P.; Brako, R.; Coraux, J.; N'Diaye, A. T.; Busse, C.; Michely, T. Dirac Cones and Minigaps for Graphene on Ir(111). *Phys. Rev. Lett.* **2009**, *102*, 056808.
- (173) Busse, C.; Lazić, P.; Djemour, R.; Coraux, J.; Gerber, T.; Atodiresei, N.; Caciuc, V.; Brako, R.; N'Diaye, A. T.; Blügel, S.; et al., Graphene on Ir(111): Physisorption with Chemical Modulation. *Phys. Rev. Lett.* **2011**, *107*, 036101.
- (174) Sutter, P.; Sadowski, J. T.; Sutter, E. Graphene on Pt(111): Growth and substrate interaction. *Phys. Rev. B* **2009**, *80*, 245411.

- (175) Ćavar, E.; Westerström, R.; Mikkelsen, A.; Lundgren, E.; Vinogradov, A.; Ng, M. L.; Preobrajenski, A.; Zakharov, A.; Mårtensson, N. A single h-BN layer on Pt(111). *Surf. Sci.* **2008**, *602*, 1722–1726.
- (176) Joshi, S.; Ecija, D.; Koitz, R.; Iannuzzi, M.; Seitsonen, A. P.; Hutter, J.; Sachdev, H.; Vijayaraghavan, S.; Bischoff, F.; Seufert, K.; et al., Boron Nitride on Cu(111): An Electronically Corrugated Monolayer. *Nano Lett.* **2012**, *12*, 5821–5828.
- (177) Moritz, W.; Wang, B.; Bocquet, M.-L.; Brugger, T.; Greber, T.; Wintterlin, J.; Günther, S. Structure Determination of the Coincidence Phase of Graphene on Ru(0001). *Phys. Rev. Lett.* **2010**, *104*, 136102.
- (178) Wang, B.; Caffio, M.; Bromley, C.; Früchtl, H.; Schaub, R. Coupling Epitaxy, Chemical Bonding, and Work Function at the Local Scale in Transition Metal-Supported Graphene. *ACS Nano* **2010**, *4*, 5773–5782.
- (179) Dil, H.; Lobo-Checa, J.; Laskowski, R.; Blaha, P.; Berner, S.; Osterwalder, J.; Greber, T. Surface Trapping of Atoms and Molecules with Dipole Rings. *Science* **2008**, *319*, 1824–1826.
- (180) Mao, J.; Zhang, H.; Jiang, Y.; Pan, Y.; Gao, M.; Xiao, W.; Gao, H.-J. Tunability of Supramolecular Kagome Lattices of Magnetic Phthalocyanines Using Graphene-Based Moiré Patterns as Templates. *J. Am. Chem. Soc.* **2009**, *131*, 14136–14137.
- (181) Zhou, H. T.; Mao, J. H.; Li, G.; Wang, Y. L.; Feng, X. L.; Du, S. X.; Müllen, K.; Gao, H.-J. Direct imaging of intrinsic molecular orbitals using two-dimensional, epitaxially-grown, nanostructured graphene for study of single molecule and interactions. *Appl. Phys. Lett.* **2011**, *99*, 153101.
- (182) Järvinen, P.; Hämäläinen, S. K.; Ijäs, M.; Harju, A.; Liljeroth, P. Self-Assembly and Orbital Imaging of Metal Phthalocyanines on a Graphene Model Surface. *J. Phys. Chem. C* **2014**, *118*, 13320–13325.

- (183) Schulz, F.; Drost, R.; Hämäläinen, S. K.; Liljeroth, P. Templated Self-Assembly and Local Doping of Molecules on Epitaxial Hexagonal Boron Nitride. *ACS Nano* **2013**, *7*, 11121–11128.
- (184) Joshi, S.; Bischoff, F.; Koitz, R.; Ecija, D.; Seufert, K.; Seitsonen, A. P.; Hutter, J.; Diller, K.; Urgel, J. I.; Sachdev, H.; et al., Control of Molecular Organization and Energy Level Alignment by an Electronically Nanopatterned Boron Nitride Template. *ACS Nano* **2014**, *8*, 430–442.
- (185) Sørensen, S. G.; Füchtbauer, H. G.; Tuxen, A. K.; Walton, A. S.; Lauritsen, J. V. Structure and Electronic Properties of In Situ Synthesized Single-Layer MoS<sub>2</sub> on a Gold Surface. *ACS Nano* **2014**, *8*, 6788–6796.
- (186) Le, D.; Sun, D.; Lu, W.; Bartels, L.; Rahman, T. S. Single layer MoS<sub>2</sub> on the Cu(111) surface: First-principles electronic structure calculations. *Phys. Rev. B* **2012**, *85*, 075429.
- (187) Kang, J.; Li, J.; Li, S.-S.; Xia, J.-B.; Wang, L.-W. Electronic Structural Moiré Pattern Effects on MoS<sub>2</sub>/MoSe<sub>2</sub> 2D Heterostructures. *Nano Lett.* **2013**, *13*, 5485–5490.
- (188) Fang, H.; Battaglia, C.; Carraro, C.; Nemsak, S.; Ozdol, B.; Kang, J. S.; Bechtel, H. A.; Desai, S. B.; Kronast, F.; Unal, A. A.; et al., Strong interlayer coupling in van der Waals heterostructures built from single-layer chalcogenides. *Proc. Natl. Acad. Sci.* **2014**, *111*, 6198–6202.
- (189) Georgakilas, V.; Otyepka, M.; Bourlinos, A. B.; Chandra, V.; Kim, N.; Kemp, K. C.; Hobza, P.; Zboril, R.; Kim, K. S. Functionalization of Graphene: Covalent and Non-Covalent Approaches, Derivatives and Applications. *Chem. Rev.* **2012**, *112*, 6156–6214.
- (190) Lee, H.; Yang, S.; Choi, J.; Park, Y.; Kim, S. Evidence of Chemical Functionalized Molecules Adsorbed on the Interface Region of Epitaxial Graphene: Interface Rough-

ness and Modification of the Electronic Properties. *J. Phys. Chem. C* **2011**, *115*, 18736–18739.

- (191) Zhang, L.; Yu, J.; Yang, M.; Xie, Q.; Peng, H.; Liu, Z. Janus graphene from asymmetric two-dimensional chemistry. *Nat. Commun.* **2013**, *4*, 1443.
- (192) Voiry, D.; Goswami, A.; Kappera, R.; Silva, C. d. C. C. e.; Kaplan, D.; Fujita, T.; Chen, M.; Asefa, T.; Chhowalla, M. Covalent functionalization of monolayered transition metal dichalcogenides by phase engineering. *Nat. Chem.* **2014**, *7*, 45–49.
- (193) Vishnoi, P.; Sampath, A.; Waghmare, U. V.; Rao, C. N. R. Covalent Functionalization of Nanosheets of MoS<sub>2</sub> and MoSe<sub>2</sub> by Substituted Benzenes and Other Organic Molecules. *Chem. Eur. J.* **2016**, *23*, 886–895.
- (194) Liu, H.; Liu, Y.; Zhu, D. Chemical doping of graphene. *J. Mater. Chem.* **2011**, *21*, 3335–3345.
- (195) Choi, J.; Lee, H.; Kim, K.-j.; Kim, B.; Kim, S. Chemical Doping of Epitaxial Graphene by Organic Free Radicals. *J. Phys. Chem. Lett.* **2010**, *1*, 505–509.
- (196) Bekyarova, E.; Itkis, M. E.; Ramesh, P.; Berger, C.; Sprinkle, M.; de Heer, W. A.; Haddon, R. C. Chemical Modification of Epitaxial Graphene: Spontaneous Grafting of Aryl Groups. *J. Am. Chem. Soc.* **2009**, *131*, 1336–1337.
- (197) Hossain, M. Z.; Walsh, M. A.; Hersam, M. C. Scanning Tunneling Microscopy, Spectroscopy, and Nanolithography of Epitaxial Graphene Chemically Modified with Aryl Moieties. *J. Am. Chem. Soc.* **2010**, *132*, 15399–15403.
- (198) Wang, Q. H.; Jin, Z.; Kim, K. K.; Hilmer, A. J.; Paulus, G. L. C.; Shih, C.-J.; Ham, M.-H.; Sanchez-Yamagishi, J. D.; Watanabe, K.; Taniguchi, T.; et al., Understanding and controlling the substrate effect on graphene electron-transfer chemistry via reactivity imprint lithography. *Nat. Chem.* **2012**, *4*, 724–732.

- (199) Knirsch, K. C.; Berner, N. C.; Nerl, H. C.; Cucinotta, C. S.; Gholamvand, Z.; McEvoy, N.; Wang, Z.; Abramovic, I.; Vecera, P.; Halik, M.; et al., Basal-Plane Functionalization of Chemically Exfoliated Molybdenum Disulfide by Diazonium Salts. *ACS Nano* **2015**, *9*, 6018–6030.
- (200) Tian, T.; Rice, P.; Santos, E. J. G.; Shih, C.-J. Multiscale Analysis for Field-Effect Penetration through Two-Dimensional Materials. *Nano Lett.* **2016**, *16*, 5044–5052.
- (201) Kratzer, M.; Klima, S.; Teichert, C.; Vasić, B.; Matković, A.; Milićević, M.; Gajić, R. Layer Dependent Wetting in Parahexaphenyl Thin Film Growth on Graphene. *e-J. Surf. Sci. Nanotech.* **2014**, *12*, 31–39.
- (202) Jeong, D. W.; Park, S.; Choi, W. J.; Bae, G.; Chung, Y. J.; Yang, C.-S.; Lee, Y. K.; Kim, J.-J.; Park, N.; Lee, J.-O. Electron-transfer transparency of graphene: Fast reduction of metal ions on graphene-covered donor surfaces. *Phys. Status Solidi RRL* **2015**, *9*, 180–186.
- (203) Qi, Y.; Han, N.; Li, Y.; Zhang, Z.; Zhou, X.; Deng, B.; Li, Q.; Liu, M.; Zhao, J.; Liu, Z.; et al., Strong Adlayer–Substrate Interactions “Break” the Patching Growth of h-BN onto Graphene on Re(0001). *ACS Nano* **2017**, *11*, 1807–1815.
- (204) Lee, T. H.; Kim, K.; Kim, G.; Park, H. J.; Scullion, D.; Shaw, L.; Kim, M.-G.; Gu, X.; Bae, W.-G.; Santos, E. J. G.; et al., Chemical Vapor-Deposited Hexagonal Boron Nitride as a Scalable Template for High-Performance Organic Field-Effect Transistors. *Chem. Mater.* **2017**, *29*, 2341–2347.
- (205) Ojeda-Aristizabal, C.; Santos, E. J. G.; Onishi, S.; Yan, A.; Rasool, H. I.; Kahn, S.; Lv, Y.; Latzke, D. W.; Velasco, J.; Crommie, M. F.; et al., Molecular Arrangement and Charge Transfer in C<sub>60</sub>/Graphene Heterostructures. *ACS Nano* **2017**, *11*, 4686–4693.
- (206) Chow, C. M.; Yu, H.; Jones, A. M.; Yan, J.; Mandrus, D. G.; Taniguchi, T.; Watan-

abe, K.; Yao, W.; Xu, X. Unusual Exciton–Phonon Interactions at van der Waals Engineered Interfaces. *Nano Lett.* **2017**, *17*, 1194–1199.

- (207) Kong, L.; Perez Medina, G.; Colón Santana, J.; Wong, F.; Bonilla, M.; Colón Amill, D.; Rosa, L.; Routaboul, L.; Braunstein, P.; Doudin, B.; et al., Weak screening of a large dipolar molecule adsorbed on graphene. *Carbon* **2012**, *50*, 1981–1986.
- (208) Tsoi, S.; Dev, P.; Friedman, A. . L.; Stine, R.; Robinson, J. T.; Reinecke, T. L.; Sheehan, P. E. van der Waals Screening by Single-Layer Graphene and Molybdenum Disulfide. *ACS Nano* **2014**, *8*, 12410–12417.
- (209) Zheng, Y. J.; Huang, Y. L.; Chen, Y.; Zhao, W.; Eda, G.; Spataru, C. D.; Zhang, W.; Chang, Y.-H.; Li, L.-J.; Chi, D.; et al., Heterointerface Screening Effects between Organic Monolayers and Monolayer Transition Metal Dichalcogenides. *ACS Nano* **2016**, *10*, 2476–2484.
- (210) Gurarslan, A.; Jiao, S.; Li, T.-D.; Li, G.; Yu, Y.; Gao, Y.; Riedo, E.; Xu, Z.; Cao, L. Van der Waals Force Isolation of Monolayer MoS<sub>2</sub>. *Adv. Mater.* **2016**, *28*, 10055–10060.
- (211) Jeffrey, G. A. *An Introduction to Hydrogen Bonding*; Oxford University Press, 1997.
- (212) Lazar, P.; Karlický, F.; Jurečka, P.; Kocman, M.; Otyepková, E.; Šafářová, K.; Otyepka, M. Adsorption of Small Organic Molecules on Graphene. *J. Am. Chem. Soc.* **2013**, *135*, 6372–6377.
- (213) Zhao, Y.; Wu, Q.; Chen, Q.; Wang, J. Molecular Self-Assembly on Two-Dimensional Atomic Crystals: Insights from Molecular Dynamics Simulations. *J. Phys. Chem. Lett.* **2015**, *6*, 4518–4524.
- (214) Mukhopadhyay, T. K.; Datta, A. Ordering and Dynamics for the Formation of Two-

Dimensional Molecular Crystals on Black Phosphorene. *J. Phys. Chem. C* **2017**, *121*, 10210–10223.

- (215) Goriachko, A.; He,; Knapp, M.; Over, H.; Corso, M.; Brugger, T.; Berner, S.; Osterwalder, J.; Greber, T. Self-Assembly of a Hexagonal Boron Nitride Nanomesh on Ru(0001). *Langmuir* **2007**, *23*, 2928–2931.
- (216) Goriachko, A.; He, Y. B.; Over, H. Complex Growth of NanoAu on BN Nanomeshes Supported by Ru(0001). *J. Phys. Chem. C* **2008**, *112*, 8147–8152.
- (217) Pan, Y.; Gao, M.; Huang, L.; Liu, F.; Gao, H.-J. Directed self-assembly of monodispersed platinum nanoclusters on graphene Moiré template. *Appl. Phys. Lett.* **2009**, *95*, 093106.
- (218) Zhou, Z.; Gao, F.; Goodman, D. W. Deposition of metal clusters on single-layer graphene/Ru(0001): Factors that govern cluster growth. *Surf. Sci.* **2010**, *604*, L31–L38.
- (219) Sicot, M.; Bouvron, S.; Zander, O.; Rüdiger, U.; Dedkov, Y. S.; Fonin, M. Nucleation and growth of nickel nanoclusters on graphene Moiré on Rh(111). *Appl. Phys. Lett.* **2010**, *96*, 093115.
- (220) Wang, B.; Bocquet, M.-L. Monolayer Graphene andh-BN on Metal Substrates as Versatile Templates for Metallic Nanoclusters. *J. Phys. Chem. Lett.* **2011**, 2341–2345.
- (221) Zhang, L. Z.; Du, S. X.; Sun, J. T.; Huang, L.; Meng, L.; Xu, W. Y.; Pan, L. D.; Pan, Y.; Wang, Y. L.; Hofer, W. A.; et al., Growth Mechanism of Metal Clusters on a Graphene/Ru(0001) Template. *Adv. Mater. Interfaces* **2014**, *1*, 1300104.
- (222) Roos, M.; Künzel, D.; Uhl, B.; Huang, H.-H.; Branda Alves, O.; Hoster, H. E.; Gross, A.; Behm, R. J. Hierarchical Interactions and Their Influence upon the Ad-

sorption of Organic Molecules on a Graphene Film. *J. Am. Chem. Soc.* **2011**, *133*, 9208–9211.

- (223) N'Diaye, A. T.; Bleikamp, S.; Feibelman, P. J.; Michely, T. Two-Dimensional Ir Cluster Lattice on a Graphene Moiré on Ir(111). *Phys. Rev. Lett.* **2006**, *97*, 215501.
- (224) Atwood, J. L. Kagomé lattice: A molecular toolkit for magnetism. *Nat. Mater.* **2002**, *1*, 91–92.
- (225) Bazarnik, M.; Brede, J.; Decker, R.; Wiesendanger, R. Tailoring Molecular Self-Assembly of Magnetic Phthalocyanine Molecules on Fe- and Co-Intercalated Graphene. *ACS Nano* **2013**, *7*, 11341–11349.
- (226) De Feyter, S.; De Schryver, F. C. Two-dimensional supramolecular self-assembly probed by scanning tunneling microscopy. *Chem. Soc. Rev.* **2003**, *32*, 139–150.
- (227) Slater, A. G.; Perdigão, L. M. A.; Beton, P. H.; Champness, N. R. Surface-Based Supramolecular Chemistry Using Hydrogen Bonds. *Acc. Chem. Res.* **2014**, *47*, 3417–3427.
- (228) Theobald, J. A.; Oxtoby, N. S.; Phillips, M. A.; Champness, N. R.; Beton, P. H. Controlling molecular deposition and layer structure with supramolecular surface assemblies. *Nature* **2003**, *424*, 1029–1031.
- (229) Deshpande, A.; Sham, C.-H.; Alaboson, J. M. P.; Mullin, J. M.; Schatz, G. C.; Hersam, M. C. Self-Assembly and Photopolymerization of Sub-2 nm One-Dimensional Organic Nanostructures on Graphene. *J. Am. Chem. Soc.* **2012**, *134*, 16759–16764.
- (230) Huang, C.; He, M.; Liu, D.; Sun, X.; Gao, B. Oriented Organic Nanowires Self-Assembled on a Graphene Surface. *J. Phys. Chem. C* **2016**, *120*, 17564–17569.
- (231) Li, B.; Tahara, K.; Adisoejoso, J.; Vanderlinden, W.; Mali, K. S.; De Gendt, S.;

Tobe, Y.; De Feyter, S. Self-Assembled Air-Stable Supramolecular Porous Networks on Graphene. *ACS Nano* **2013**, *7*, 10764–10772.

- (232) Hung, S.-W.; Hsiao, P.-Y.; Chen, C.-P.; Chieng, C.-C. Wettability of Graphene-Coated Surface: Free Energy Investigations Using Molecular Dynamics Simulation. *J. Phys. Chem. C* **2015**, *119*, 8103–8111.
- (233) Järvinen, P.; Hämäläinen, S. K.; Banerjee, K.; Häkkinen, P.; Ijäs, M.; Harju, A.; Liljeroth, P. Molecular Self-Assembly on Graphene on SiO<sub>2</sub>and h-BN Substrates. *Nano Lett.* **2013**, *13*, 3199–3204.
- (234) Cai, Y.; Zhang, H.; Song, J.; Zhang, Y.; Bao, S.; He, P. Adsorption properties of CoPc molecule on epitaxial graphene/Ru(0001). *Appl. Surf. Sci.* **2015**, *327*, 517–522.
- (235) Emery, J. D.; Wang, Q. H.; Zarrouati, M.; Fenter, P.; Hersam, M. C.; Bedzyk, M. J. Structural analysis of PTCDA monolayers on epitaxial graphene with ultra-high vacuum scanning tunneling microscopy and high-resolution X-ray reflectivity. *Surf. Sci.* **2011**, *605*, 1685–1693.
- (236) Zhou, H.; Zhang, L.; Mao, J.; Li, G.; Zhang, Y.; Wang, Y.; Du, S.; Hofer, W. A.; Gao, H.-J. Template-directed assembly of pentacene molecules on epitaxial graphene on Ru(0001). *Nano Res.* **2013**, *6*, 131–137.
- (237) He, D.; Pan, Y.; Nan, H.; Gu, S.; Yang, Z.; Wu, B.; Luo, X.; Xu, B.; Zhang, Y.; Li, Y.; et al., A van der Waals pn heterojunction with organic/inorganic semiconductors. *Appl. Phys. Lett.* **2015**, *107*, 183103.
- (238) He, D.; Zhang, Y.; Wu, Q.; Xu, R.; Nan, H.; Liu, J.; Yao, J.; Wang, Z.; Yuan, S.; Li, Y.; et al., Two-dimensional quasi-freestanding molecular crystals for high-performance organic field-effect transistors. *Nat. Commun.* **2014**, *5*, 5162.

- (239) Hara, M.; Sasabe, H.; Yamada, A.; Garito, A. F. Epitaxial Growth of Organic Thin Films by Organic Molecular Beam Epitaxy. *Jpn. J. Appl. Phys.* **1989**, *28*, L306–L308.
- (240) Koma, A. Summary Abstract: Fabrication of ultrathin heterostructures with van der Waals epitaxy. *J. Vac. Sci. Technol. B* **1985**, *3*, 724.
- (241) Ueno, K.; Saiki, K.; Shimada, T.; Koma, A. Epitaxial growth of transition metal dichalcogenides on cleaved faces of mica. *J. Vac. Sci. Technol. B* **1990**, *8*, 68–72.
- (242) Ohuchi, F. S.; Parkinson, B. A.; Ueno, K.; Koma, A. van der Waals epitaxial growth and characterization of MoSe<sub>2</sub>thin films on SnS<sub>2</sub>. *J. Appl. Phys.* **1990**, *68*, 2168–2175.
- (243) Parkinson, B. A.; Ohuchi, F. S.; Ueno, K.; Koma, A. Periodic lattice distortions as a result of lattice mismatch in epitaxial films of two-dimensional materials. *Appl. Phys. Lett.* **1991**, *58*, 472–474.
- (244) Wang, Q.; Xu, K.; Wang, Z.; Wang, F.; Huang, Y.; Safdar, M.; Zhan, X.; Wang, F.; Cheng, Z.; He, J. van der Waals Epitaxial Ultrathin Two-Dimensional Nonlayered Semiconductor for Highly Efficient Flexible Optoelectronic Devices. *Nano Lett.* **2015**, *15*, 1183–1189.
- (245) Wu, Q.; Jang, S. K.; Park, S.; Jung, S. J.; Suh, H.; Lee, Y. H.; Lee, S.; Song, Y. J. In situ synthesis of a large area boron nitride/graphene monolayer/boron nitride film by chemical vapor deposition. *Nanoscale* **2015**, *7*, 7574–7579.
- (246) Chen, W.; Huang, H.; Thye, A.; Wee, S. Molecular orientation transition of organic thin films on graphite: the effect of intermolecular electrostatic and interfacial dispersion forces. *Chem. Commun.* **2008**, 4276–4278.
- (247) Ruiz, R.; Choudhary, D.; Nickel, B.; Toccoli, T.; Chang, K.-C.; Mayer, A. C.; Clancy, P.; Blakely, J. M.; Headrick, R. L.; Iannotta, S.; et al., Pentacene Thin Film Growth. *Chem. Mater.* **2004**, *16*, 4497–4508.

- (248) Chatraphorn, P. P.; Toroczkai, Z.; Das Sarma, S. Epitaxial mounding in limited-mobility models of surface growth. *Phys. Rev. B* **2001**, *64*, 205407.
- (249) Yang, J. L.; Schumann, S.; Jones, T. S. Nanowire-array films of copper hexadecafluorophthalocyanine (F16CuPc) fabricated by templated growth. *J. Mater. Chem.* **2011**, *21*, 5812–5816.
- (250) Breuer, T.; Salzmann, I.; Götzen, J.; Oehzelt, M.; Morherr, A.; Koch, N.; Witte, G. Interrelation between Substrate Roughness and Thin-Film Structure of Functionalized Acenes on Graphite. *Cryst. Growth Des.* **2011**, *11*, 4996–5001.
- (251) Makimoto, T.; Kumakura, K.; Kobayashi, Y.; Akasaka, T.; Yamamoto, H. A Vertical InGaN/GaN Light-Emitting Diode Fabricated on a Flexible Substrate by a Mechanical Transfer Method Using BN. *Appl. Phys. Express* **2012**, *5*, 072102.
- (252) Dlubak, B.; Kidambi, P. R.; Weatherup, R. S.; Hofmann, S.; Robertson, J. Substrate-assisted nucleation of ultra-thin dielectric layers on graphene by atomic layer deposition. *Appl. Phys. Lett.* **2012**, *100*, 173113.
- (253) Hong, H.; Liu, C.; Cao, T.; Jin, C.; Wang, S.; Wang, F.; Liu, K. Interfacial Engineering of Van der Waals Coupled 2D Layered Materials. *Adv. Mater. Interfaces* **2017**, *4*, 1601054.
- (254) Dong, X.; Fu, D.; Fang, W.; Shi, Y.; Chen, P.; Li, L.-J. Doping Single-Layer Graphene with Aromatic Molecules. *Small* **2009**, *5*, 1422–1426.
- (255) Voloshina, E.; Dedkov, Y. Graphene on metallic surfaces: problems and perspectives. *Phys. Chem. Chem. Phys.* **2012**, *14*, 13502.
- (256) Endlich, M.; Gozdzik, S.; Néel, N.; da Rosa, A. L.; Frauenheim, T.; Wehling, T. O.; Kröger, J. Phthalocyanine adsorption to graphene on Ir(111): Evidence for decoupling from vibrational spectroscopy. *J. Chem. Phys.* **2014**, *141*, 184308.

- (257) Huang, H.; Huang, Y.; Wang, S.; Zhu, M.; Xie, H.; Zhang, L.; Zheng, X.; Xie, Q.; Niu, D.; Gao, Y. Van Der Waals Heterostructures between Small Organic Molecules and Layered Substrates. *Crystals* **2016**, *6*, 113.
- (258) Xu, C.; Song, S.; Liu, Z.; Chen, L.; Wang, L.; Fan, D.; Kang, N.; Ma, X.; Cheng, H.-M.; Ren, W. Strongly Coupled High-Quality Graphene/2D Superconducting Mo<sub>2</sub>C Vertical Heterostructures with Aligned Orientation. *ACS Nano* **2017**, *11*, 5906–5914.
- (259) Hunt, B.; Sanchez-Yamagishi, J. D.; Young, A. F.; Yankowitz, M.; LeRoy, B. J.; Watanabe, K.; Taniguchi, T.; Moon, P.; Koshino, M.; Jarillo-Herrero, P.; et al., Massive Dirac Fermions and Hofstadter Butterfly in a van der Waals Heterostructure. *Science* **2013**, *340*, 1427–1430.
- (260) Dean, C. R.; Wang, L.; Maher, P.; Forsythe, C.; Ghahari, F.; Gao, Y.; Katoch, J.; Ishigami, M.; Moon, P.; Koshino, M.; et al., Hofstadter’s butterfly and the fractal quantum Hall effect in moiré superlattices. *Nature* **2013**, *497*, 598–602.
- (261) Li, Y.; Qin, J.-K.; Xu, C.-Y.; Cao, J.; Sun, Z.-Y.; Ma, L.-P.; Hu, P. A.; Ren, W.; Zhen, L. Electric Field Tunable Interlayer Relaxation Process and Interlayer Coupling in WSe<sub>2</sub>/Graphene Heterostructures. *Adv. Funct. Mater.* **2016**, *26*, 4319–4328.
- (262) Li, Y.; Xu, C.-Y.; Qin, J.-K.; Feng, W.; Wang, J.-Y.; Zhang, S.; Ma, L.-P.; Cao, J.; Hu, P. A.; Ren, W.; et al., Tuning the Excitonic States in MoS<sub>2</sub>/Graphene van der Waals Heterostructures via Electrochemical Gating. *Adv. Funct. Mater.* **2015**, *26*, 293–302.
- (263) Hong, X.; Kim, J.; Shi, S.-F.; Zhang, Y.; Jin, C.; Sun, Y.; Tongay, S.; Wu, J.; Zhang, Y.; Wang, F. Ultrafast charge transfer in atomically thin MoS<sub>2</sub>/WS<sub>2</sub> heterostructures. *Nat. Nanotechnol.* **2014**, *9*, 682–686.
- (264) Virkar, A. A.; Mannsfeld, S.; Bao, Z.; Stingelin, N. Organic Semiconductor Growth

and Morphology Considerations for Organic Thin-Film Transistors. *Adv. Mater.* **2010**, *22*, 3857–3875.

- (265) Bettis Homan, S.; Sangwan, V. K.; Balla, I.; Bergeron, H.; Weiss, E. A.; Hersam, M. C. Ultrafast Exciton Dissociation and Long-Lived Charge Separation in a Photovoltaic Pentacene–MoS<sub>2</sub> van der Waals Heterojunction. *Nano Lett.* **2017**, *17*, 164–169.
- (266) Wang, Y.; Torres, J. A.; Stieg, A. Z.; Jiang, S.; Yeung, M. T.; Rubin, Y.; Chaudhuri, S.; Duan, X.; Kaner, R. B. Graphene-Assisted Solution Growth of Vertically Oriented Organic Semiconducting Single Crystals. *ACS Nano* **2015**, *9*, 9486–9496.
- (267) Zheng, J.-Y.; Xu, H.; Wang, J. J.; Winters, S.; Motta, C.; Karademir, E.; Zhu, W.; Varrla, E.; Duesberg, G. S.; Sanvito, S.; et al., Vertical Single-Crystalline Organic Nanowires on Graphene: Solution-Phase Epitaxy and Optical Microcavities. *Nano Lett.* **2016**, *16*, 4754–4762.
- (268) Li, X.; Cai, W.; An, J.; Kim, S.; Nah, J.; Yang, D.; Piner, R.; Velamakanni, A.; Jung, I.; Tutuc, E.; et al., Large-Area Synthesis of High-Quality and Uniform Graphene Films on Copper Foils. *Science* **2009**, *324*, 1312–1314.
- (269) Erni, R.; Rossell, M. D.; Nguyen, M.-T.; Blankenburg, S.; Passerone, D.; Hartel, P.; Alem, N.; Erickson, K.; Gannett, W.; Zettl, A. Stability and dynamics of small molecules trapped on graphene. *Phys. Rev. B* **2010**, *82*, 165443.
- (270) van Engers, C. D.; Cousens, N. E. A.; Babenko, V.; Britton, J.; Zappone, B.; Grobert, N.; Perkin, S. Direct Measurement of the Surface Energy of Graphene. *Nano Lett.* **2017**, *17*, 3815–3821.
- (271) Lee, Y.-H.; Zhang, X.-Q.; Zhang, W.; Chang, M.-T.; Lin, C.-T.; Chang, K.-D.; Yu, Y.-C.; Wang, J. T.-W.; Chang, C.-S.; Li, L.-J.; et al., Synthesis of Large-Area MoS<sub>2</sub>Atomic Layers with Chemical Vapor Deposition. *Adv. Mater.* **2012**, *24*, 2320–2325.

- (272) Steinmann, S. N.; Piemontesi, C.; Delachat, A.; Corminboeuf, C. Why are the Interaction Energies of Charge-Transfer Complexes Challenging for DFT? *J. Chem. Theory Comput.* **2012**, *8*, 1629–1640.
- (273) Hermann, J.; DiStasio, R. A.; Tkatchenko, A. First-Principles Models for van der Waals Interactions in Molecules and Materials: Concepts, Theory, and Applications. *Chemical Reviews* **2017**, *117*, 4714–4758.
- (274) Rappé, A. K.; Casewit, C. J.; Colwell, K. S.; Goddard Iii, W. A.; Skiff, W. M. UFF, a full periodic table force field for molecular mechanics and molecular dynamics simulations. *J. Am. Chem. Soc.* **1992**, *114*, 10024–10035.

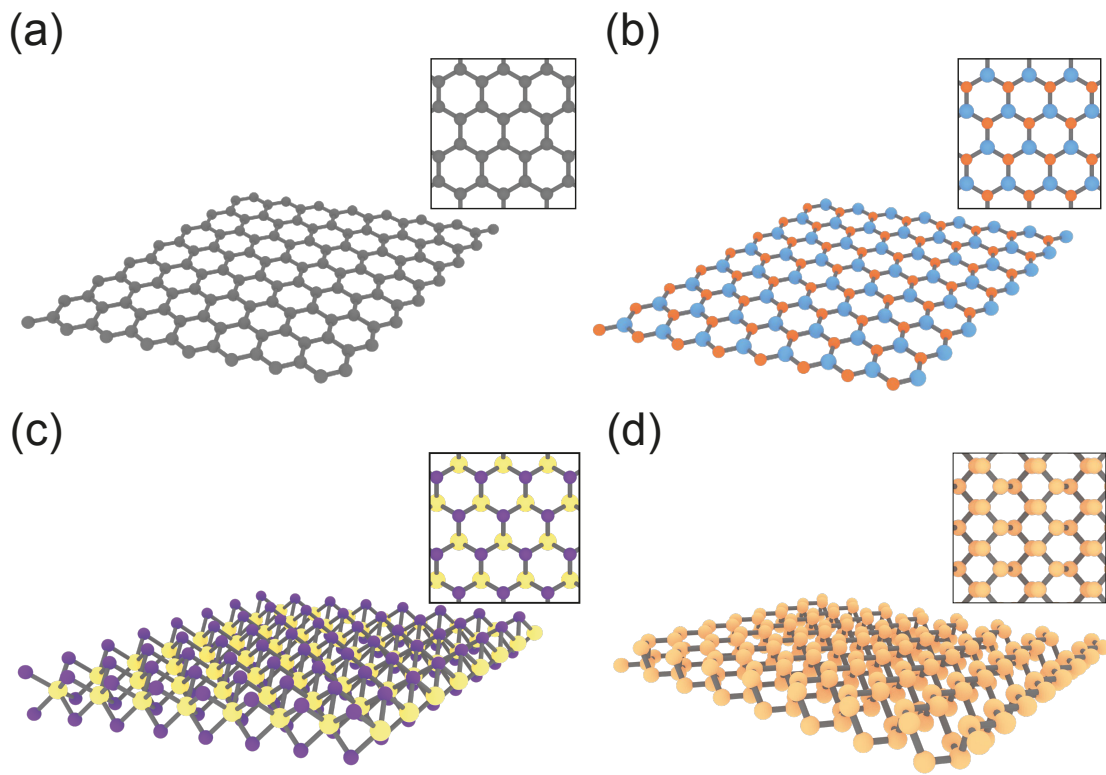


Figure 1: Structures of 2D materials. (a) graphene, (b) hBN, (c) TMDC (2H-type), (d) phosphorene. The inset of each subfigure shows the structure of the 2D material viewed from the top.

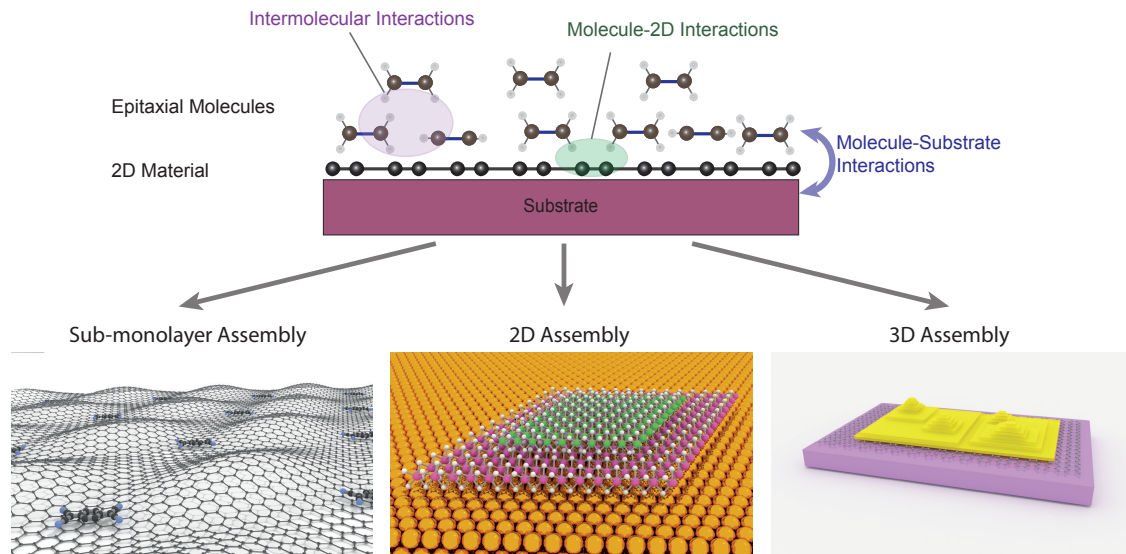


Figure 2: Types of molecular interactions involved in the molecular epitaxy on 2D materials, categorized into intermolecular interaction of epitaxial molecules, molecule-2D material and molecule-substrate interactions. Multidimensional epitaxial structures from sub-2D to 3D **assembled assemblies** are reviewed in the context of this article.

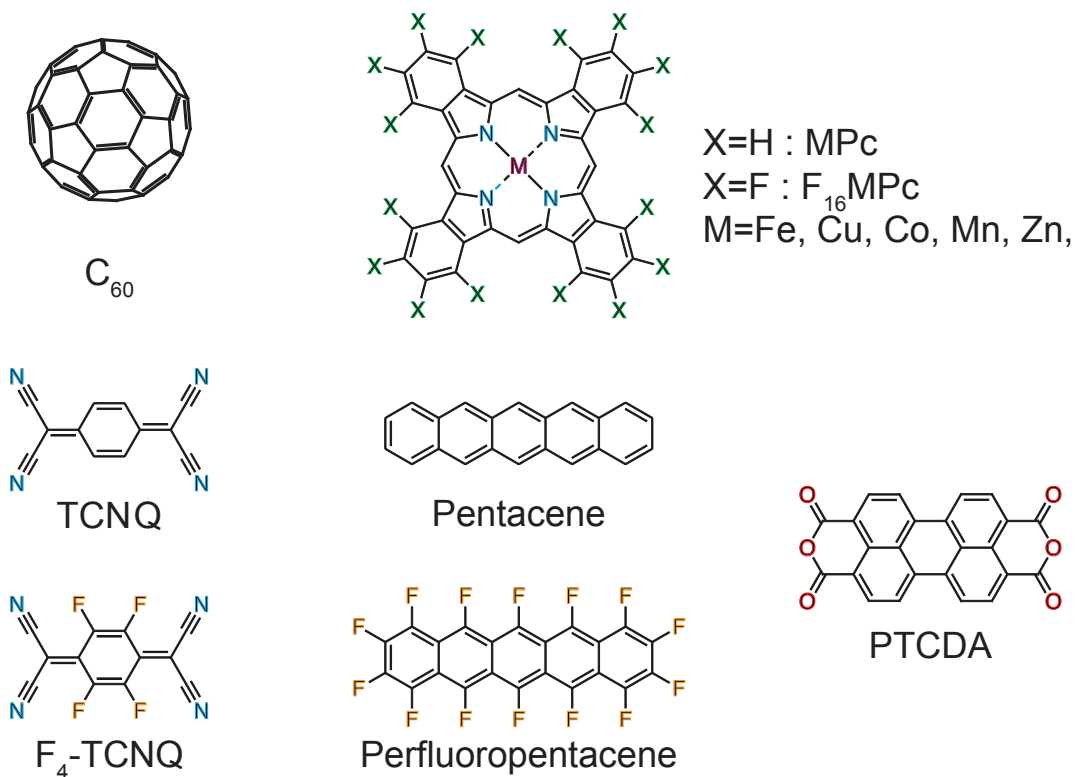


Figure 3: Chemical structures of organic molecules frequently quoted in this review: C<sub>60</sub>, MPc, TCNQ, F<sub>4</sub>-TCNQ, pentacene, perfluoropentacene and PTCDA

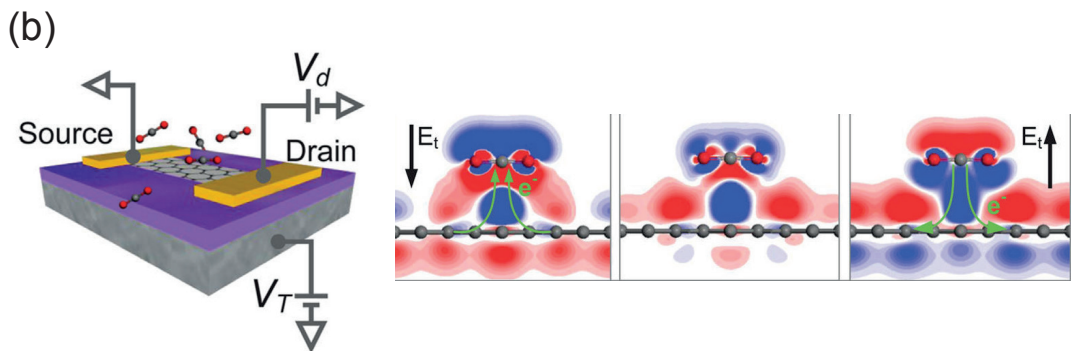
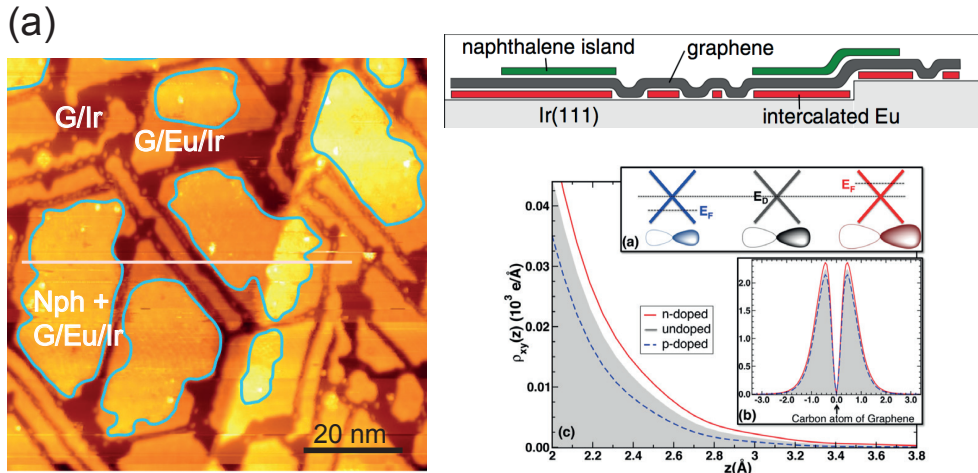


Figure 4: Tunable molecule-2D [interaction](#) by doping of 2D material. (a) Tunable vdW interaction between naphthalene (Nph) and graphene by substrate doping of intercalating Eu between graphene/Ir(111) (G/Ir) surface, indicated by exclusive adsorption of naphthalene (Nph) molecules on Eu intercalated region (G/Eu/Ir).<sup>15</sup> ([Huttman et al. Adapted with permission from Ref. 15. Copyright 2015, American Physical Society.](#)) (b) Tunable vdW interaction between  $CO_2$  and graphene by electrostatic doping. Molecular orbitals of  $CO_2$  on pristine and doped graphene are shown.<sup>16</sup> [Figures adapted \(Muruganathan et al. Adapted with permission from RefsRef. 16. Copyright 2015, American Chemical Society.\)](#)

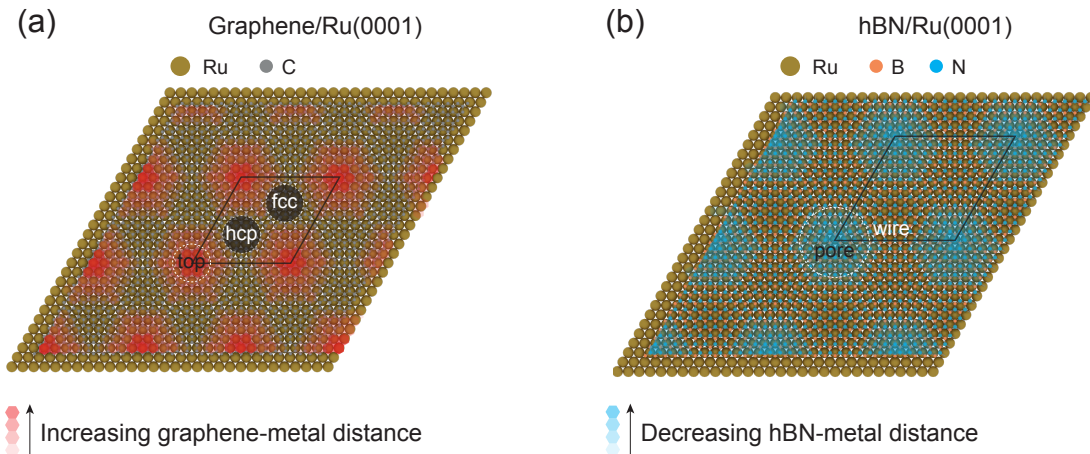


Figure 5: Scheme of the moiré patterns formed in-on (a) graphene/Ru(0001), with valley (fcc, hcp) and hill (top) regions labeled and (b) hBN/Ru(0001) with pore and wire regions marked. The distance between the 2D material and the metal surface is indicated by the transparency of the color hexagonal grids.

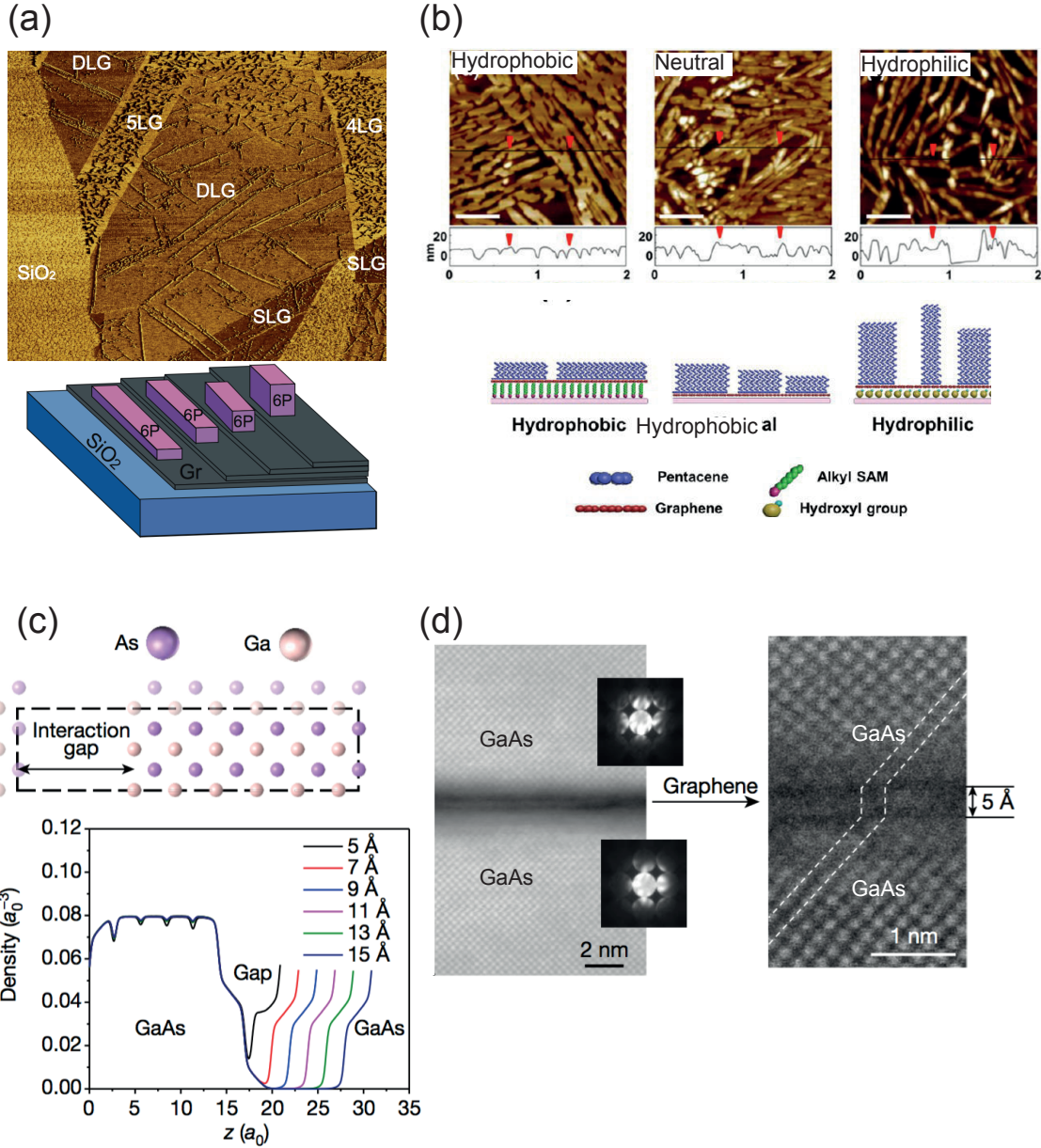


Figure 6: Examples which show the penetration of vdW interaction from the substrate through 2D material. (a) Layer-dependent morphology of 6P epitaxy on graphene/SiO<sub>2</sub>. The proposed morphology change is shown below, with the thickness of the epitaxial layer increasing on 2D materials with more layers.<sup>201</sup> (Kratzer et al. Adapted with permission from Ref. 201. Copyright 2014, The Surface Science Society of Japan.) (b) Substrate hydrophobicity-dependent epitaxial morphology of pentacene on different graphene-covered surfaces.<sup>63</sup> The morphology changes significantly from hydrophobic to hydrophilic substrate. (Nguyen et al. Adapted with permission from Ref. 63. Copyright 2015, American Chemical Society.) (c) Spatial electron density of separating two GaN slabs with a certain distance from first principles calculation. At a distance  $< 9 \text{ \AA}$  the vdW interaction is continuous in the gap.<sup>133</sup> (Kim et al. Adapted with permission from Ref. 133. Copyright 2017, Springer Nature.) (d) Cross sectional high resolution transmission electron microscopy image of the homoepitaxial GaAs on graphene/GaAs in (c). The lattice of the epitaxy and substrate GaN shows perfect match (Kim et al. Figures adapted. Adapted with permission from Refs Ref. 133. Copyright 2017, Springer Nature.)

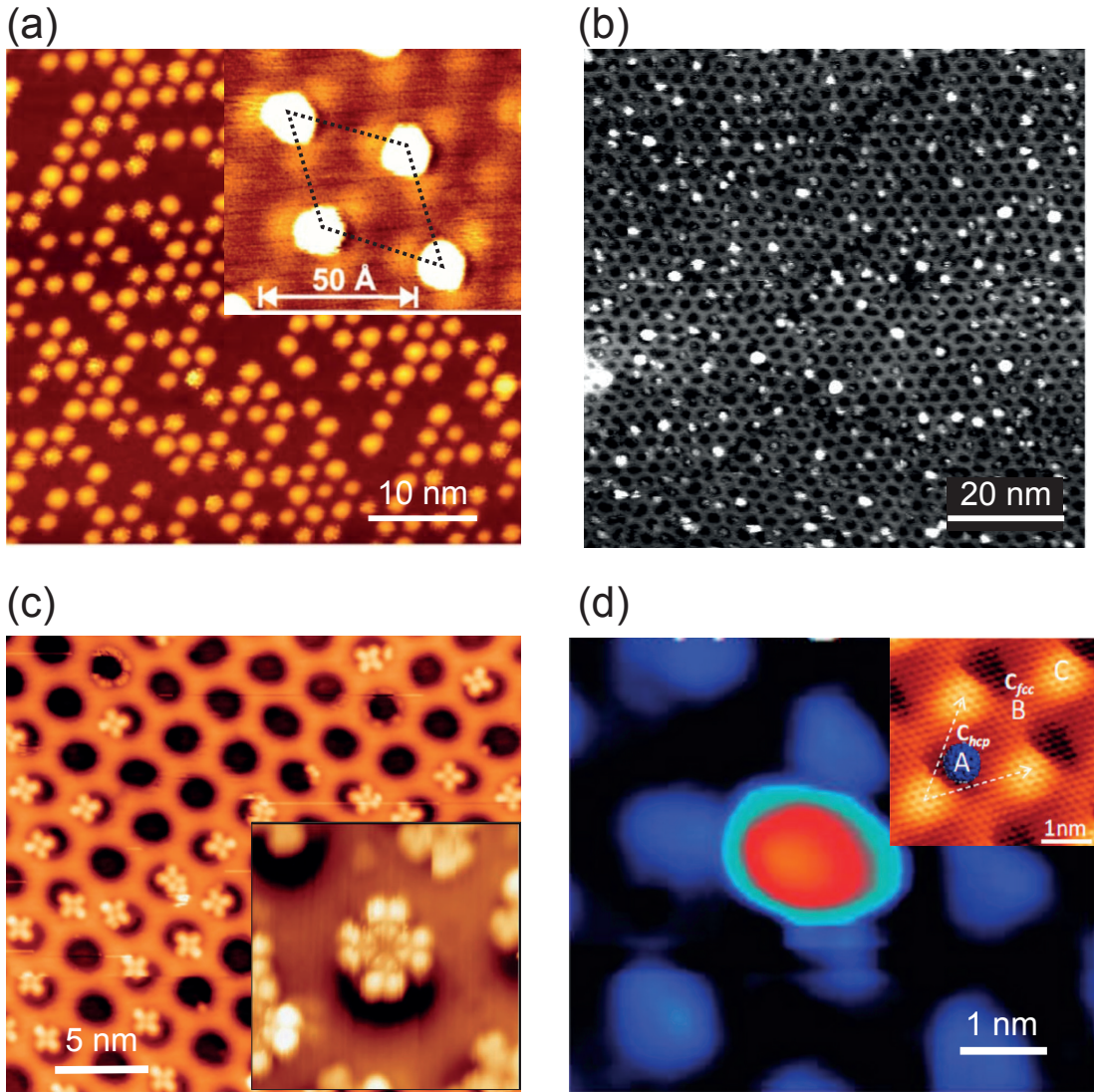


Figure 7: STM images of 0D assemblies formed on strongly interacting 2D surfaces. (a) Isolated Ir clusters on graphene/Ir surface [showing hexagonal arrangement](#). Inset shows details about the adsorption on the hcp sites.<sup>223</sup> ([N'Diaye et al. Adapted with permission from Ref. 223. Copyright 2006, American Physical Society.](#)) (b) Au 0D clusters on hBN/Ru nanomesh [with individual clusters located at the pore edges](#).<sup>216</sup> ([Goriachko et al. Adapted with permission from Ref. 216. Copyright 2008, American Chemical Society.](#)) (c) Trapped CuPc molecules in the pore regions of hBN/Ru. Inset shows off-center adsorption in the pore for a single molecule.<sup>52</sup> ([Iannuzzi et al. Adapted with permission from Ref. 52. Copyright 2014, The PCCP Owner Societies.](#)) (d) Trapping of single C<sub>60</sub> molecule in the hcp valley of a graphene/Ru surface.<sup>29</sup> [Figures adapted](#) ([Lu et al. Adapted with permission from Refs. Ref. 29. Copyright 2012, American Chemical Society.](#))

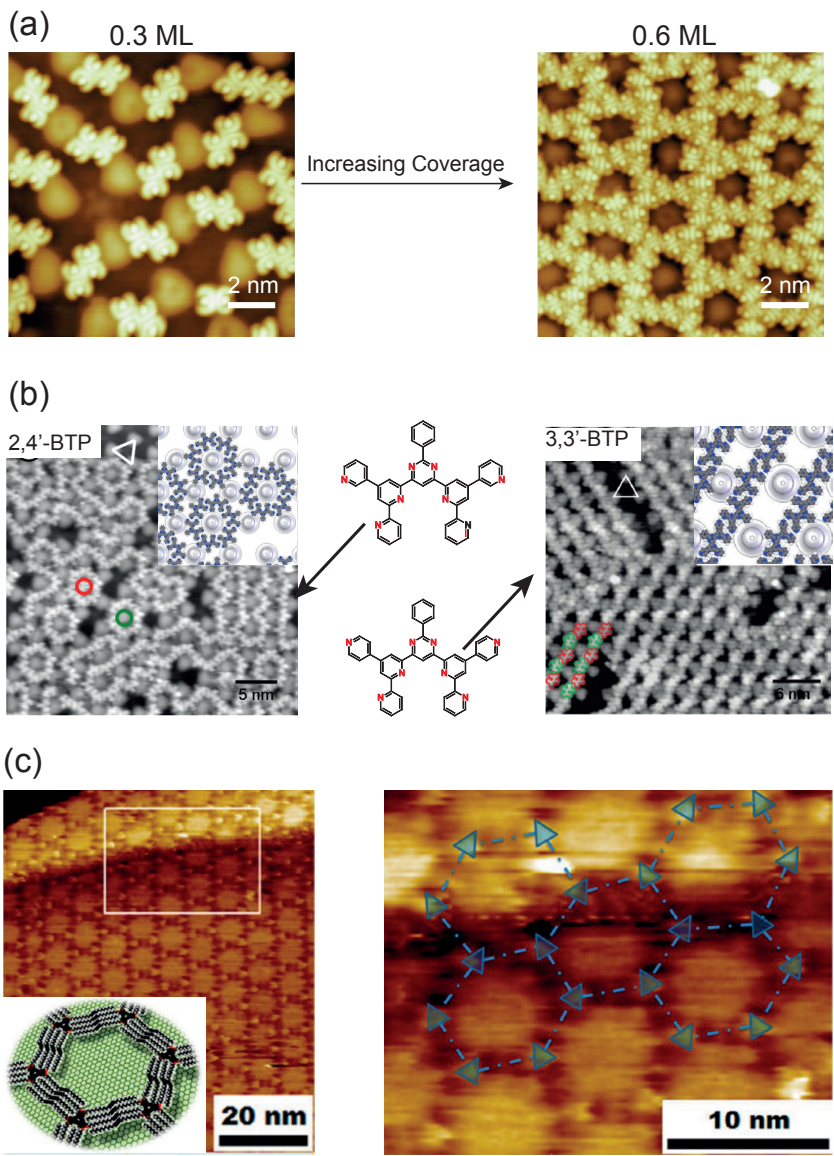


Figure 8: Examples of sub-2D assembly formation by various intermolecular interactions on 2D materials. (a) Transition of 0D assembly of TNCQ on graphene/Ru at 0.3 ML coverage to Kagome lattice formation at 0.6 ML.<sup>82</sup> (Maccariello et al. Adapted with permission from Ref. 82. Copyright 2014, American Chemical Society.) (b) Distinct assembly of hydrogen-bonded 2,4'-BTP (left) with nanorope structure and 3,3'-BTP (right) with linear assembly, on graphene/Ru surface.<sup>92,222</sup> (Roos et al. Adapted with permission from Ref. 92. Copyright 2011, Beilstein-Institut. Roos et al. Adapted with permission from Ref. 222. Copyright 2011, American Chemical Society.) (c) Kagome lattice formation of alkyl-DBA on graphene/SiC, stabilized by interactions between hydrocarbon chains.<sup>231</sup> (Li et al. Adapted with permission from RefsRef. 231. Copyright 2013, American Chemical Society.)

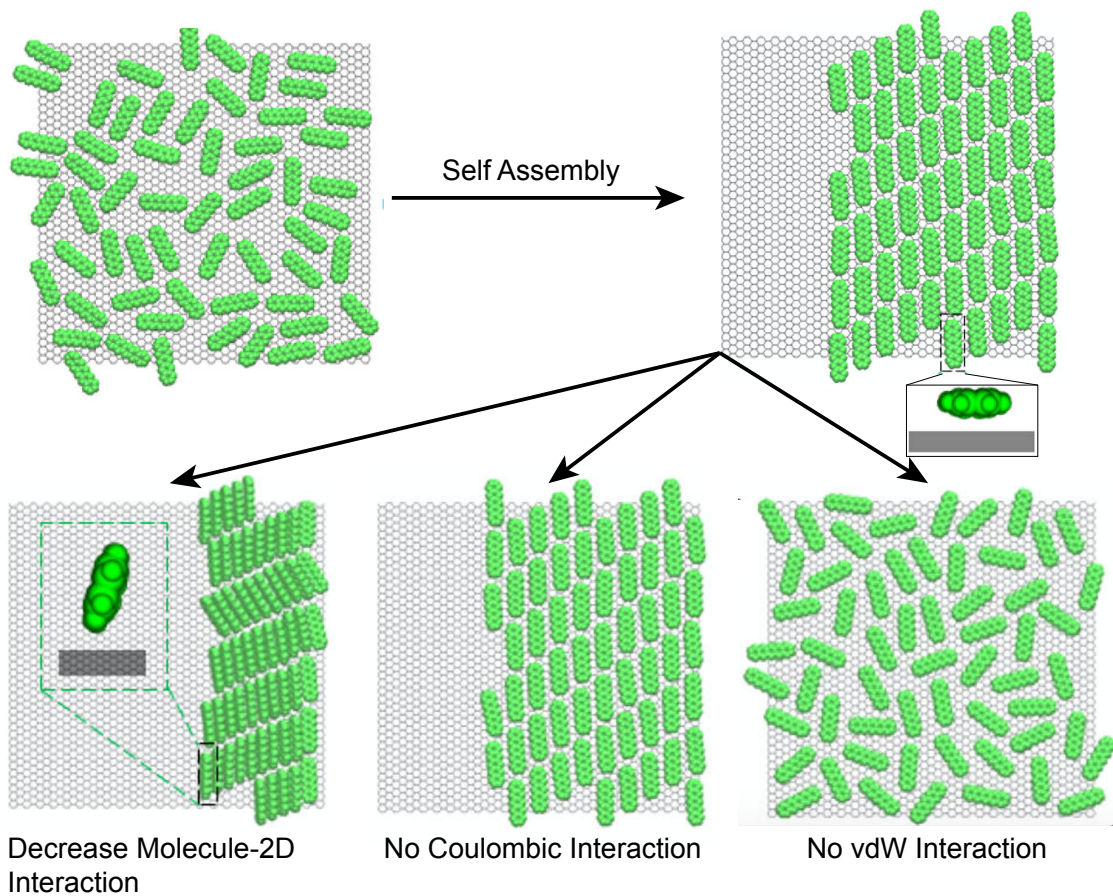


Figure 9: Mechanism of 2D vdW assembly of pentacene on graphene by MD simulation. The ordered assembly forms simultaneously from a random assembly configuration. The influence of changing the molecule-2D, Coulombic and vdW interactions are shown below.<sup>213</sup> Figure adapted from Ref. 213. ([Zhao et al. Adapted with permission from Ref. 213. Copyright 2015, American Chemical Society.](#))

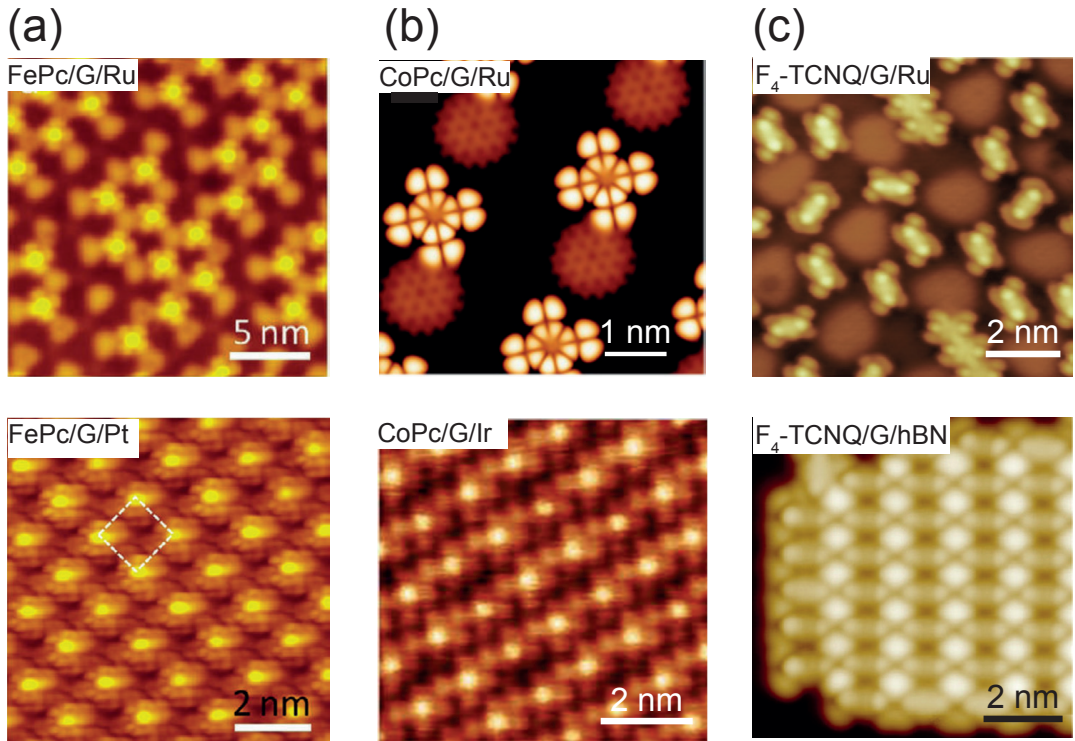


Figure 10: The influence of molecule-2D material interactions on the 2D assembly, shown by STM images of (a) FePc on graphene/Ru and graphene/Ir,<sup>43</sup> (Yang et al. Adapted with permission from Ref. 43. Copyright 2012, American Chemical Society.) (b) CoPc on graphene/Ru (simulated)<sup>234</sup> (Cai et al. Adapted with permission from Ref. 234. Copyright 2015, Elsevier B.V.) and graphen/Ir,<sup>42</sup> (Hämäläinen et al. Adapted with permission from Ref. 42. Copyright 2013, American Physical Society) and (c) F<sub>4</sub>-TCNQ on graphene/Ru<sup>83</sup> (Stradi et al. Adapted with permission from Ref. 83. Copyright 2014, Royal Society of Chemistry) and graphene/hBN.<sup>84</sup> (Tsai et al. Adapted with permission from Ref. 84. Copyright 2015, American Chemical Society.) On strongly interacting graphene surfaces the molecules pack in a sub-2D assembly while on weakly interacting surface close packing is always observed. Figures adapted from Refs.—

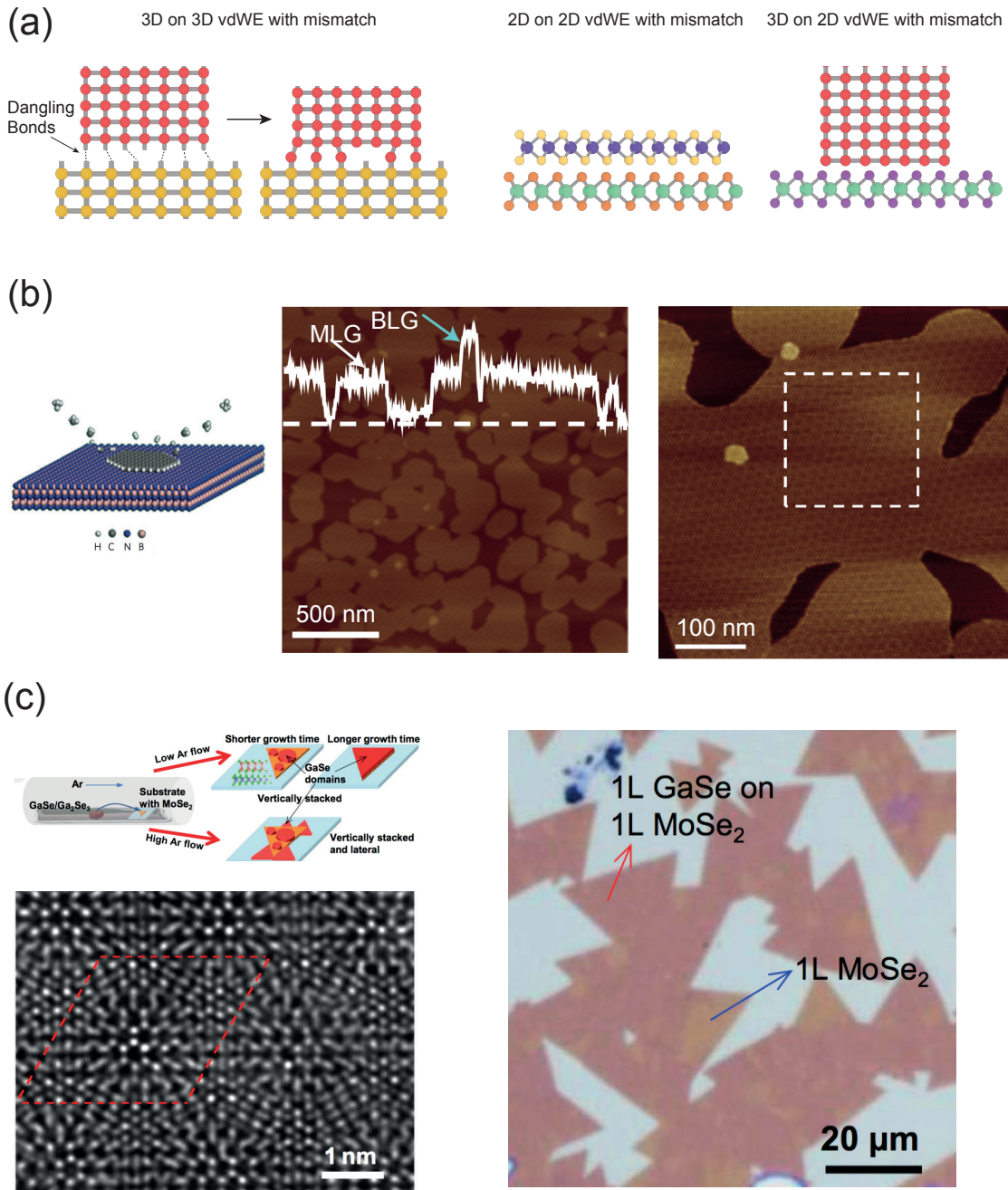


Figure 11: Van der Waals epitaxy of 2D heterostructures. (a) The principle of vdWE process, which has less limit of lattice mismatch than conventional heteroepitaxy, for both 2D and 3D epitaxy on 2D materials. (b) Growing of single crystal graohene on hBN by plasma-enhanced CVD. Large area graphene/hBN heterostructure with ordered moiré pattern can be seen.<sup>110</sup> (Yang et al. Adapted with permission from Ref. 110. Copyright 2013, Springer Nature.) (c) Epitaxial growth of single layer GaSe on single layer MoSe<sub>2</sub> flakes.<sup>120</sup> Figures adapted (Li et al. Adapted with permission from Refs Ref. 120. Copyright 2016, American Association for the Advancement of Science.) The STM image shows moiré pattern as a result of highly ordered interlayer packing.

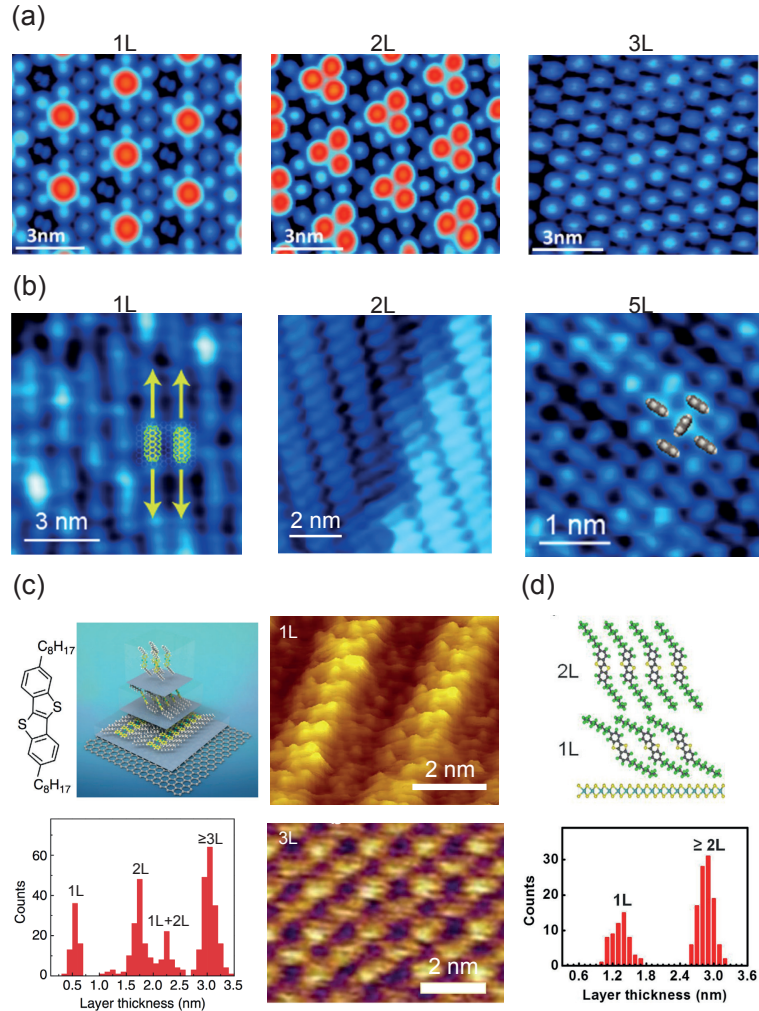


Figure 12: The influence of interfacial interactions on layer-by-layer epitaxy structure. (a)  $\text{C}_{60}$  deposited on graphene/Ru surface. The trapped nucleation sites influence the packing of the first two layers, while the third layer has a packing as in the bulk phase.<sup>29</sup> (Lu et al. Adapted with permission from Ref. 29. Copyright 2012, American Chemical Society.) (b) Layer-dependent morphology of pentacene on epitaxial graphene/SiC. The interface-induced face-on orientation is shown to be partially inherited in the second layer, while the third layer adopts the herringbone packing like in the bulk phase.<sup>61</sup> (Jung et al. Adapted with permission from Ref. 61. Copyright 2014, American Institute of Physics.) (c) Packing of C8-TBTB on graphene.<sup>238</sup> (He et al. Adapted with permission from Ref. 238. Copyright 2014, Springer Nature.) The graphene-induced faced-on orientation propagate within the first 2 layers. (d) Packing of C8-TBTB on  $\text{MoS}_2$ . The  $\text{MoS}_2$  is found to have less orientation guiding for the C8-TBTB molecule.<sup>237</sup> Figures adapted fro Refs(He et al. Adapted with permission from Ref. 237. Copyright 2015, American Institute of Physics.)

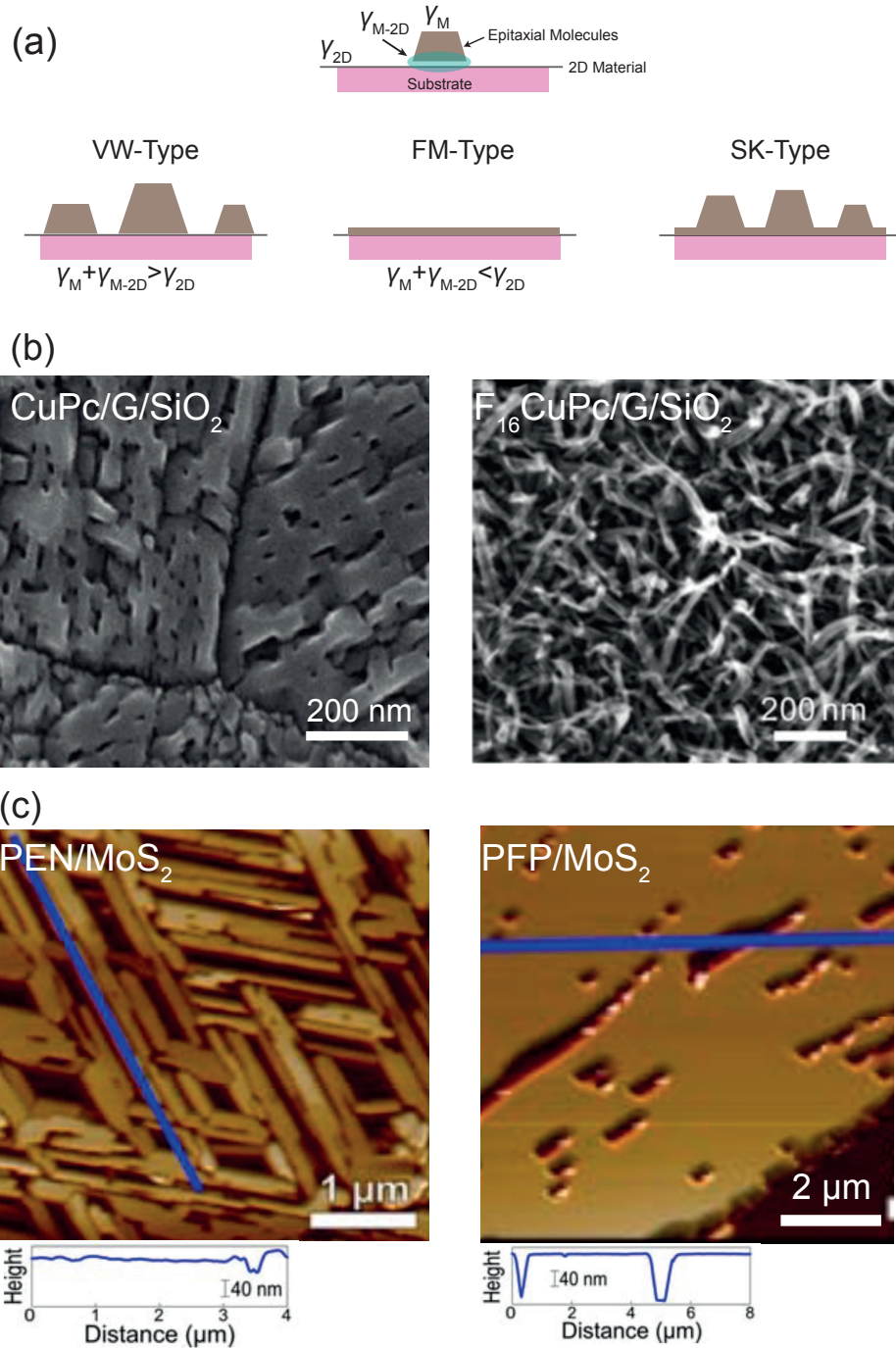


Figure 13: Macroscopic morphology of 3D molecular epitaxy. (a) The VW, FM and SK growth models. (b) The difference between the morphology of CuPc and  $\text{F}_{16}\text{CuPc}$  on graphene/PTCDA.<sup>35,249</sup> (Singha Roy et al. Adapted with permission from Ref. 35. Copyright 2012, American Chemical Society. Yang et al. Adapted with permission from Ref. 249. Copyright 2011, Royal Society of Chemistry.) (c) The difference between the morphology of pentacene (PEN) and perfluoropentacene (PFP) on  $\text{MoS}_2$ .<sup>68</sup> (Breuer et al. Adapted with permission from Ref. 68. Copyright 2016, WILEY-VCH Verlag GmbH & Co. KGaA, Weinheim.) In both cases the orientation of the H- and F- substituted molecule are the same. **Figures adapted from Refs.**

# Graphical TOC Entry

